DISSERTATION

DEVELOPMENT OF ASYMMETRIC N-HETEROCYCLIC CARBENE-CATALYZED REACTIONS

Submitted by

Darrin Miles Flanigan

Department of Chemistry

In partial fulfillment of the requirements

For the Degree of Doctor of Philosophy

Colorado State University

Fort Collins, Colorado

Summer 2017

Doctoral Committee:

Advisor: Tomislav Rovis

Eugene Chen
Yian Shi
Delphi Chatterjee

ABSTRACT

DEVELOPMENT OF ASYMMETRIC N-HETEROCYCLIC CARBENE-CATALYZED REACTIONS

N-Heterocyclic carbenes (NHCs) are ubiquitous organocatalysts in a variety of asymmetric transformations. The benzoin and Stetter reactions, which couple aldehydes to other aldehydes or Michael acceptors, respectively are the most commonly reported reactivity manifold employing NHC catalysts. However, other umpolung reactivity pathways exist, for example, when α,β-unsaturated aldehydes are reacted with NHCs, the Breslow intermediate can react through the double bond of the aldehyde to functionalize at the beta position of the carbonyl. A process that has come to be known has homoenolate reactivity.

A range of reactivity manifolds were investigated, including the asymmetric intermolecular Stetter reaction and an enantioselective NHC-catalyzed nucleophilic dearomatization of pyridiniums. In the dearomatization chemistry, a homoenolate equivalent is first generated from an enal and an NHC, which then adds to the pyridinium to generate 1,4-dihydropyridines with high enantioselectivity. This is a rare example of catalytic, asymmetric addition of a nucleophile to the activated pyridinium that prefers C-4 functionalization leading to the 1,4-dihydropyridine product.

The asymmetric intermolecular Stetter reaction was also investigated in an attempt to broaden the scope of the reaction to include less activated Michael acceptors, specifically, α,β-unsaturated ketones. The coupling of heteroaryl aldehydes to enones could be achieved with appreciable levels of enantioselectivity (up to 80% ee), but reactivity remains a major challenge with this methodology.

ACKNOWLEDGEMENTS

I would like to thank my advisor Tom Rovis for his guidance and mentorship over the last several years. Tom's willingness and patience to let people explore their own intellectual pursuits during graduate school is truly special and greatly contributes to everyone's growth as a scientist and as a person. His unwavering confidence in my ability throughout my time in graduate school has inspired me to accomplish more than I ever thought possible.

I would also like to thank the many great people that I have met in the Rovis group. The last several years have been incredible, largely because of the excitement and energy for constant learning by everyone in the group. I am very blessed and proud to have been a part of such a wonderful group of people. Specifically, I must thank Tiffany Piou, Claire Filloux, Kyle Ruhl, and Jamie Neely who not only made going to lab everyday a fun and intellectually challenging environment, but were great friends outside of the lab as well.

Finally, I would like to thank my family for supporting me while I have been going through graduate school and always encouraging me in whatever I am trying to achieve. They have been a steady source of encouragement throughout my time in graduate school and I could not have made it to this point without their constant support. I would especially like to thank my parents for their constant love and support, I am truly blessed to have them in my life.

TABLE OF CONTENTS

Chapter 1. History of N-Heterocyclic Carbene-Catalyzed Reactions

Although N-Heterocyclic carbenes had been used for benzoin reactions as early as the 1940's, broad interest in their reactivity and chemical properties was not generated until independent reports of stable carbenes by Bertrand[1] and Arduengo.[2] Since these initial reports, N-heterocyclic carbenes (NHCs) have impacted many fields of organic chemistry including organocatalysis,[3,4] transition metal catalysis,[5] and polymer chemistry.[6] Thiazolium-derived NHC scaffolds were initially popular because of their similarity to Thiamine. However, high enantioselectivity could not be achieved with these catalysts and triazolium-based N-heterocyclic carbene (NHC) precursors were developed. Since the introduction of triazolium scaffolds for catalysis, many reports have appeared demonstrating reliably high enantioselectivity across a range of different NHC-catalyzed reactions can be achieved. The high activity and selectivity across such varying reactivity, powered, the need for fine-tuning the NHC structure and has led to an impressive number of reported carbene-catalysts.

1.1 Umpolung Acyl Anion Catalysis

The most studied umpolung reaction employing NHC organocatalysts is the benzoin reaction. This was first discovered by Wöhler and Liebig in 1832 using cyanide as the catalyst to couple benzaldehyde to form benzoin.[7] The currently accepted mechanism of this transformation was first proposed by Lapworth[8] and is shown in scheme 1.1.1 First, cyanide adds to benzaldehyde generating tetrahedral intermediate **1**, which then undergoes a proton transfer to give intermediate **2**. This intermediate where the anionic charge is localized on the carbon of the aldehyde is responsible for the umpolung reactivity observed in this reaction. Carbanion **2** then adds to another

equivalent of aldehyde to give intermediate **3**, which, after proton transfer, collapses to generate the observed benzoin product (**4**) and the cyanide catalyst.

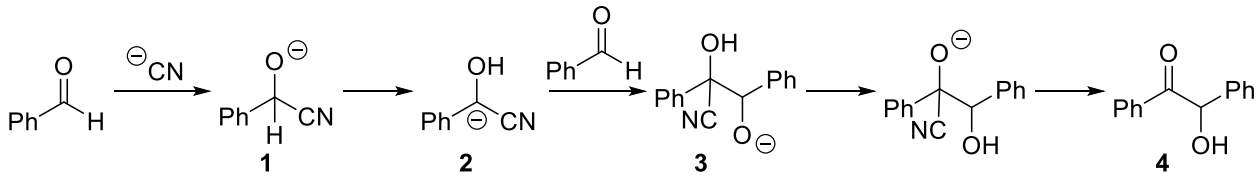

Scheme 1.1.1

In 1943, Ukai demonstrated the same reaction could be carried out with catalytic amounts of thiazolium in the presence of base.[9] Inspired by the Lapworth mechanism, Breslow proposed a similar pathway for the thiazolium catalyzed benzoin reaction while investigating the mechanism of thiamine action.[10] Breslow's key insight was that the thiazolium could be deprotonated a the 2-position to generate an ylide where the carbanion acts as the reactive center of the catalyst. This hypothesis was supported by deuterium exchange experiments with thiamine in D_2O. After this finding, it was reasoned that the deprotonated thiazolium bearing a carbanion at the C-2 position could react similarly to the cyanide ion and catalyze benzoin formation.

The currently accepted mechanism for the thiazolium-catalyzed benzoin reaction is shown in scheme 1.1.2. The thiazolium is first deprotonated to give an ylide (a resonance form of the free carbene), which then adds to an aldehyde generating tetrahedral intermediate **5**. This then undergoes proton transfer, to give carbanion **6**, which is in resonance with neutral enaminol **7**, commonly referred to as the Breslow intermediate. Addition of **6** to another equivalent of aldehyde gives tetrahedral intermediate **8**, followed by proton transfer and collapse to form **4** and regenerate the active catalyst. In-depth kinetic studies were later performed on the mechanism of the benzoin reaction by White and Leeper.[11] The authors determined the three kinetically significant steps were initial addition of the NHC to the aldehyde, tautomerization to form the Breslow intermediate, and

addition of this intermediate to another equivalent of benzaldehyde. Interestingly, all three steps contributed to the rate of the reaction and were partially rate-limiting.

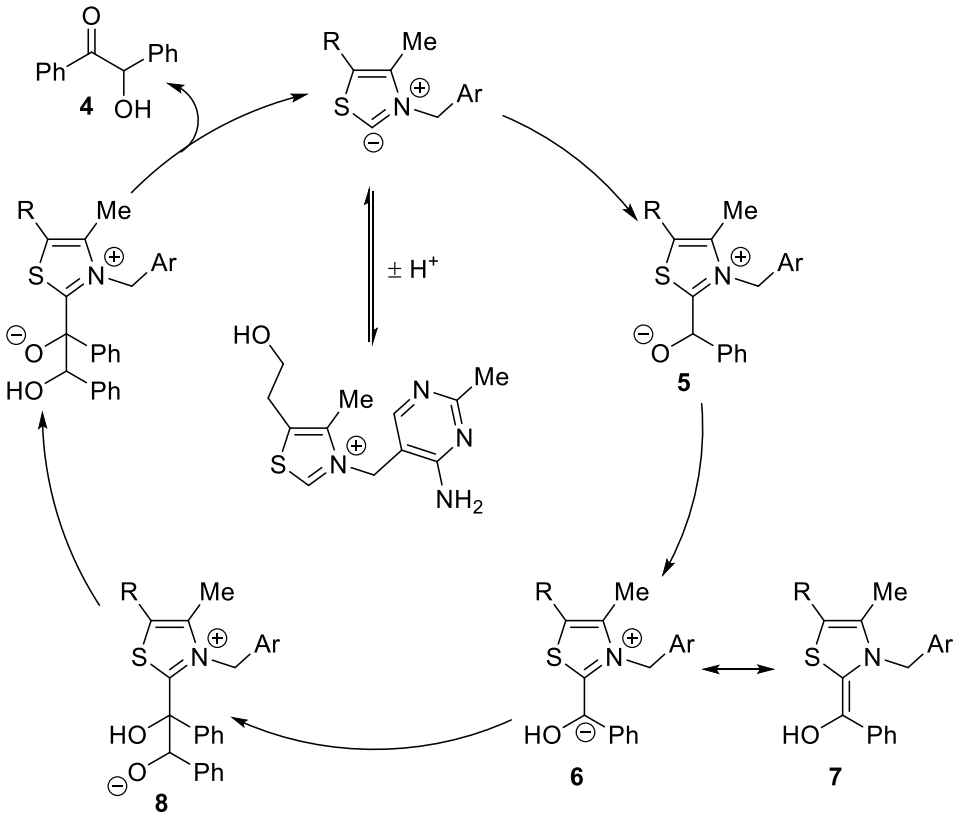

Scheme 1.1.2

The Breslow intermediate generated upon addition of the carbene to an aldehyde was later demonstrated to couple aldehydes with other electrophiles, such as Michael acceptors. This reactivity was heavily investigated by Stetter in the 1970's and has since become known as the Stetter reaction.[12] Due to its importance in NHC catalysis, much work has been devoted to the isolation and characterization of the Breslow intermediate.[13] Berkessel isolated and characterized the Breslow intermediate derived from imidazolinium-derived NHCs and aryl aldehydes.[14] Through competition experiments with these isolated intermediates, he demonstrated the reversibility of Breslow intermediate formation that has been proposed previously.

1.2 Asymmetric Benzoin Reactions

The benzoin reaction has been widely studied and has become a benchmark reaction to test new carbene scaffolds. Sheehan reported an asymmetric variant of the reaction in 1966 using a chiral thiazolium that gave the benzoin product in 22% ee.[15] Since this time, many groups have sought to improve the efficiency of the reaction by designing catalysts to increase the yield and enantioselectivity of the process.[16] Figure 1.2.1 illustrates the major advances during the evolution of catalyst design that took place over 50 years and allowed for high enantioselectivity to be achieved in the reaction. In 1997, Leeper and Rawal introduced a bicyclic thiazolium-derived catalyst that provided an important basis for future catalyst design, despite no improvement in the enantioselectivity of the reaction over Sheehan's original report.[17] A major advance was later reported by Enders using a triazolium-derived scaffold, which provides the product with much improved enantioselectivity (75% ee).[18] This was followed up by a bicyclic triazolium-derived catalyst that provided the benzoin product in high enantioselectivity for the first time (90% ee).[19] Currently, the most selective catalyst for the asymmetric benzoin reaction, reported Connon and Zietler delivers the product in 99% ee.[20]

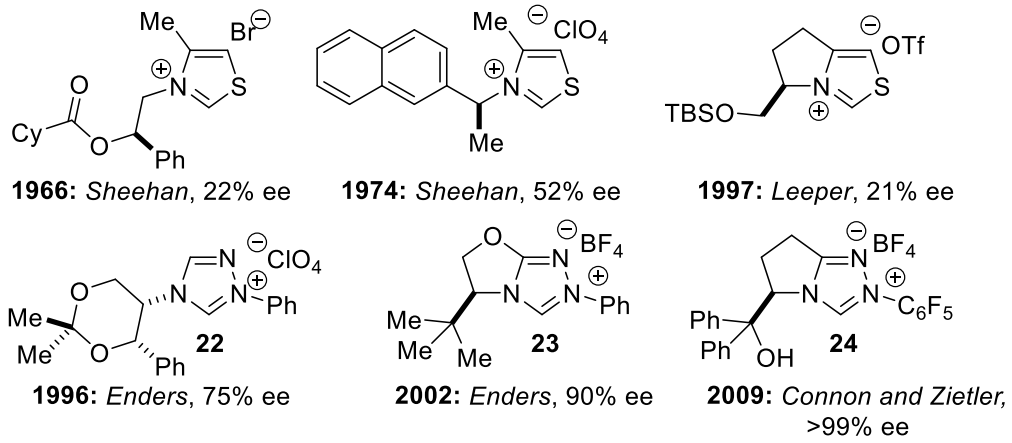

Figure 1.2.1 Catalyst development for the asymmetric benzoin reaction.

This reaction is not limited to homo-benzoin reactions and a variety of cross-benzoin reactions have also been reported. Cookson reported an intramolecular cross-benzoin reaction of tethered aliphatic aldehydes in 1976.[21] Importantly, the substrates lacked chemoselectivity issues between the two aldehydes; when more than one benzoin products is possible, a statistical mixture of products is observed. In the intermolecular cross-benzoin reaction, the product distribution could be controlled by increasing the amount of one coupling partner (Scheme 1.2.1).[22]

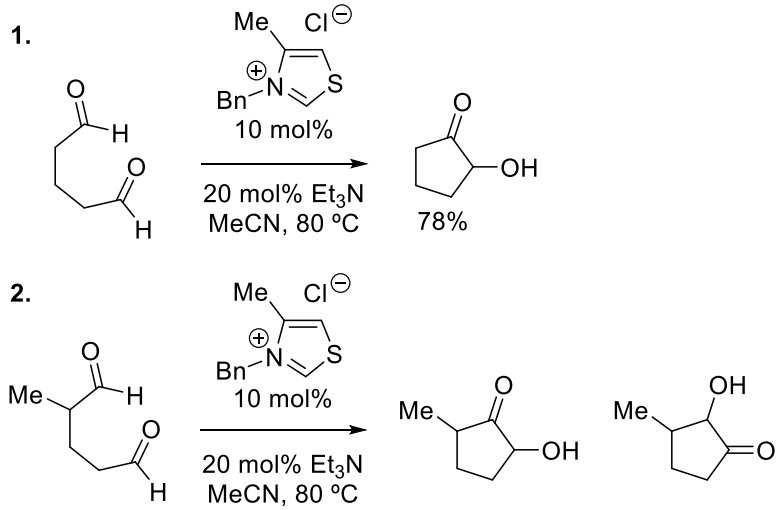

Scheme 1.2.1

Several groups aimed to improve the chemoselectivity issues inherent in the cross reaction. Johnson reported the use of acyl-silanes as an acyl anion equivalent, which essentially removed the chemoselectivity issues observed by other groups.[23] Gravel could increase the selectivity of the cross-benzoin reaction between aliphatic aldehyde donors and aryl aldehydes acceptors through catalyst design.[24] He proposes the selectivity arises from steric interactions between the larger catalyst and the aromatic aldehyde disfavor formation of the Breslow intermediate with the aryl aldehyde. Therefore, using the bulkier NHC catalyst will encourage the formation of the aliphatic aldehyde-derived Breslow intermediate which then preferentially reacts with the aromatic aldehyde. Thus, the [4.3.0]-bicyclic triazolium **14** delivers the benzoin product **9** in a 40:1 ratio

over the other three possible products. In contrast, sterically smaller [3.3.0]-triazolium **13** favors **9** in only a 1.4:1 ratio over the other three possible benzoin products. Efforts to render this reaction asymmetric were met with limited success, but the cross-benzoin product could be generated in 63% yield and a promising 40% ee (Scheme 1.2.2).

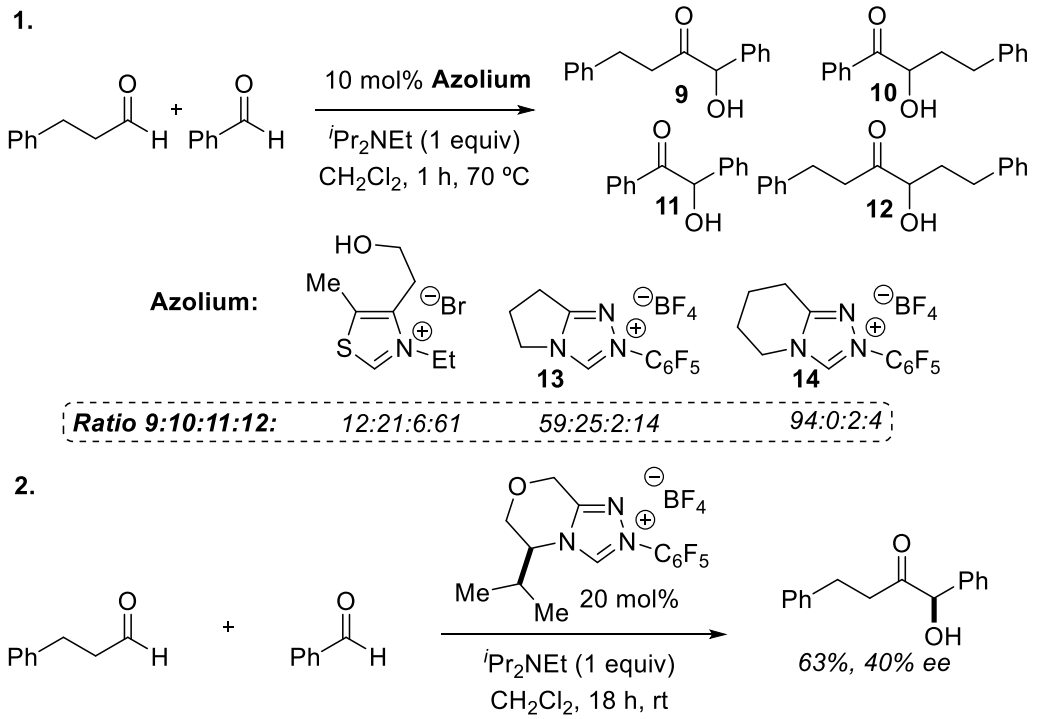

Scheme 1.2.2

In addition to the reaction between two different aldehydes, the cross-benzoin reaction has also been employed to couple aldehydes with imines and ketones. Enders reported the coupling of aldehydes and trifluoromethyl ketones in good yields and modest enantioselectivity (up to 85% ee).[25] Ketoesters have been shown to be competent acceptors in the cross-benzoin reaction between aryl and aliphatic aldehydes and ethyl pyruvate by Connon and Zeitler.[26] Other ketoesters were also competent in the reaction, but branched aliphatic ketones were less reactive. This process was later rendered asymmetric by Gravel using triazolium **15** as the precatalyst giving the expected cross-benzoin product in up to 98% yield and up to 94% ee (Scheme 1.2.3).[27]

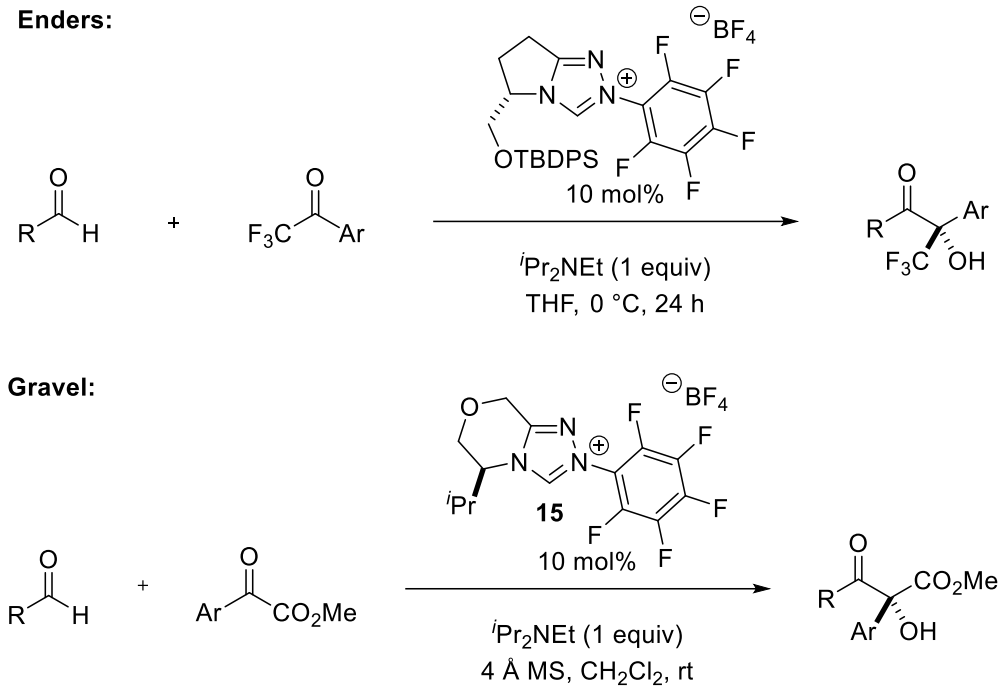

Scheme 1.2.3

Imines were first reported in cross-benzoin reactions to give α-amino ketones by Murry and Frantz.[28] The enantioselective cross-benzoin reaction between aldehydes and imines was first reported by Miller who employed a peptide-derived thiazolium catalyst to impart selectivity.[29] A triazolium-derived catalyst was reported by Rovis for the cross-aza-benzoin reaction between aldehydes and *N*-Boc imines that offers improved selectivity and a more general substrate scope than the peptide-catalyzed reaction.[30] In this methodology, the NHC can add to the imine generating a stable NHC-imine adduct, which is highly reversible in the presence of a weak acid. This is generated in the reaction by deprotonation of the triazolium with CsOAc. Trifluoromethyl ketimines have also been demonstrated to be competent substrates in the cross-aza-benzoin reaction. High enantioselectivity could be achieved in the reaction when triazolium **16** is used as the pre-catalyst. This triazolium was also effective in coupling other imines bearing an electron withdrawing group including iminoesters and iminonitriles with high yields and enantioselectivity (Scheme 1.2.4).[31] The benzoin reaction remains the most studied NHC-catalyzed process and the

advances in catalyst design for this reaction were crucial to the development of new carbene organocatalysts that could impart high levels of enantioselectivity for this and many other transformations.

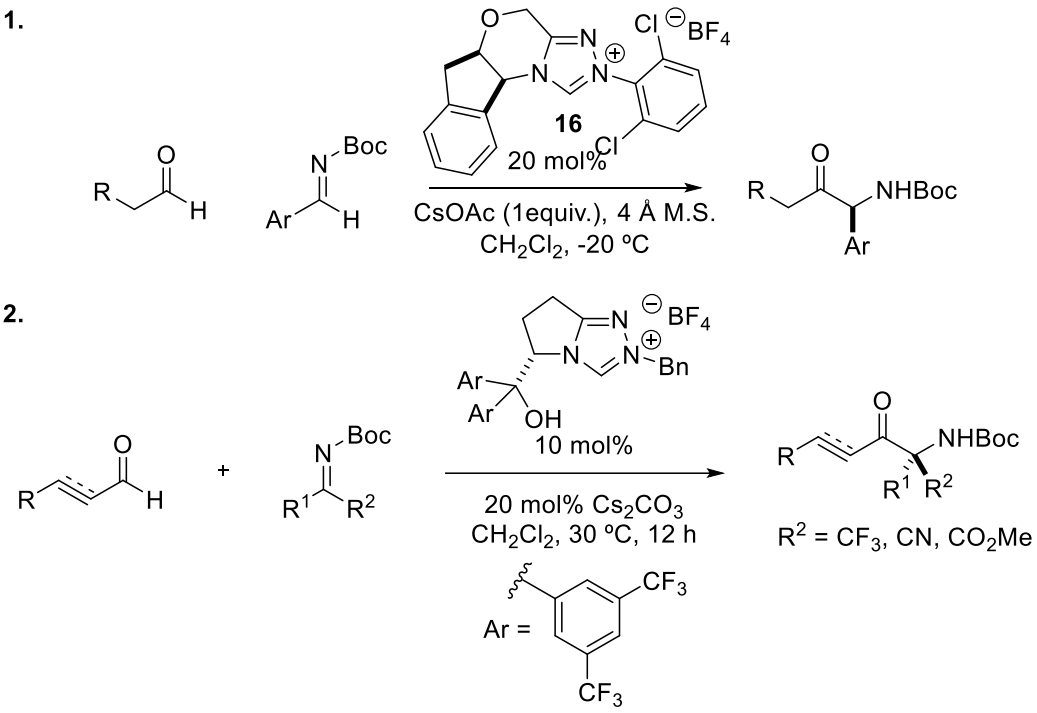

Scheme 1.2.4

1.3 Asymmetric Intermolecular Stetter Reactions

The Stetter reaction proceeds, similarly to the benzoin reaction, by initial generation of an acyl anion equivalent. The addition of this acyl anion to a carbon-heteroatom double bond in a 1,2 fashion leads to the benzoin product. However, in the Stetter reaction, this intermediate adds conjugately to Michael acceptor to give γ-functionalized ketones. This reactivity was systematically investigated by Stetter during the 1970's using cyanide or achiral thiazolium-derived catalysts.[12,32]

The intramolecular version of the reaction proved much more amenable toward the development of an asymmetric variant. This was first reported by Enders in 1996 using triazolium

precatalyst **17**.[33] The Rovis group published highly efficient catalyst scaffolds for this reaction in 2002, providing the products in high yield and enantioselectivity (Scheme 1.3.1).[34]

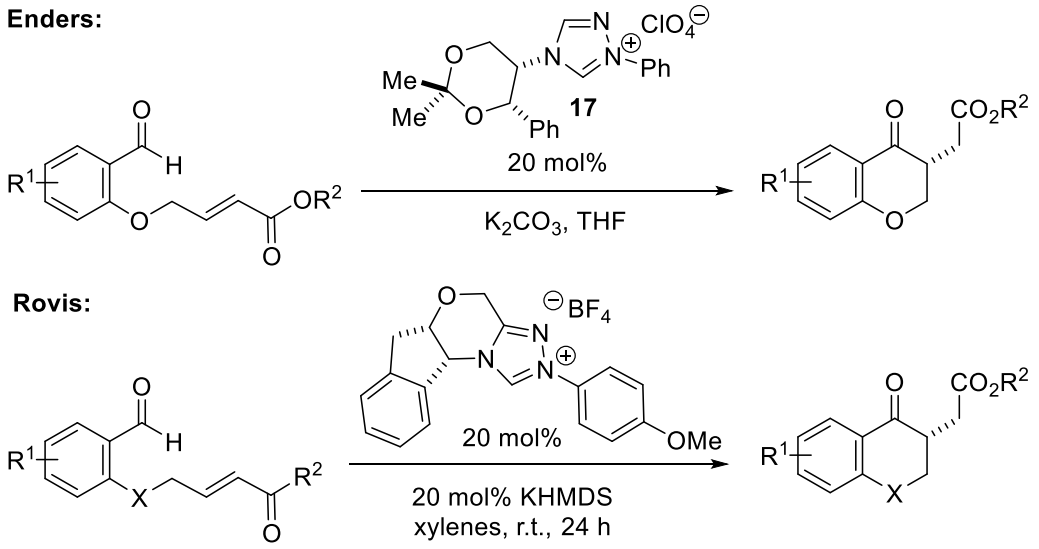

Scheme 1.3.1

Since these initial reports, our group[35] and others[36] have reported a variety of catalysts for the efficient coupling of aldehydes to Michael acceptors. The scope of the reaction has also been expanded dramatically to include unsaturated amides, thioesters, ketones, esters, phosphonates and aldehydes. The mechanism of the intramolecular Stetter reaction was studied experimentally by Rovis.[37] Through competition experiments, it was determined that the rate limiting step of the reaction is likely deprotonation to form the Breslow intermediate (Scheme 1.3.2). Interestingly, this is experimental evidence for previous computational investigations into the mechanism that found a high barrier for the symmetry forbidden 1,2-proton transfer (29.2 kcal/mol), which suggests the mechanism is proceeding in an alternate path. In a separate study, the proton transfer to generate the Breslow intermediate had a >43 kcal/mol barrier for the 1,2-proton shift, which could be reduced to 21 kcal/mol when an exogenous base (triethylamine) shuttles the proton.[38] Finally, Yates found that the mechanism for the Stetter reaction is different than the benzoin

reaction by following a two-step process for addition of the Breslow intermediate to the Michael acceptor, rather than a one step process as in the benzoin reaction.[39]

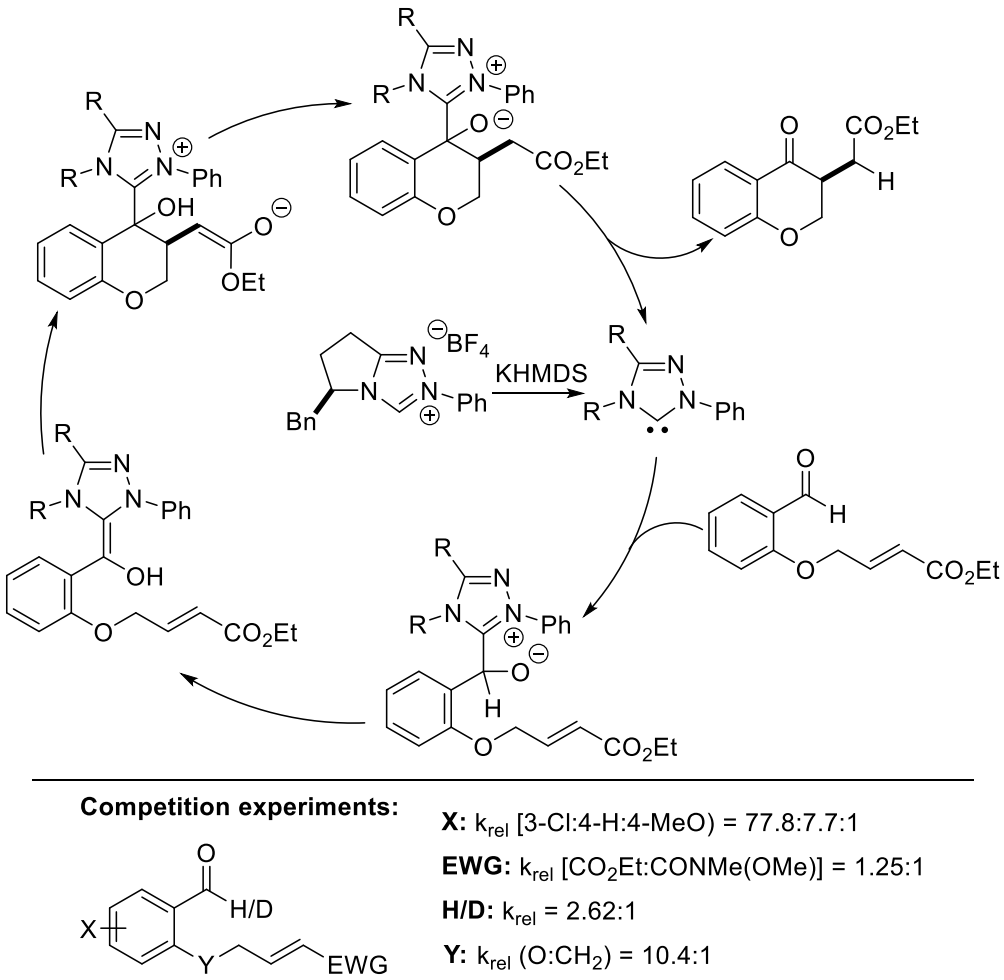

Scheme 1.3.2

Although the asymmetric intramolecular Stetter reaction has been demonstrated with many substrates, expanding the scope of the enantioselective intermolecular Stetter reaction has proven more difficult because the reaction often requires highly activated Michael acceptors to achieve good reactivity. First attempts at an enantioselective variant of this reaction were reported by Enders in 1990 coupling butenal with chalcone. The corresponding 1,4-diketone was generated in 29% yield and 30% ee. The enantioselectivity could be slightly improved (39% ee) with a different thiazolium-derived catalyst, but reactivity drops off significantly (4% yield).[40] The first major

advances toward developing an asymmetric intermolecular Stetter reaction were reported in 2008. Rovis reported the coupling of glyoxamides to alkylidene malonate acceptors with good yield and high enantioselectivity.[41] The use of trisubstituted alkylidene ketoamides was later demonstrated to give the Stetter product with high levels of diastereocontrol.[42] Concurrently, Enders published the coupling of aryl aldehydes to chalcones in good yield and modest enantioselectivity (Scheme 1.3.3).[43] Subsequently, acetaldehyde was demonstrated to be a competent coupling partner in the reaction, but with lower levels of enantioselectivity.[44]

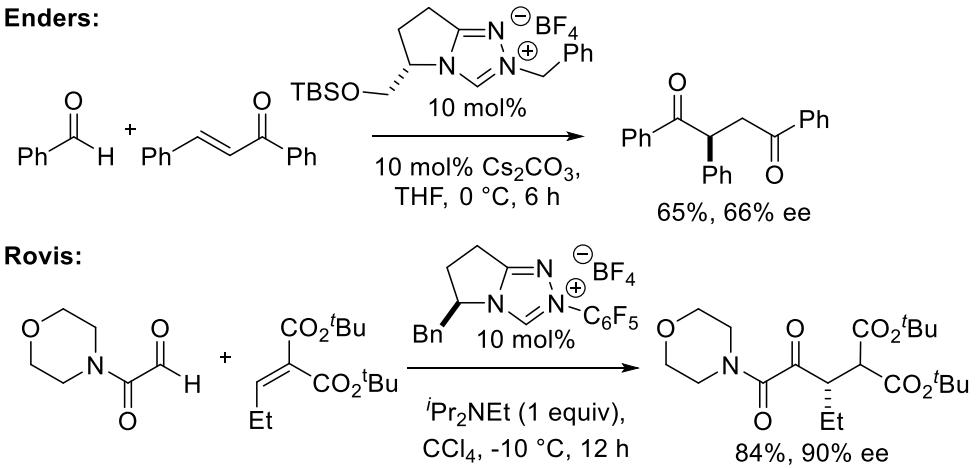

Scheme 1.3.3

Following these seminal reports, the coupling of heteroaryl aldehydes to nitroalkenes was demonstrated.[45] Fluorinated catalyst **19** was found to give the Stetter products in higher enantioselectivity compared to the non-fluorinated catalyst **18** demonstrating the impact of fluorination of the catalyst backbone on the efficiency of the catalyst (Scheme 1.3.4). This catalyst was further applied to the coupling of aryl aldehydes to unsaturated ketoesters.[46] The improved selectivity with this catalyst was originally proposed to result from conformational changes in the catalyst that enhance the steric environment around the carbene center on the catalyst. A subsequent computational study found the selectivity could arise from attractive interactions on

the developing positive charge of the Breslow intermediate and the developing negative charge of the nitroalkene during the carbon-carbon bond forming step.[47]

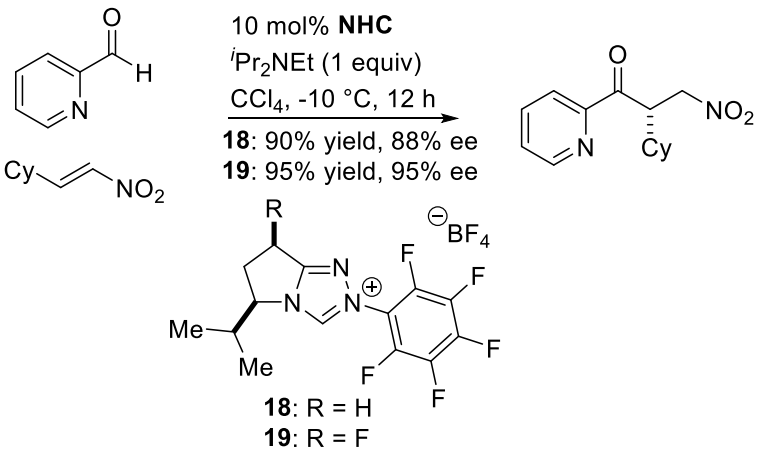

Scheme 1.3.4

Triazolium **19** was later used to expand the scope of the Stetter reaction to include the coupling of α,β-unsaturated aldehydes with nitroalkenes.[48] Interestingly, adding catechol to the reaction greatly increased the yield of the process, going from 5% yield after 8 hours to 80% yield after 2 hours. The addition of catechol to the intramolecular Stetter reaction was also tested and permitted catalyst loadings as low as 0.1 mol%. The increased activity from adding catechol to the reaction mixture was proposed to stem from catechol assisting the proton transfer of the tetrahedral intermediate to generate the Breslow intermediate (Scheme 1.3.5). This hypothesis is based on previous mechanistic studies on the intramolecular Stetter reaction which demonstrate that proton transfer to generate the Breslow intermediate is likely the rate limiting step of the intramolecular Stetter reaction.[37] Kinetic isotope measurements with deutero-aldehyde and deutero-catechol support that catechol is assisting the proton transfer giving a k_H/k_D = 4.2. Alternatively, the increased reactivity could result from hydrogen bonding to the nitroalkene, activating it toward nucleophilic addition; however, Further control experiments with chiral diols and achiral NHC

catalysts give racemic Stetter product, suggesting the enhanced reactivity is not a result of activation of the Michael acceptor by hydrogen bonding.

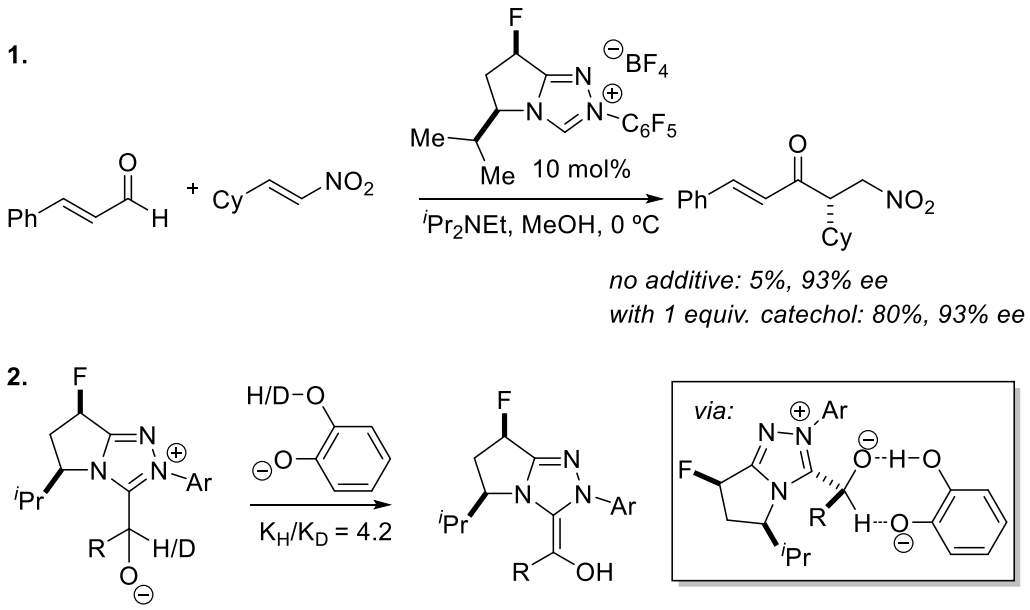

Scheme 1.3.5

Aliphatic aldehydes could also be coupled to nitroalkenes. In this case, the *trans*-fluorinated NHC **20** was more efficient than either **18** or **19** (Scheme 1.3.6). This was also studied computationally and it was again proposed that electrostatic interactions between the fluorine on the catalyst and the nitro group of the acceptor is the reason for the high selectivity of this catalyst.

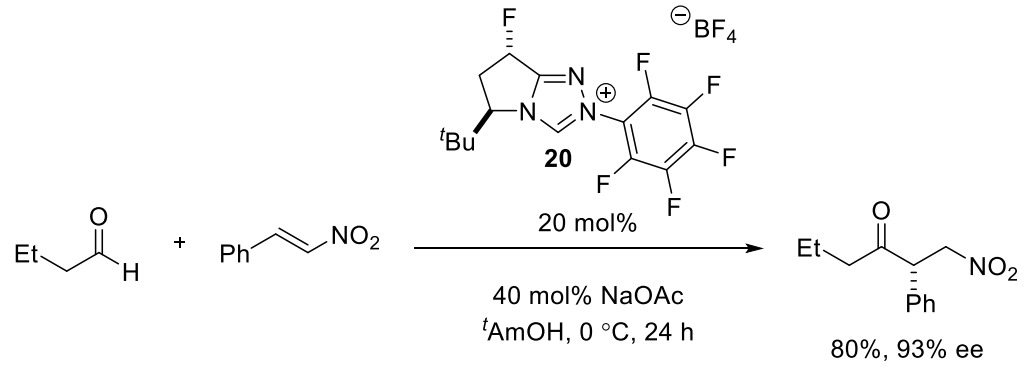

Scheme 1.3.6

Chi reported enal coupling partners with modified chalcones in good yield and enantioselectivity.[49] While the scope of Michael acceptors in this reaction is generally limited to highly activated Michael acceptors, there have been reports using less activated substrates. The coupling of aryl aldehydes to acetamido-acrylates proceeds with good yield and enantioselectivity.[50] This was later expanded to α-substituted acrylates lacking a second activating group.[51] These reactions are limited to the use of α-substituted Michael acceptors. Importantly, the use of β-substituted enoates gives the product in diminished yield and enantioselectivity. When *Z*-methyloct-2-enoate is used in the reaction, the Stetter product is afforded in 59% yield and 80% ee (Scheme 1.3.7). This is the only published example of an asymmetric Stetter reaction carried out on a β-substituted Michael acceptor lacking highly activating groups.

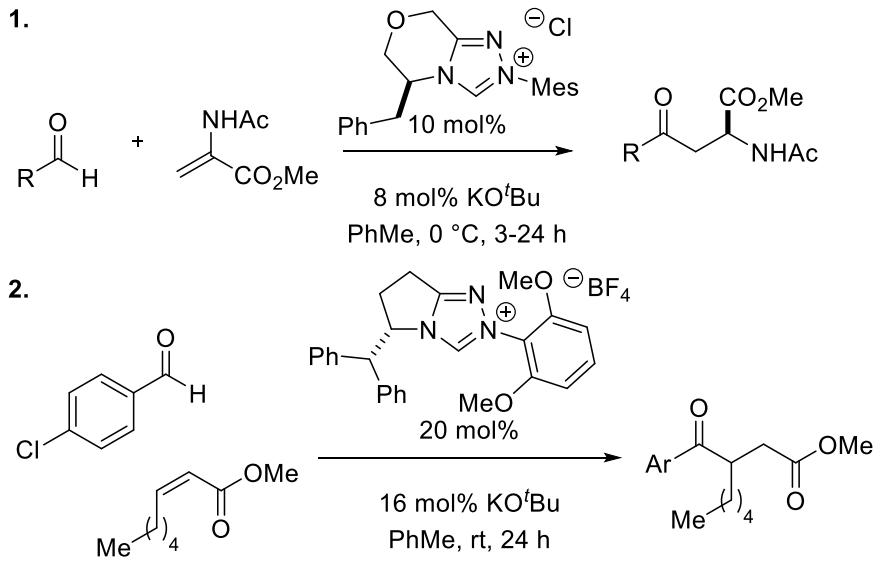

Scheme 1.3.7

1.4 Annulation Reaction Involving Extended Breslow Intermediates

As mentioned above, α,β-unsaturated aldehydes can be used in umpolung acyl anion reactions, but because of the conjugated alkene, enals are also capable of substitution at the alpha or beta positions providing an alternate reactivity pathway that is not accessible with other

aldehydes (Scheme 1.4.1). Nucleophilic addition at the beta carbon of the extended Breslow intermediate **21** to an electrophile generates an enol azolium (**22**), which can also intercept electrophiles at the alpha position of the aldehyde. Protonation of the azolium enolate generates the electrophilic acyl azolium species **23**, which can then be intercepted by a nucleophile to release the carbene catalyst and form the desired product.

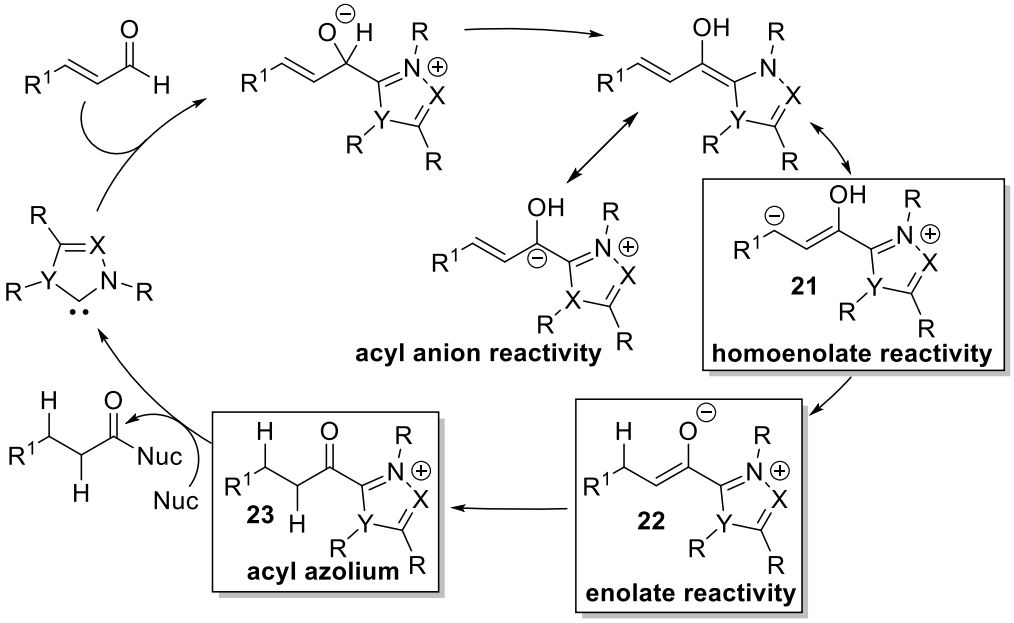

Scheme 1.4.1

Often this type of reactivity is carried out with a tethered nucleophile that can add to the acyl azolium generated to give cyclic products. A variety of annulation reactions are possible which can proceed by functionalization at the beta position through the homoenolate intermediate followed by cyclization onto either the enol azolium in a [4+2] fashion or at the acyl azolium to give [3+3] cycloaddition-type products. Cyclic products can also be accessed by initial beta protonation of the homoenolate intermediate to generate the enol azolium, which has been used to generate 5- and 6-membered rings.

NHC-catalyzed homoenolate annulation reactions were first reported by Bode[52] and Glorius[53] in 2004 who demonstrated the synthesis of γ-lactones from enals and aryl aldehydes. This reactivity can also be exploited to synthesize γ-lactams, which was first reported by Bode in 2005 using IMES as the NHC precursor (Scheme 1.4.2.).[54] The proposed reaction is believed to proceed by initial formation of the Breslow intermediate **24**, which then adds at the beta position to the aromatic aldehyde to give intermediate **25**. This can then tautomerize to acyl azolium **26** followed by intramolecular trapping of **26** by the tethered alkoxide to form the observed lactone product and regenerate the NHC catalyst.

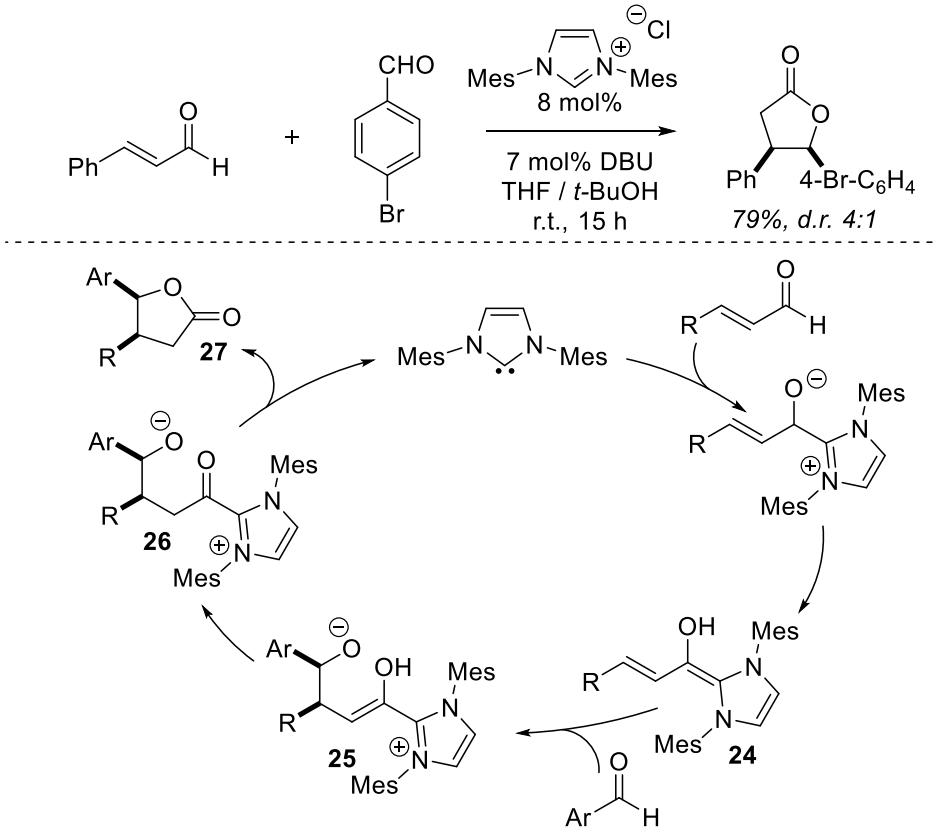

Scheme 1.4.2

Since this initial report, several other studies have expanded the scope of the reaction demonstrating a variety of enals and aldehydes are tolerated as well as ketones[55] and isatins.[56] An enantioselective version of this reaction was reported by Scheidt, but was limited to

acylphosphonates as the carbonyl partner.[57] Shortly after, the asymmetric homoenolate addition to cyclic ketimines was reported.[58] Scheidt reported a synthesis of γ-lactams from *N*-acyl hydrazones and enals (Scheme 1.4.3).[59] Interestingly, a Lewis acid co-catalyst was required to achieve high levels of reactivity and selectivity. It is proposed that the hydrazone is first activated by binding to the Lewis acid co-catalyst, followed by nucleophilic addition of the homoenolate equivalent. Rovis reported that a chiral NHC with catalytic amounts of a Brønsted acid enables the synthesis of γ-lactams in good yield and enantioselectivity.[60] A related annulation reaction was reported by Scheidt who found that aryl nitrones can undergo a beta functionalization followed by trapping with the tethered nitrone-oxygen.[61] The [3+3] cycloadduct could then be opened with sodium methoxide and methanol to generate the straight chain product.

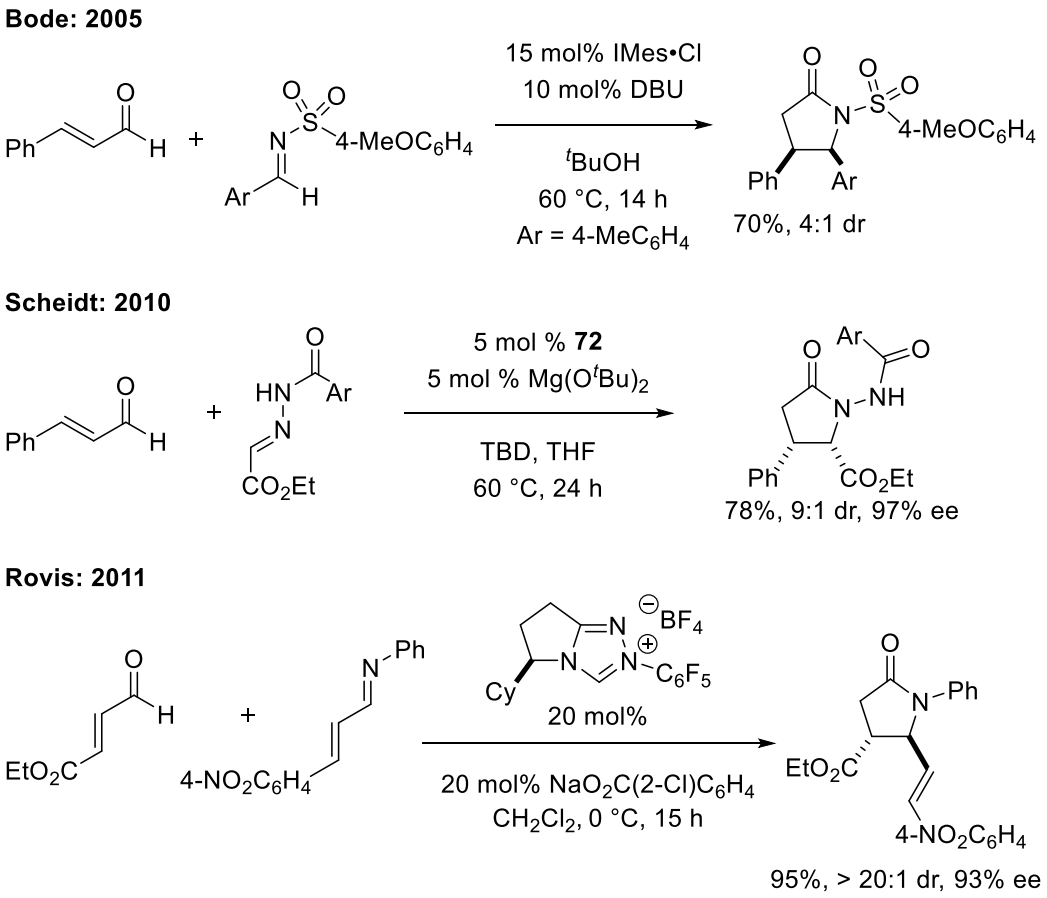

Scheme 1.4.3

1.5 Non-Ring Forming Reactions

Although much less common, the umpolung beta functionalization of enals can also be employed where the acyl azolium is not intercepted by a tethered nucleophile. The first NHC-catalyzed reactions involving beta functionalization of enals were reported by Scheidt[62] and Bode[63] who developed an internal redox esterification process where the extended Breslow intermediate is first protonated at the beta position of the aldehyde to generate an azolium enolate (Scheme 1.5.1). This can then undergo proton transfer to form an acyl azolium species, which is intercepted by an alcohol to give the saturated ester and regenerate the NHC catalyst. This mirrors reactivity reported forty years prior by Walia and Vishwakarma where cyanide was demonstrated to catalyze the transformations to their corresponding saturated amides in the presence of water.[64]

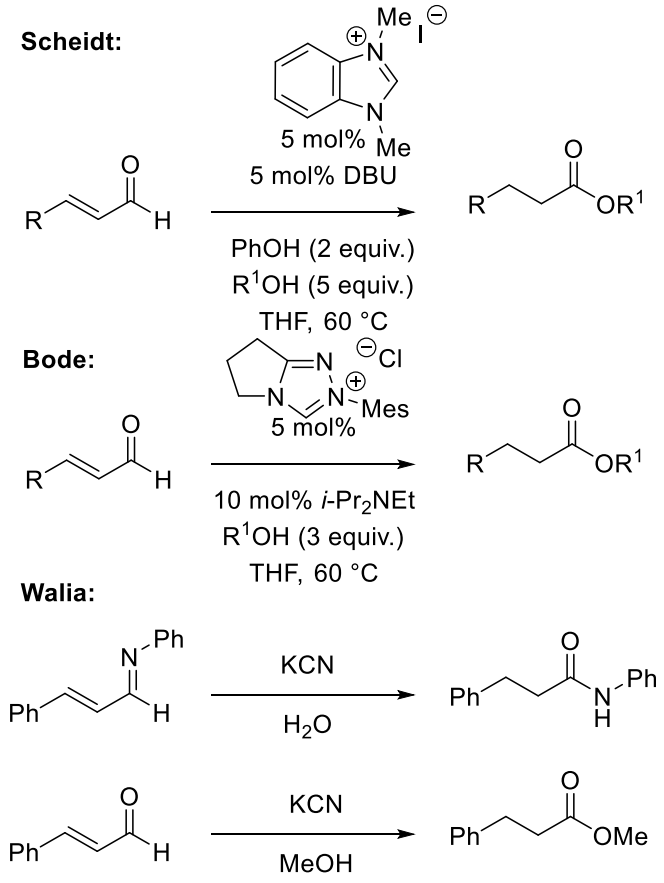

Scheme 1.5.1

Nair reported a beta addition of enals to nitroalkenes generating functionalized δ-nitroesters, which is believed to proceed by generation of the homoenolate equivalent, followed by conjugate addition to the nitroalkene. Liu[65] and Rovis[66] later published enantioselective versions of this reaction. Interestingly, the method reported by Nair and the enantioselective variant reported by Liu favor formation of the *anti*-isomer, while the *syn* product was favored when catalyst **28** was used (Scheme 1.5.2).

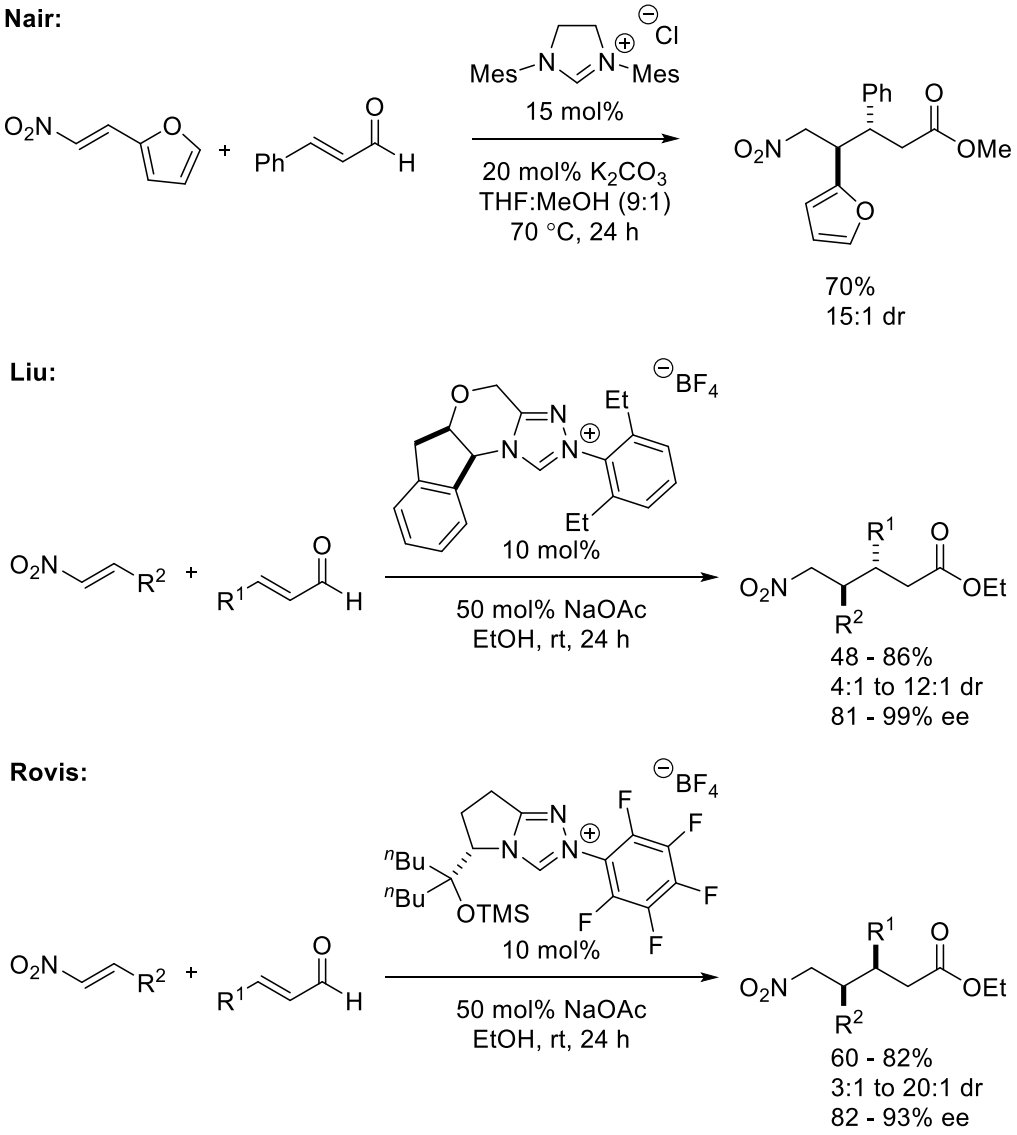

Scheme 1.5.2

The change in diastereoselectivity was proposed to result from an inversion in the Breslow intermediate geometry, which would allow for the reaction to occur on the same enantiotopic face of the enal, despite the pseudo-enantiomeric catalysts used in this methodology. It has also been proposed that Liu's reaction proceeds via an open transition state (**29**) which leads to the formation of the *anti*-diastereomer. In Rovis' case, the reaction is proposed to proceed through a closed transition state (**30**) which gives the *syn* product (Scheme 1.5.3). The mechanism and stereochemical outcome were later studied computationally and a transition state barrier of 15.3 kcal/mol was calculated for the *syn* product.[67] A possible reason for the high *syn* diastereoselectivity of the reaction results from lowering steric interaction on the enal and nitroalkene substituents in the C-C bond-forming step, as well as hydrogen bonding between the enol oxygen of the Breslow intermediate and the nitro group. Combined, these interactions lower the transition state energy enough to favor *syn* addition.

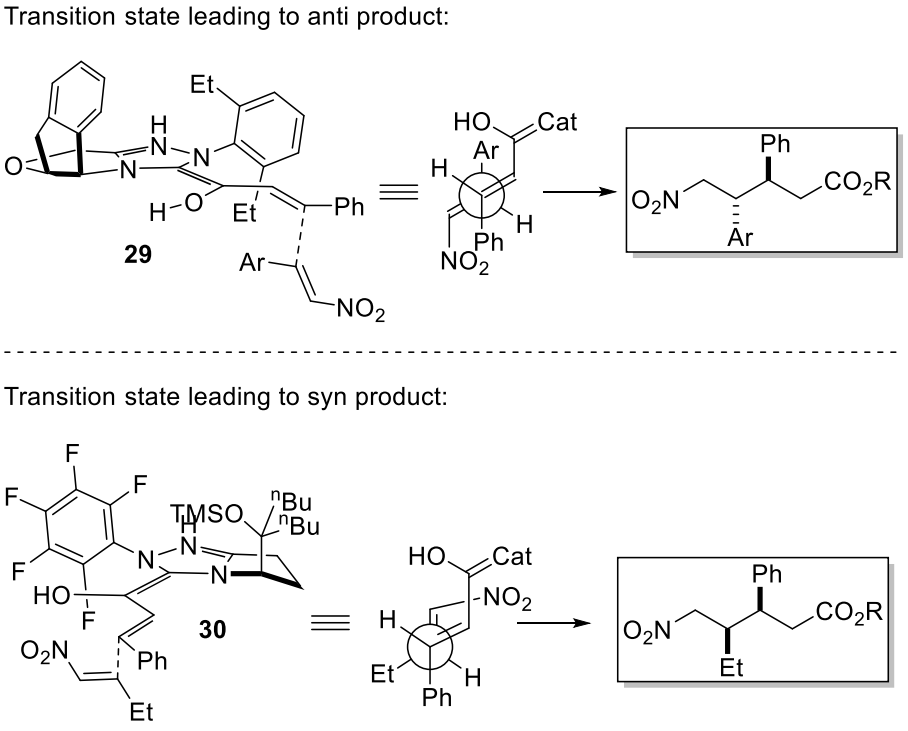

Scheme 1.5.3

1.6 Conclusion

Despite a resurgence of interest in NHCs as organocatalysts after the landmark papers of Bertrand[1] and Arduengo[2] that elucidated the structure of these stable carbenes, it was not until the 2000's that broad interest was generated. During this time, many new reactivity pathways were discovered and consequently, more efficient catalysts. Importantly, triazolium-derived NHCs were quickly identified as modular, easily modifiable catalysts that could impart high selectivity across a spectrum of reactivity.

References

[1] Igau, A.; Grutzmacher, H.; Baceiredo, A.; Bertrand, G. *J. Am. Chem. Soc.* **1988**, *110*, 6463.
[2] Arduengo, A. J.; Harlow, R. L.; Kline, M. *J. Am. Chem. Soc.* **1991**, *113*, 361.
[3] Enders, D.; Niemeier, O.; Henseler, A. *Chemical Reviews* **2007**, *107*, 5606.
[4] Flanigan, D. M.; Romanov-Michailidis, F.; White, N. A.; Rovis, T. *Chem. Rev.* **2015**, *115*, 9307.
[5] (a) Fliedel, C.; Braunstein, P. *Journal of Organomet. Chem.* **2014**, *751*, 286. (b) Bellemin-Laponnaz, S.; Dagorne, S. *Chem. Rev.* **2014**, *114*, 8747. (c) Izquierdo, F.; Manzini, S.; Nolan, S. P. *Chem. Commun.* **2014**, *50*, 14926. (d) Hopkinson, M. N.; Richter, C.; Schedler, M.; Glorius, F. *Nature* **2014**, *510*, 485. (e) Nelson, D. J.; Nolan, S. P. *Chem. Soc. Rev.* **2013**, *42*, 6723. (f) Samojłowicz, C.; Bieniek, M.; Grela, K. *Chem. Rev.* **2009**, *109*, 3708. (g) Herrmann, W. A. *Angew. Chem., Int. Ed.* **2002**, *41*, 1290.
[6] (a) Matsuoka, S.-i. *Polym. J.* **2015**, *47*, 713. (b) Naumann, S.; Dove, A. P. *Polym. Chem,* **2015**, *6*, 3185. (c) Naumann, S.; Buchmeiser, M. R. *Catal. Sci. Tech.* **2014**, *4*, 2466. (d) Fevre, M.; Pinaud, J.; Gnanou, Y.; Vignolle, J.; Taton, D. *Chem. Soc. Rev.* **2013**, *42*, 2142. (e) Mercs, L.; Albrecht, M. *Chem. Soc. Rev.* **2010**, *39*, 1903. (f) Bielawski, C. W.; Benitez, D.; Grubbs, R. H. *Science* **2002**, *297*, 2041.
[7] Wöhler, F.; Liebig, J. *Annalen der Pharmacie* **1832**, *3*, 249.
[8] Lapworth, A. *J. Chem. Soc.* **1903**, *83*, 995.
[9] Ukai, T.; Tanaka, R.; Dokawa, T. *J. Pharm. Soc. Jpn* **1943**, *63*, 296.
[10] Breslow, R. *J. Am. Chem. Soc.* **1958**, *80*, 3719.
[11] White, M. J.; Leeper, F. J. *J. Org. Chem.* **2001**, *66*, 5124.
[12] (a) Stetter, H.; Kuhlmann, H. *Angew. Chem., Int. Ed.* **1974**, *13*, 539. (b) Stetter, H.; Schreckenberg, M. *Angew. Chem., Int. Ed.* **1973**, *12*, 81.
[13] (a) Jordan, F.; Kudzin, Z. H.; Rios, C. B. *J. Am. Chem. Soc.* **1987**, *109*, 4415. (b) Hollóczki, O.; Kelemen, Z.; Nyulászi, L. *J. Org. Chem.* **2012**, *77*, 6014. (c) He, Y.; Xue, Y. *J. Phys. Chem. A* **2011**, *115*, 1408. (d) Dudding, T.; Houk, K. N. *Proc. Nat. Acad. Sci.* **2004**, *101*, 5770. (e) Collett, C. J.; Massey, R. S.; Maguire, O. R.; Batsanov, A. S.; O'Donoghue, A. C.; Smith, A. D. *Chem. Sci.* **2013**, *4*, 1514. (f) Mahatthananchai, J.; Bode, J. W. *Chem. Sci.* **2012**, *3*, 192. (g) Maji, B.; Mayr, H. *Angew. Chem., Int. Ed.* **2012**, *51*, 10408.
[14] Berkessel, A.; Elfert, S.; Yatham, V. R.; Neudörfl, J.-M.; Schlörer, N. E.; Teles, J. H. *Angew. Chem., Int. Ed.* **2012**, *51*, 12370.
[15] Sheehan, J. C.; Hunneman, D. H. *J. Am. Chem. Soc.* **1966**, *88*, 3666.
[16] (a) Sheehan, J. C.; Hara, T. *J. Org. Chem.* **1974**, *39*, 1196. (b) Tagaki, W.; Tamura, Y.; Yano, Y. *Bull. Chem. Soc. Jpn.* **1980**, *53*, 478. (c) L. Knight, R.; J. Leeper, F. *J. Chem. Soc., Perkin Trans. 1* **1998**, 1891.
[17] (a) Knight, R. L.; Leeper, F. J. *Tetrahedron Lett.* **1997**, *38*, 3611. (b) Gerhard, A. U.; Leeper, F. J. *Tetrahedron Lett.* **1997**, *38*, 3615. (c) Dvorak, C. A.; Rawal, V. H. *Tetrahedron Lett.* **1998**, *39*, 2925.
[18] Enders, D.; Breuer, K.; Raabe, G.; Runsink, J.; Teles, J. H.; Melder, J.-P.; Ebel, K.; Brode, S. *Angew. Chem., Int. Ed.* **1995**, *34*, 1021.
[19] Enders, D.; Kallfass, U. *Angew. Chem., Int. Ed.* **2002**, *41*, 1743.
[20] Baragwanath, L.; Rose, C. A.; Zeitler, K.; Connon, S. J. *J. Org. Chem.* **2009**, *74*, 9214.

[21] Cookson, R. C.; Lane, R. M. *J. Chem. Soc., Chem. Comm.* **1976**, 804.
[22] Stetter, H.; Dämbkes, G. *Synthesis* **1977**, 403.
[23] Tarr, J. C.; Johnson, J. S. *Org. Lett.* **2009**, *11*, 3870.
[24] Langdon, S. M.; Wilde, M. M. D.; Thai, K.; Gravel, M. *J. Am. Chem. Soc.* **2014**, *136*, 7539.
[25] Enders, D.; Henseler, A. *Adv. Syn. Catal.* **2009**, *351*, 1749.
[26] Rose, C. A.; Gundala, S.; Fagan, C.-L.; Franz, J. F.; Connon, S. J.; Zeitler, K. *Chem. Sci.* **2012**, *3*, 735.
[27] Thai, K.; Langdon, S. M.; Bilodeau, F.; Gravel, M. *Org. Lett.* **2013**, *15*, 2214.
[28] Murry, J. A.; Frantz, D. E.; Soheili, A.; Tillyer, R.; Grabowski, E. J. J.; Reider, P. J. *J. Am. Chem. Soc.* **2001**, *123*, 9696.
[29] Mennen, S. M.; Gipson, J. D.; Kim, Y. R.; Miller, S. J. *J. Am. Chem. Soc.* **2005**, *127*, 1654.
[30] DiRocco, D. A.; Rovis, T. *Angew. Chem., Int. Ed.* **2012**, *51*, 5904.
[31] (a) Enders, D.; Henseler, A.; Lowins, S. *Synthesis* **2009**, *2009*, 4125. (b) Sun, L.-H.; Liang, Z.-Q.; Jia, W.-Q.; Ye, S. *Angew. Chem., Int. Ed.* **2013**, *52*, 5803.
[32] Stetter, H.; Kuhlmann, H., The Catalyzed NucleophilicAddition of Aldehydes to Electrophilic Double Bonds. In *Organic Reactions*, John Wiley & Sons, Inc.: 2004; Vol. 40, pp 407.
[33] Enders, D.; Breuer, K.; Runsink, J.; Teles, J. H. *Helvetica Chimica Acta* **1996**, *79*, 1899.
[34] Kerr, M. S.; Read de Alaniz, J.; Rovis, T. *J. Am. Chem. Soc.* **2002**, *124*, 10298.
[35] (a) Read de Alaniz, J. R.; Rovis, T. *Synlett* **2009**, 1189. (b) Moore, J. L.; Kerr, M. S.; Rovis, T. *Tetrahedron* **2006**, *62*, 11477. (c) Read de Alaniz, J.; Rovis, T. *J. Am. Chem. Soc.* **2005**, *127*, 6284. (d) Reynolds, N. T.; Rovis, T. *Tetrahedron* **2005**, *61*, 6368. (e) Kerr, M. S.; Rovis, T. *J. Am. Chem. Soc.* **2004**, *126*, 8876. (f) Rovis, T.; Kerr, M. S. *Synlett* **2003**, 1934.
[36] (a) Pesch, J.; Harms, K.; Bach, T. *Eur. J. Org. Chem.* **2004**, *2004*, 2025. (b) Matsumoto, Y.; Tomioka, K. *Tetrahedron Lett.* **2006**, *47*, 5843. (c) Jia, M.-Q.; Li, Y.; Rong, Z.-Q.; You, S.-L. *Org. Biomol. Chem.* **2011**, *9*, 2072. (d) Rong, Z.-Q.; Li, Y.; Yang, G.-Q.; You, S.-L. *Synlett* **2011**, 1033. (e) Soeta, T.; Tabatake, Y.; Ukaji, Y. *Tetrahedron* **2012**, *68*, 10188. (f) Jia, M.-Q.; You, S.-L. *Chem. Commun.* **2012**, *48*, 6363. (g) Jia, M.-Q.; Liu, C.; You, S.-L. *J. Org. Chem.* **2012**, *77*, 10996. (h) Jia, M.-Q.; You, S.-L. *Synlett* **2013**, *24*, 1201. (i) Rafiński, Z.; Kozakiewicz, A.; Rafińska, K. *ACS Catalysis* **2014**, *4*, 1404.
[37] Moore, J. L.; Silvestri, A. P.; de Alaniz, J. R.; DiRocco, D. A.; Rovis, T. *Org. Lett.* **2011**, *13*, 1742.
[38] Domingo, L. R.; Zaragozá, R. J.; Saéz, J. A.; Arnó, M. *Molecules* **2012**, *17*, 1335.
[39] Hawkes, K. J.; Yates, B. F. *Eur. J. Org. Chem.* **2008**, 5563.
[40] Tiebes, J. Untersuchung Zur Katalytischen, Enantioselektiven C-C-Verknuepfung mit N-Chiral-Substituierten Thiazoliumsalzen. Diploma Thesis, RWTH Aachen, Aachen, Germany, 1990.
[41] Liu, Q.; Perreault, S.; Rovis, T. *J. Am. Chem. Soc.* **2008**, *130*, 14066.
[42] Liu, Q.; Rovis, T. *Org. Lett.* **2009**, *11*, 2856.
[43] Enders, D.; Han, J.; Henseler, A. *Chem. Commun.* **2008**, 3989.
[44] Enders, D.; Han, J. *Synthesis* **2008**, *2008*, 3864.
[45] DiRocco, D. A.; Oberg, K. M.; Dalton, D. M.; Rovis, T. *J. Am. Chem. Soc.* **2009**, *131*, 10872.
[46] Um, J. M.; DiRocco, D. A.; Noey, E. L.; Rovis, T.; Houk, K. N. *J. Am. Chem. Soc.* **2011**, *133*, 11249.
[47] Sánchez-Larios, E.; Thai, K.; Bilodeau, F.; Gravel, M. *Org. Lett.* **2011**, *13*, 4942.
[48] DiRocco, D. A.; Rovis, T. *J. Am. Chem. Soc.* **2011**, *133*, 10402.

[49] Fang, X.; Chen, X.; Lv, H.; Chi, Y. R. *Angew. Chem., Int. Ed.* **2011**, *50*, 11782.
[50] Jousseaume, T.; Wurz, N. E.; Glorius, F. *Angew. Chem., Int. Ed.* **2011**, *50*, 1410.
[51] Wurz, N. E.; Daniliuc, C. G.; Glorius, F. *Chem. Euro. J.* **2012**, *18*, 16297.
[52] Sohn, S. S.; Rosen, E. L.; Bode, J. W. *J. Am. Chem. Soc.* **2004**, *126*, 14370.
[53] Burstein, C.; Glorius, F. *Angew. Chem., Int. Ed.* **2004**, *43*, 6205.
[54] He, M.; Bode, J. W. *Org. Lett.* **2005**, *7*, 3131.
[55] (a) Burstein, C.; Tschan, S.; Xie, X.; Glorius, F. *Synthesis* **2006**, *2006*, 2418. (b) Nair, V.; Vellalath, S.; Poonoth, M.; Suresh, E.; Viji, S. *Synthesis* **2007**, *2007*, 3195. (c) Li, Y.; Zhao, Z.-A.; He, H.; You, S.-L. *Adv. Syn. Catal.* **2008**, *350*, 1885.
[56] Dugal-Tessier, J.; O'Bryan, E. A.; Schroeder, T. B. H.; Cohen, D. T.; Scheidt, K. A. *Angew. Chem., Int. Ed.* **2012**, *51*, 4963.
[57] (a) Cohen, D. T.; Scheidt, K. A. *Chem. Sci.* **2012**, *3*, 53. (b) Jang, K. P.; Hutson, G. E.; Johnston, R. C.; McCusker, E. O.; Cheong, P. H. Y.; Scheidt, K. A. *J. Am. Chem. Soc.* **2014**, *136*, 76.
[58] Rommel, M.; Fukuzumi, T.; Bode, J. W. *J. Am. Chem. Soc.* **2008**, *130*, 17266.
[59] Raup, D. E. A.; Cardinal-David, B.; Holte, D.; Scheidt, K. A. *Nat Chem* **2010**, *2*, 766.
[60] Zhao, X.; DiRocco, D. A.; Rovis, T. *J. Am. Chem. Soc.* **2011**, *133*, 12466.
[61] Phillips, E. M.; Reynolds, T. E.; Scheidt, K. A. *J. Am. Chem. Soc.* **2008**, *130*, 2416.
[62] Chan, A.; Scheidt, K. A. *Org. Lett.* **2005**, *7*, 905.
[63] Sohn, S. S.; Bode, J. W. *Org. Lett.* **2005**, *7*, 3873.
[64] (a) Walia, J. *Chem. and Ind.* **1972**, 933. (b) Vishwakarma, L. *Ind. J. Chem. Sect. B.* **1976**, *14B*, 692. (c) Vishwakarma, L. *Ind. J. Chem. Sect. B.* **1976**, *14B*, 696.
[65] Maji, B.; Ji, L.; Wang, S.; Vedachalam, S.; Ganguly, R.; Liu, X.-W. *Angew. Chem., Int. Ed.* **2012**, *51*, 8276.
[66] White, N. A.; DiRocco, D. A.; Rovis, T. *J. Am. Chem. Soc.* **2013**, *135*, 8504.
[67] Zhang, Q.; Yu, H.-Z.; Fu, Y. *Organic Chemistry Frontiers* **2014**, *1*, 614.

Chapter 2. Nucleophilic Dearomatization of Pyridiniums

2.1 Introduction

Aside from being a privileged structure in drug discovery, 1,4-dihydropyridines are also useful intermediates en route to other classes of important drug scaffolds. This important class of pharmaceuticals is used to treat an assortment of illnesses and have demonstrated antimicrobial, anticancer, antihypertensive, and anticonvulsant activity.[1] In addition to the interest in these scaffolds as important drug molecules, dihydropyridines allow for easy synthetic entry into other substituted 6-membered heterocycles, such as pyridines and piperidines, and have the potential to streamline pharmaceutical syntheses.[2]

Despite the importance of the 1,4-dihydropyridine scaffold, direct and mild methods for their synthesis remain scarce. Condensation reactions, as in the Hantzsch ester synthesis, have historically been used to generate 1,4-dihydropyridines.[3] Asymmetric condensation reactions have also been reported.[4] Another strategy for the synthesis of dihydropyridines is the nucleophilic dearomatization of activated pyridines.[5] Many of the syntheses are racemic and often require strong nucleophiles (e.g. Grignards reagents) in stoichiometric amounts. To overcome this, chiral *N*-substituents on the pyridinium have been used to impart stereoselectivity for the diastereoselective synthesis of 2,3-dihydropyridines.[6] This strategy can also be used to generate 1,4-dihydropyridines when the pyridine has a chiral auxiliary at the 3-position.[7] More recently, transition metal-catalyzed reactions have been applied to the asymmetric synthesis of dihydropyridines. Several nucleophiles have been coupled to pyridiniums including cyanide,[8] alkynal cuprates,[9] dialkyl zincs,[10] and aryl boronic acids.[11] This strategy was also employed to cyclize tethered iridium-π-allyl species that were generated *in situ* from allyl carbonates.[12]

Although much less common, organocatalytic methods have also been developed. Anion-binding catalysis has been demonstrated to be an effective enantioselective strategy for the nucleophilic dearomatization of *N*-Troc pyridiniums (Scheme 2.1.1).[13] This method favored addition of silylenol ethers at the 2-position of the pyridinium, except in the cases where the pyridinium is substituted at the 3-position, in which case, addition at the 4-position is favored. High enantioselectivity could be achieved with certain substrates (up to 98% ee). However, enantioselectivity drops off dramatically when addition at the 4-position is observed (62-80% ee). This method could be extended to coupling indoles with pyridiniums, which gives the 1,4-dihydropyridine with high regioselectivity (10:1 rr) and enantioselectivity.[14]

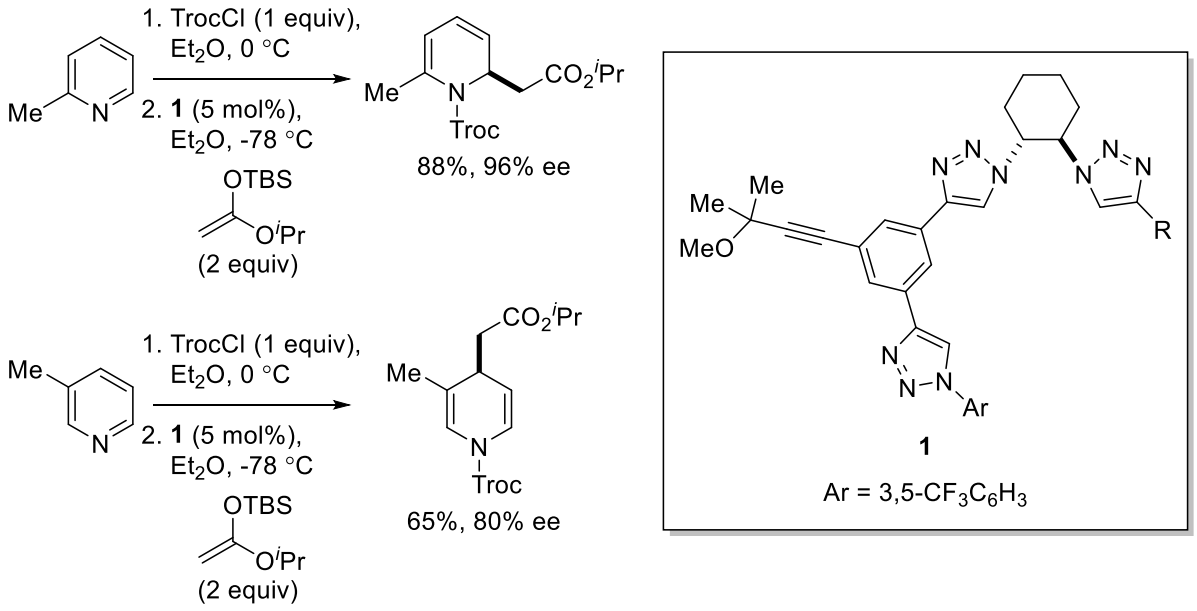

Scheme 2.1.1

More recently, enamine catalysis with chiral secondary amines was demonstrated as an efficient way to couple aldehydes at the alpha position to highly activated pyridiniums (Scheme 2.1.2).[15] Due to racemization, a one-pot procedure was developed where the product is immediately treated with Wittig salts to convert the product aldehyde to a γ-substituted enoates, before isolation. Following the two-step protocol, the dihydropyridine products were isolated in

good yields, with high levels of diastereo- and enantioselectivity (up to 19:1 and 99% ee) when 3-nitropyridiniums are used as the substrate. However, 3-cyanopyridiniums generate the product with lower levels of diastereoselectivity (3:1 dr).

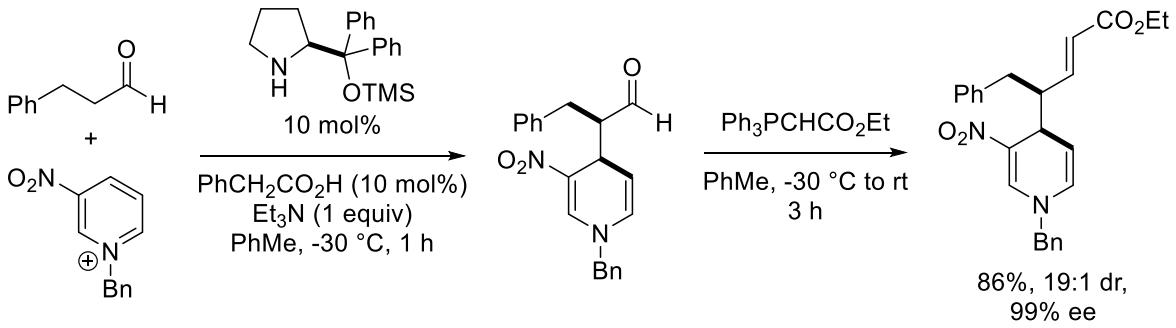

Scheme 2.1.2

2.2 Development of the Racemic Reaction

We envisioned that the NHC-catalyzed homoenolate reactivity of enals could be utilized for the nucleophilic dearomatization of pyridinium ions to generate 1,4-dihydropoyridines stereoselectively. This method could potentially couple pyridiniums with enals to provide the 1,4-dihydropyridine product directly from simple starting materials and provide a rare example of direct 1,4-dihydropyridine synthesis by catalytic nucleophilic dearomatization of pyridiniums.

We began our studies of this reaction by first investigating the racemic reaction. Initially, the reaction was conducted with achiral trichloro-triazolium **31** using cinnamaldehyde as the enal to give the product in 30% yield and 1:1 dr (Scheme 2.2.1). When catalysts bearing more electron rich aryl rings were used, no desired reactivity was observed and the pyridinium decomposed under the reaction conditions. Interestingly, more catalysts bearing more electron-deficient aryl groupgs (*e.g.* pentafluorophenyl catalyst **32**) delivers the product in much higher yields (79%). Despite the promising trends with reactivity when different achiral catalysts were tested, the diastereoselectivity of the process was still very low (1:1 dr across all catalysts).

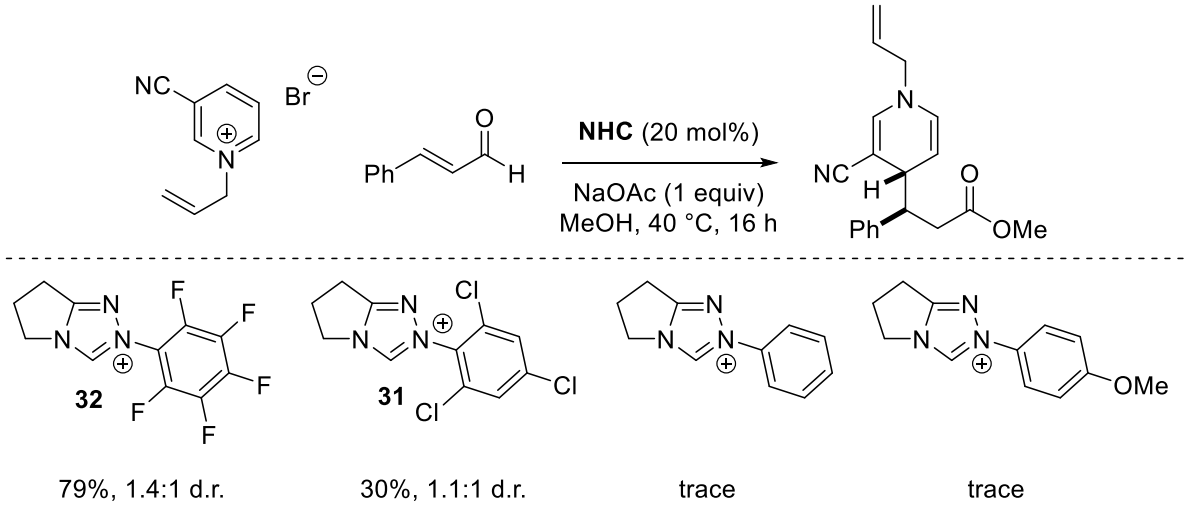

Scheme 2.2.1

After screening several different catalysts in the reaction, we then tried different classes of aldehydes to investigate the influence of the aldehyde on the selectivity of the reaction (Scheme 2.2.2). As shown above, cinnamaldehyde gives the expected product in high yield, but with no control of the diastereoselectivity. Ethyl butanoate and the conjugated 2,4-hexadienal also give the product with low levels of diastereocontrol. We also tried an aliphatic enal, Interestingly, the aliphatic aldehyde gives the product in 40% yield and 3:1 dr and was the only aldehyde class found to have any inherent diastereoselectivity in this reaction.

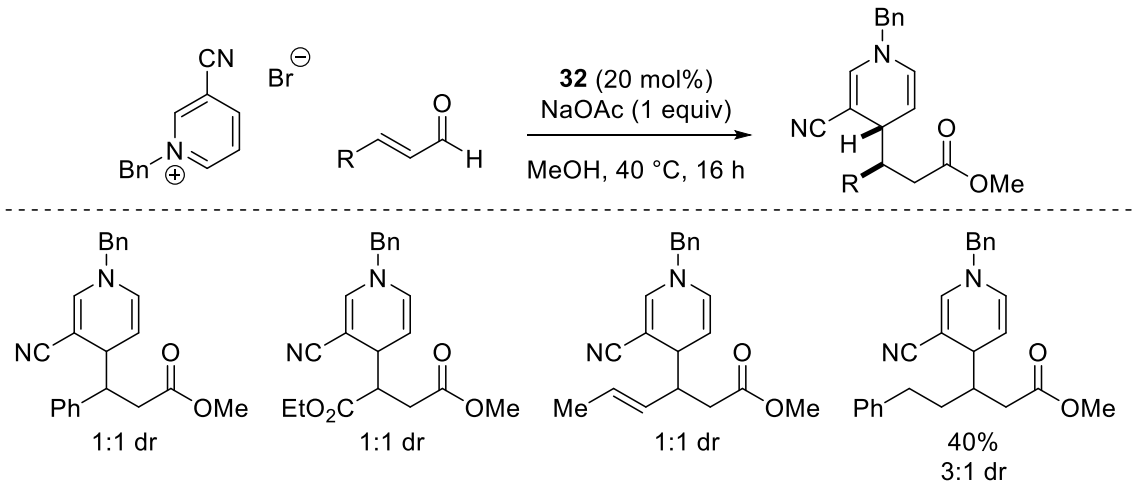

Scheme 2.2.2

2.3 Development of the Asymmetric Reaction

After discovering the high reactivity of the achiral catalyst **19**, combined with modest levels of diastereoselectivity with aliphatic enals in the reaction, we began investigating the asymmetric variant (Scheme 2.3.1). We first tested several different chiral catalysts in the reaction and found that high levels of enantioselectivity could be achieved, but the reaction required high catalyst loadings (20 mol%) and yields remained low (14-58%).

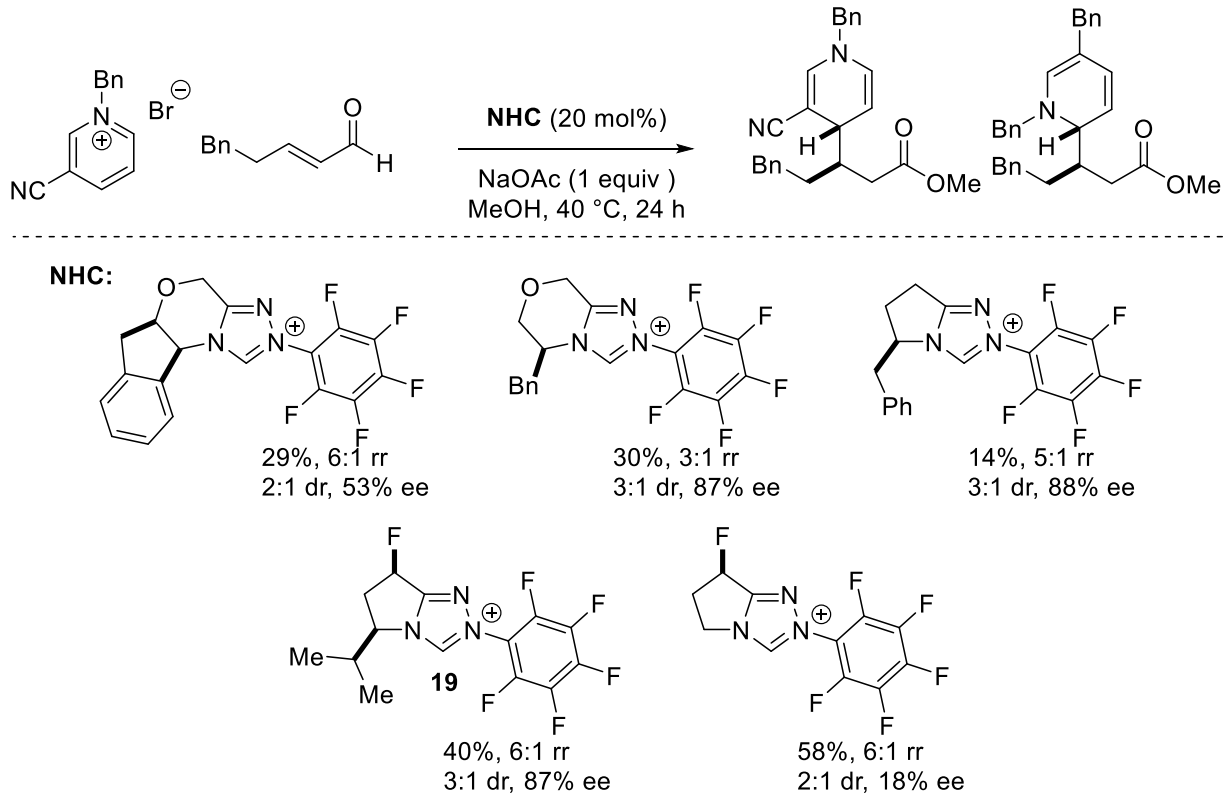

Scheme 2.3.1

After the initial catalyst screen, different conditions were investigated. However, when the reaction is run in solvents other than methanol there is a complete loss of the desired reactivity. We believed that the reason for the low reactivity in methanol could be a result of NHC addition to the pyridinium that leads to catalyst deactivation by oxidation of the NHC-pyridinium adduct. Thus, the three most selective catalysts were chosen and the reactions were conducted under an

inert atmosphere. Exclusion of oxygen from the reaction leads to a marked increase in the yields (as high as 87% yield) without affecting the selectivity. Encouraged by these results, the reaction was attempted with 10 mol% catalyst loading, which gave the product in 27% yield (Scheme 2.3.2).

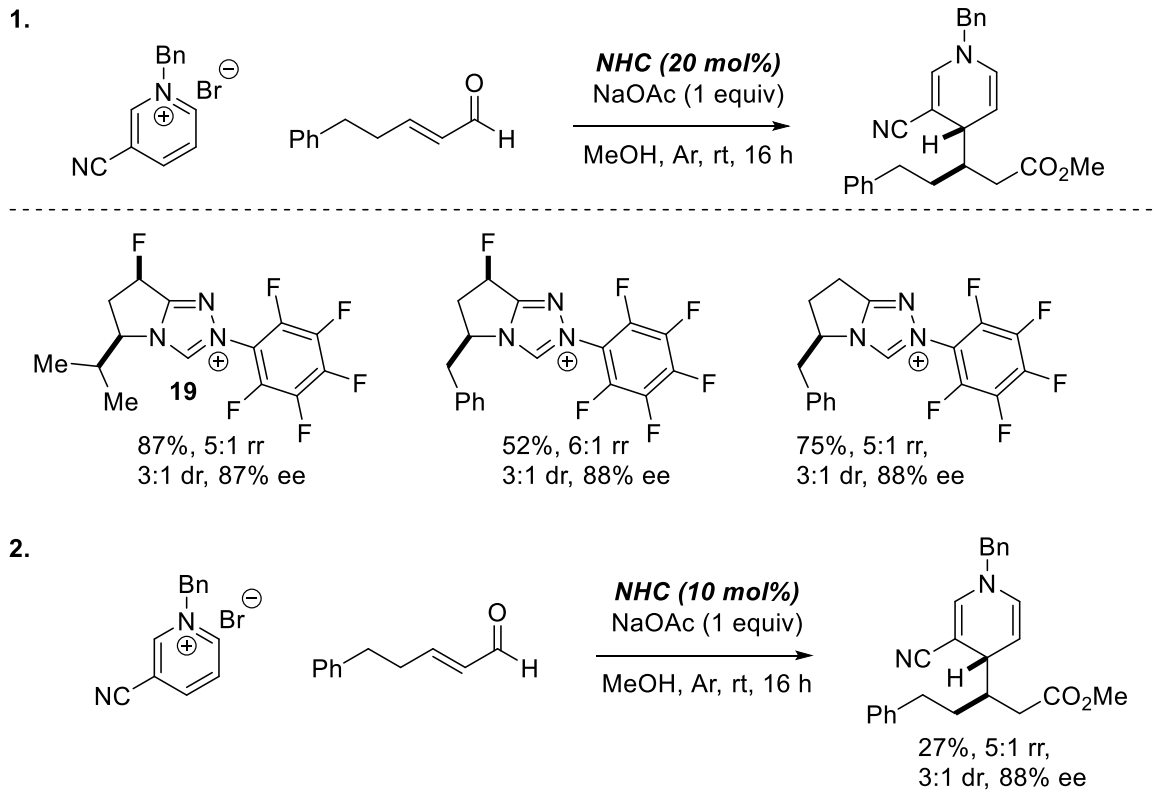

Scheme 2.3.2

Due to the lack of oxygen in these conditions, the NHC-pyridinium adduct is likely not being oxidized, but there could be an equilibrium that exists between the NHC-pyridinium adduct and the free carbene. We believed that while the unproductive addition of the NHC to the pyridinium was not leading to catalyst death when oxygen is removed from the reaction, it could possibly sequester the free carbene and arrest catalysis. Further studies were performed to test the validity of this hypothesis and are discussed in the mechanism and stereochemistry section of this chapter. To overcome the low yields when using 10 mol % catalyst loading, we then screened a

variety of additives in the reaction. Lewis acids added in 20 mol % were added to the reaction, but deliver none of the desired product, instead leading to oxidation of the enal to the enoate or no reaction (results not shown). Interestingly, addition of 20 mol % acetic acid to the reaction mixture restores the reactivity (with 10 mol % NHC) and gives the desire product in 61% yield (Scheme 2.3.3).

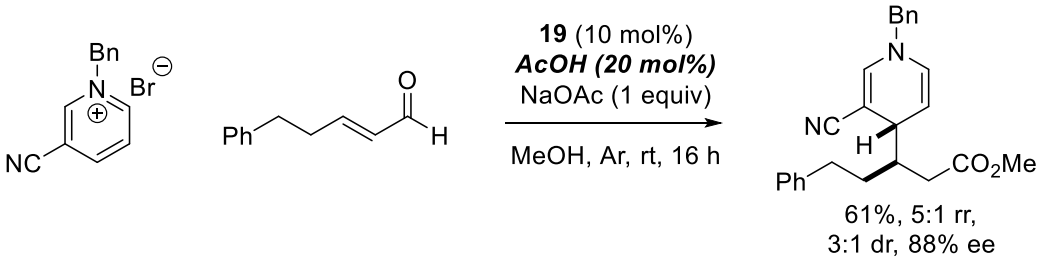

Scheme 2.3.3

2.4 Scope of the Reaction

A variety of *N*-substituents on the pyridinium were tolerated including alky groups. 4-bromenzyl and 4-methoxybenzyl groups were also tolerated without affecting the selectivity or yield of the reaction. In general, variations on the *N*-alkyl substituent had little effect on the reactivity or selectivity, although the regioselectivity decreases somewhat as the N-group becomes smaller. However, carbamates on the nitrogen of the pyridinium led to a complete loss of reactivity. An electron withdrawing group at the 3-position of the pyridinium was required to achieve good reactivity with the cyano group providing the dihydropyridine with the highest enantioselectivity. Acetyl pyridinium **34** was tolerated, but the enantioselectivity was much lower. Interestingly, the diastereoselectivity and regioselectivity are slightly higher compared to the cyano group. Other electron-withdrawing groups, including the *N*-benzyl pyridiniums derived from methyl nicotinate, nicotinic acid and nicotinamide, were also tried in the reaction, but gave only trace amounts of

product. 2-methyl-5-cyano pyridinium was tolerated in the reaction, eliminating the regioselectivity issues (Scheme 2.4.1).

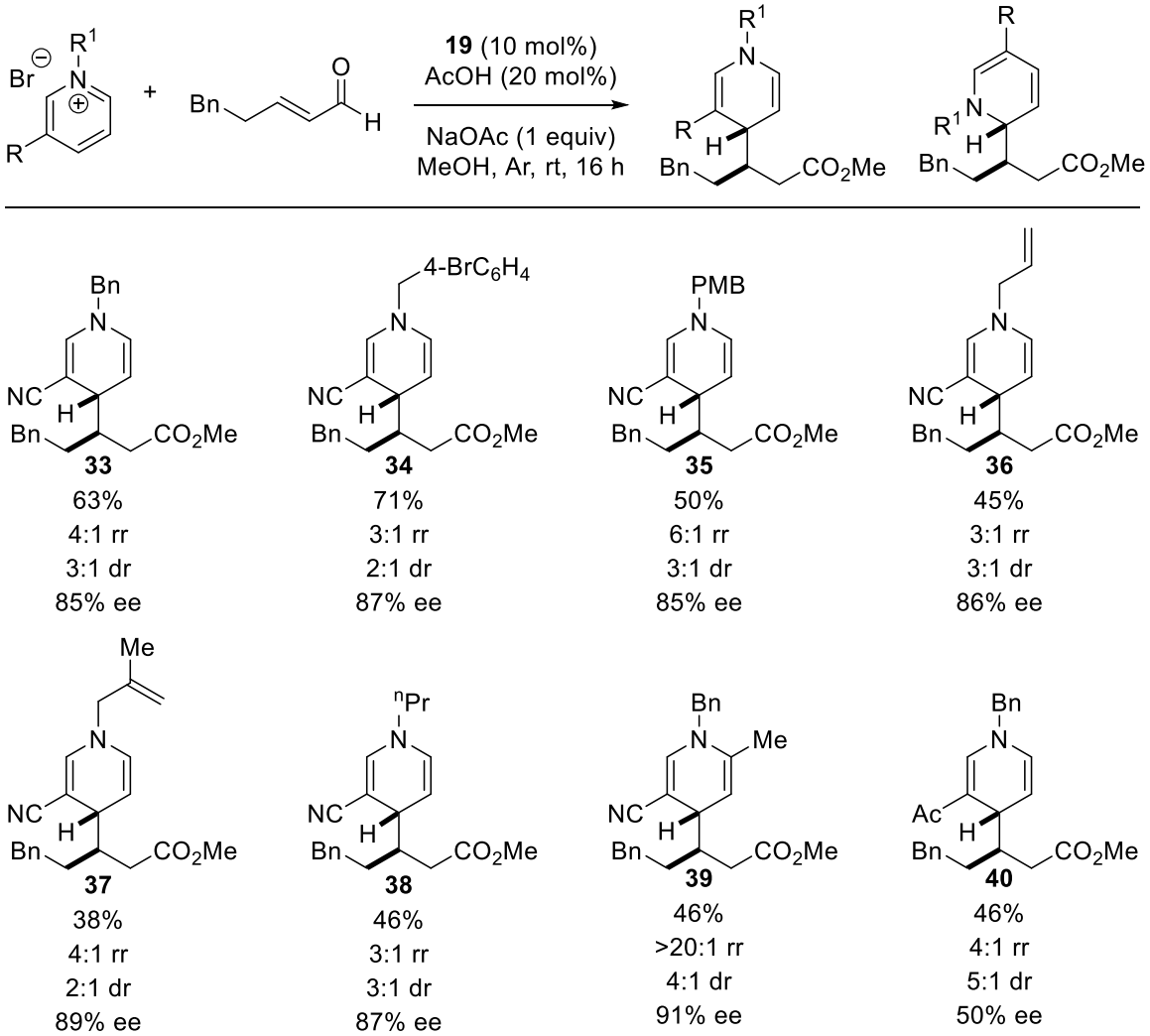

Scheme 2.4.1

A wide variety of aliphatic and aryl enals were also tolerated in the reaction with varying levels of reactivity and selectivity. Straight-chain aliphatic enals proceed with the highest enantioselectivity. Branched aliphatic aldehydes participate in the reaction, but deliver the product in only marginal ee (c.f. products **45** & **46**). Interestingly, the only exception to the depressed enantioselectivity with branched, aliphatic substrates was a cyclopropyl substituted enal that gives the corresponding dihydropyridine product **44** in comparable enantioselectivity to the straight

chain substrates. Cinnamaldehyde, as well as other conjugated enals, are competent coupling partners and proceed with good yield, but with much lower levels of selectivity (Scheme 2.4.2).

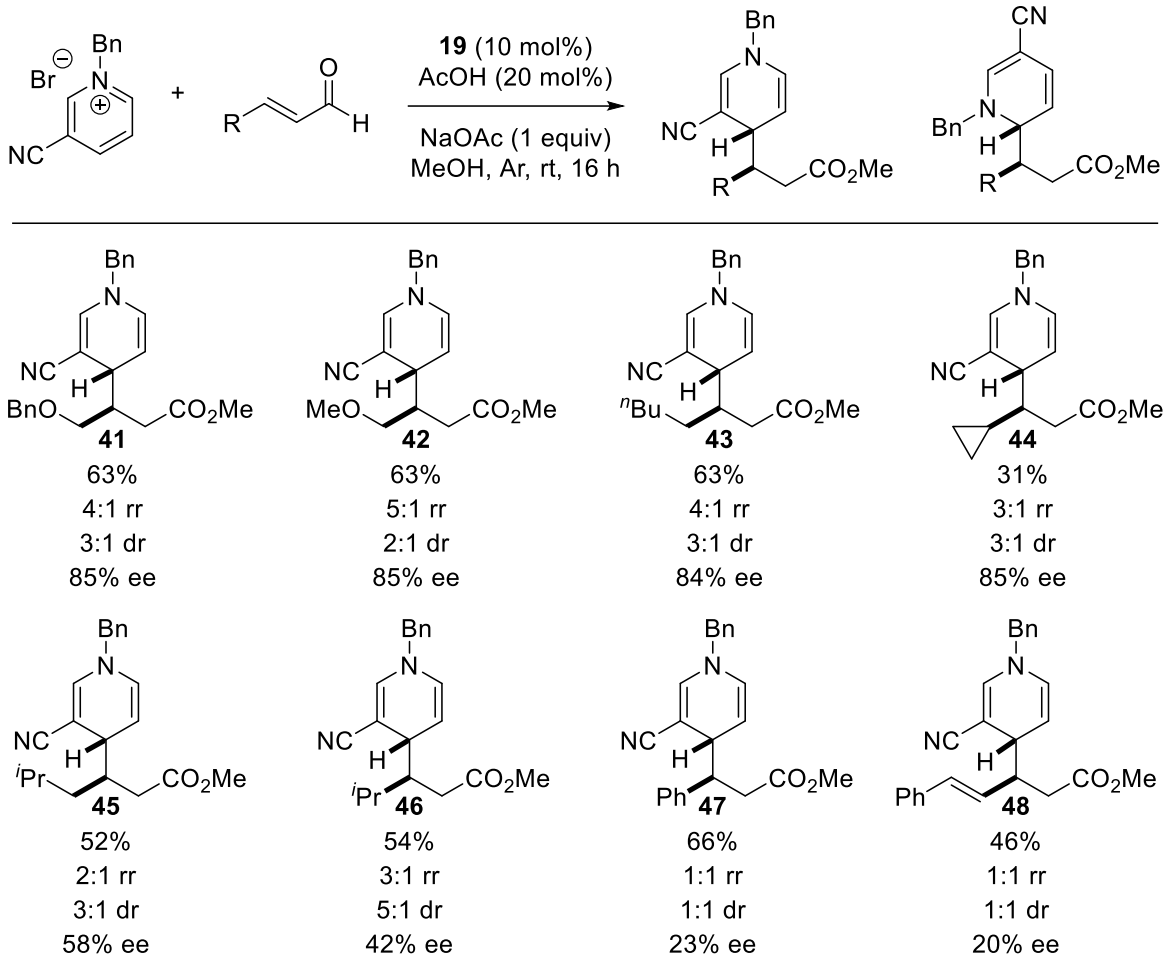

Scheme 2.4.2

A variety of other pyridiniums and heterocycles were tested in the reaction, but did not give the desired product, instead giving the saturated ester byproduct or no reaction (Scheme 2.4.3). The lack of reactivity observed when highly electron withdrawing groups are present (e.g. 3-nitropyridinium) likely results from an irreversible addition of the NHC to the pyridinium causing catalyst deactivation. In the other cases, the pyridinium is not electrophilic enough to undergo addition with the Breslow intermediate, and the free carbene is still active. This allows for the formation of the saturated ester product by protonation of the Breslow intermediate at the

β-position of the enal, followed by tautomerization of the resulting enol azolium. This can then be intercepted by methanol to deliver the ester byproduct.

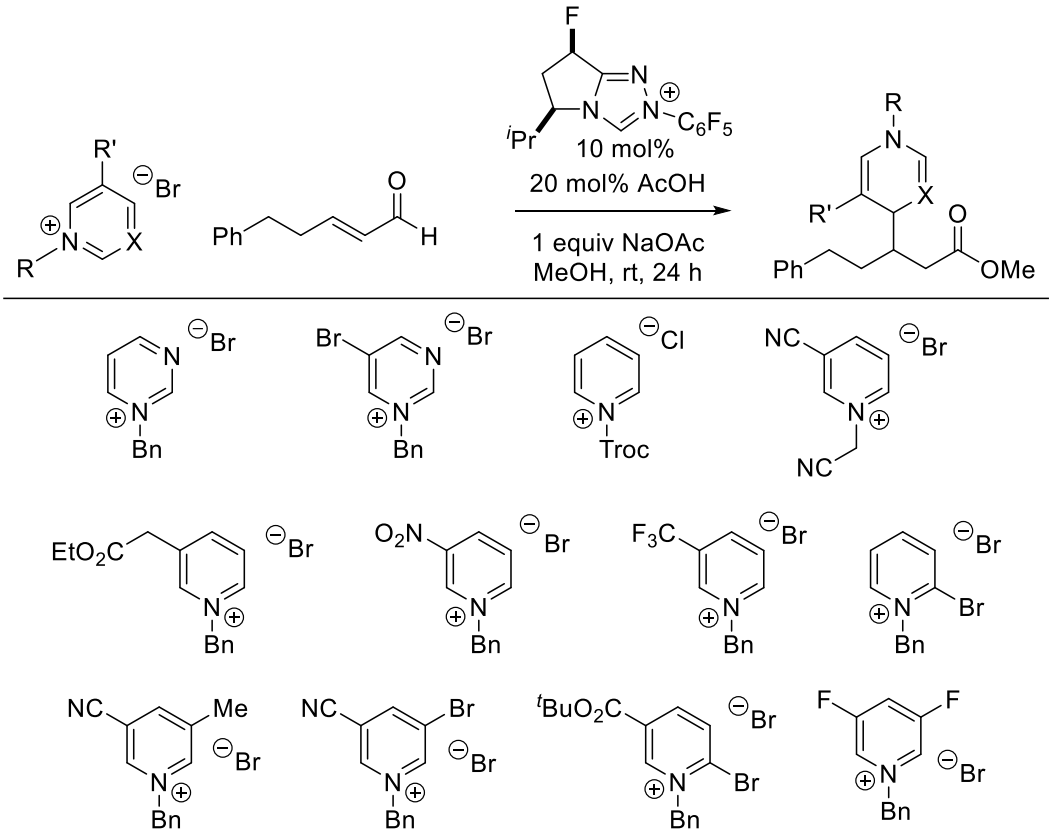

Scheme 2.4.3

2.5 Mechanism and Stereochemistry

Based on recent reports of single-electron coupling pathways,[16] we wondered whether this reaction could be proceeding via a one or two electron mechanism. Cyclic voltammetry was carried out to test this hypothesis. From these experiments, we determined that the pyridinium undergoes a quasi-reversible reduction at -0.77 V vs SCE. A related unsaturated aza-Breslow intermediate **49** has been previously isolated and characterized (Scheme 2.5.1). This species was found to have a reduction potential of E= -0.49 V vs SCE in acetonitrile. This suggests that it is unlikely the pyridinium ion is incapable of oxidizing the Breslow intermediate in the reaction. Further evidence of this comes from recent reports of single electron oxidations of the extended Breslow

intermediate, followed by functionalization of the beta position. In these reactions, electron-deficient nitroaryl compounds are believed to oxidize the Breslow intermediate to generate a radical cation, radical ion pair, which can recombine to give the observed beta hydroxylation products. The oxidants in these reactions have a reduction potential of E= -0.26 to -0.33 V vs SCE. Nitrobenzene has a reduction potential of E= -0.49 V vs SCE, which is right in line with the extended aza-Breslow intermediate, and delivers the product in trace amounts, suggesting that oxidants with a reduction potential below E= -0.49 will not be oxidizing enough to oxidize the extended Breslow intermediate.

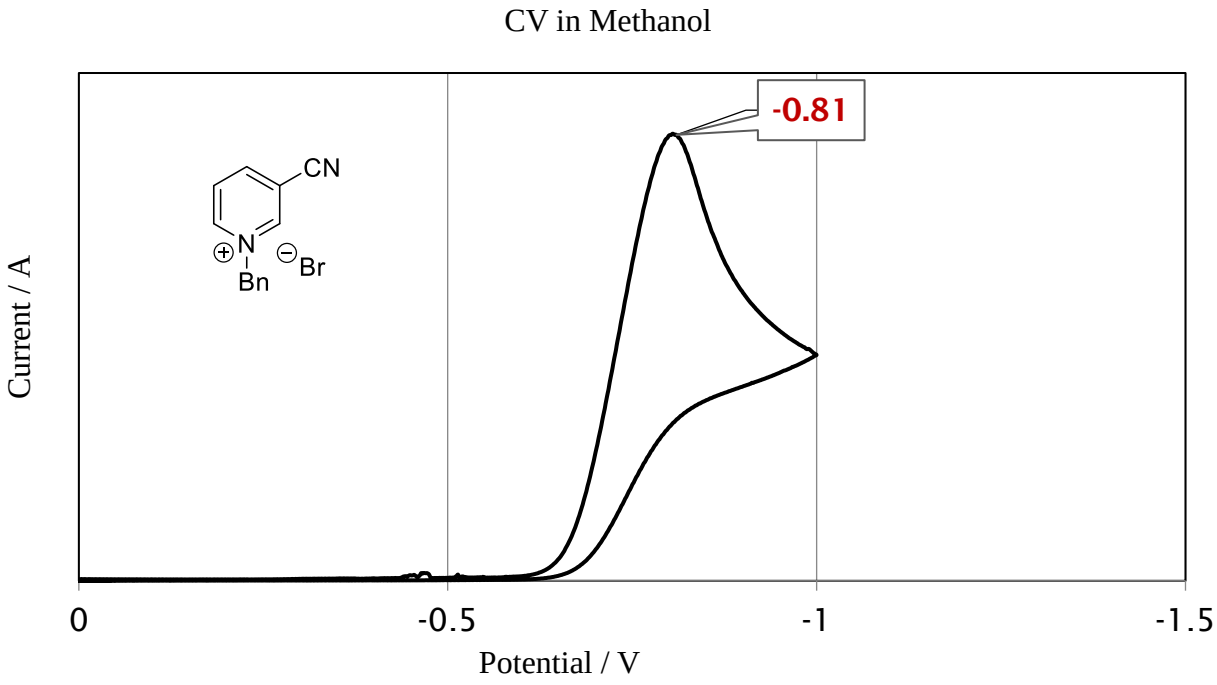

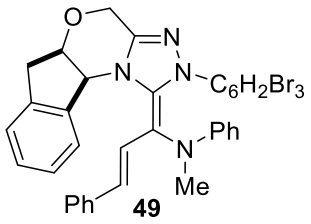

E^o_{red} = -0.49 V

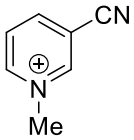

E^o_{red} = -0.76 V

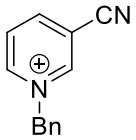

E^o_{red} = -0.77 V

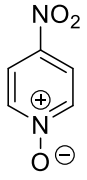

E^o_{red} = -0.33 V

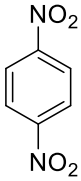

E^o_{red} = -0.26 V

Scheme 2.5.1

Because the reduction potential of the pyridinium is far outside the range of oxidants previously demonstrated to oxidize the Breslow intermediate, we believe the mechanism proceeds via a two-electron pathway as shown in scheme 2.5.2 where the extended Breslow intermediate is generated from the NHC and the enal, followed by addition of the beta carbon to the electron-deficient pyridinium.

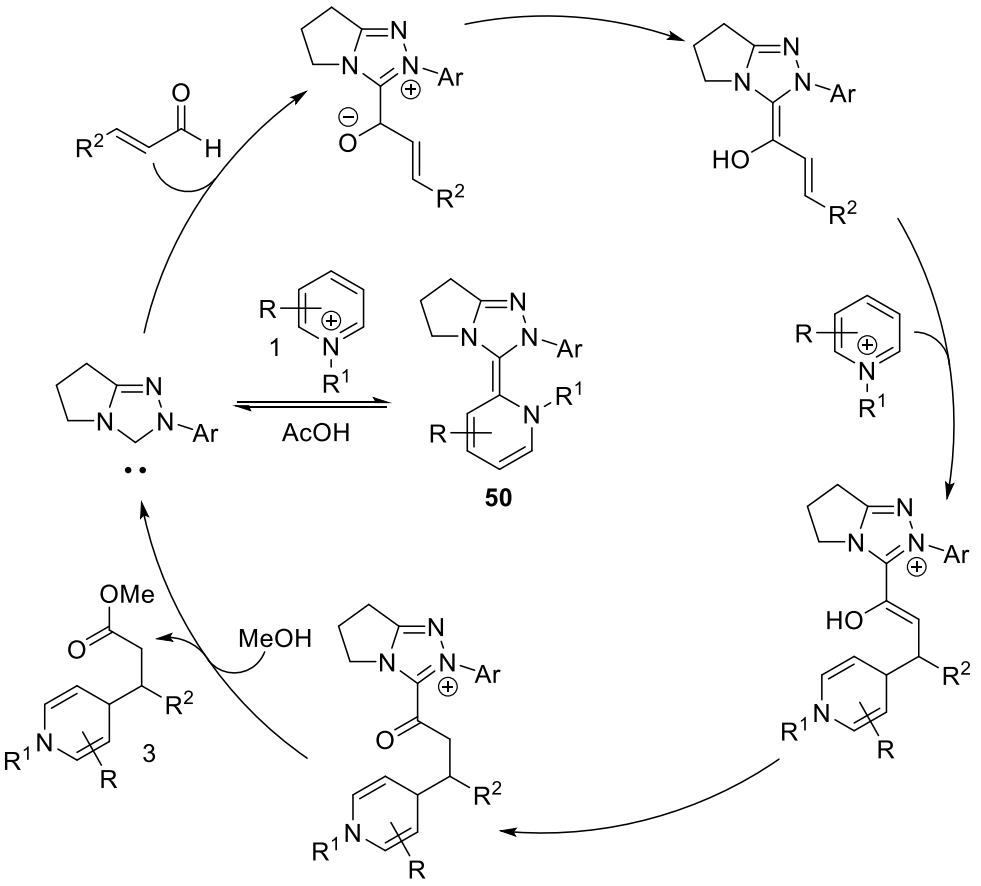

Scheme 2.5.2

During the optimization of the reaction, we found that the yield is drastically improved when oxygen is removed from the reaction. The absence of the saturated ester product, arising from trapping of the homoenolate equivalent with a proton, could suggest that the carbene adds reversibly to the pyridinium forming a 1,4-dihydropyridine which acts as a catalyst resting state. This adduct (**50**) could potentially be oxidized by oxygen leading to catalyst death and would

explain the low yields of the reaction when oxygen is present. This type of catalyst inhibition was previously noted by our group[17] while investigating cross aza-benzoin reactions between aldehydes and imines. In these cases, it is believed that the carbene can reversibly add to the imine and if oxidized by oxygen in the air, lead to catalyst death. In the case of *N*-Boc imines, the addition of acetic acid was found to restore catalytic activity to the reaction. Further studies on these aza-Breslow intermediates revealed that when treated with acid, they generate the free carbene and the corresponding imine.[18] In this case, with pyridiniums, the carbene can add to the pyridinium generating either a 1,4 or 1,2-dihydropyridine which can also be thought of as an aza-Breslow intermediate or a vinylogous aza-Breslow intermediate in the case of 1,4-addition. To test this hypothesis, an equimolar amount of achiral catalyst was mixed with the pyridinium at rt and stirred for 2 hours. After this time, ^{1}H NMR and mass spectrometry revealed the presence of the carbene-pyridinium adduct in roughly 30% conversion by ^{1}H NMR (Scheme 2.5.3).

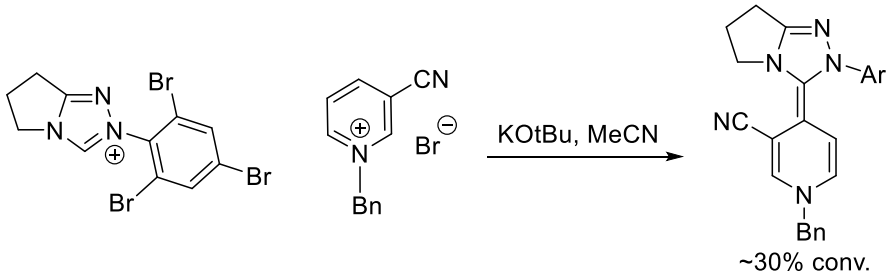

Scheme 2.5.3

Further evidence for the reversible addition of the NHC to the pyridinium was found when the reaction was conducted in MeOH-d_1 with 20 mol % acetic acid-d_1. After completion of the reaction, ^{1}H NMR revealed 66% deuterium incorporation at the 2-position of the dihydropyridine product. Deuterium was also incorporated at the 2-position of the pyridinium (75% D incorporation) and at the 6-position (39% D incorporation). This result suggests that the NHC adds to the pyridinium to generate aza-Breslow intermediate **50**, which can undergo protonation to give

the corresponding azolium. This can then be eliminated to regenerate the pyridinium and free carbene (Scheme 2.5.4).

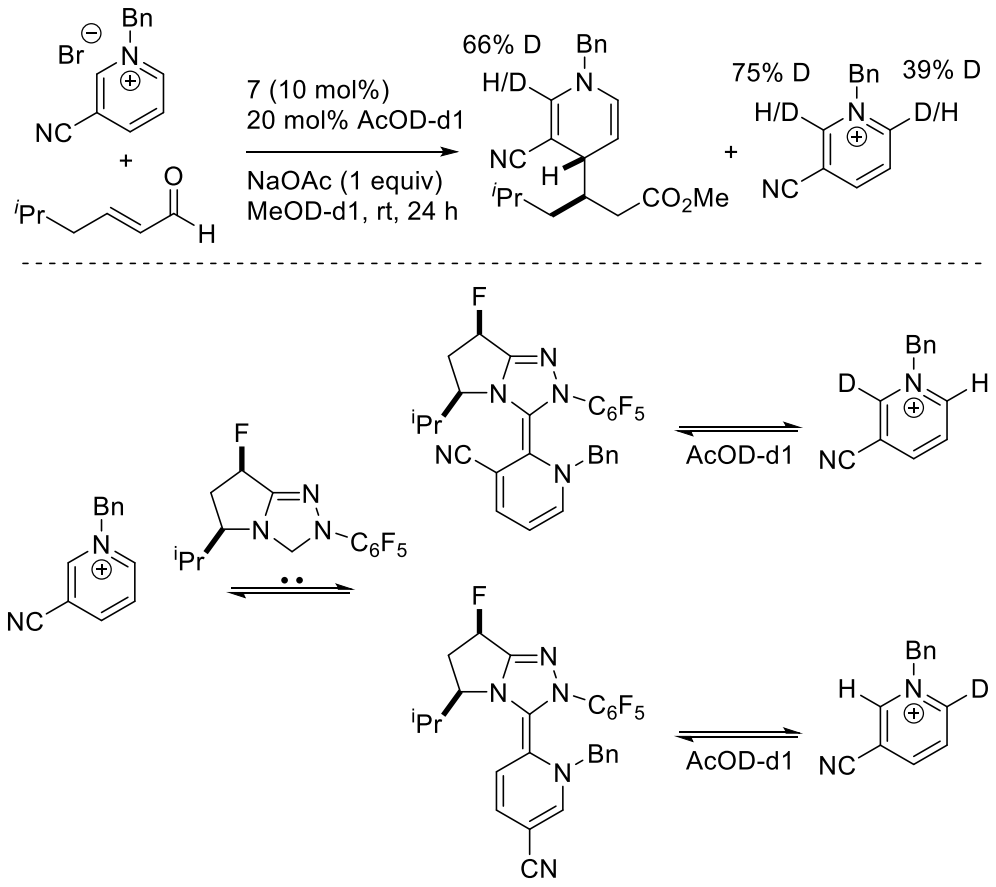

Scheme 2.5.4

Finally, the absolute stereochemistry of the product was confirmed to be the *R,S*-enantiomer by X-ray crystallography. From the crystal structure, it is apparent that the favored diastereomer is the *R-S* conformation. This stereochemical outcome matches a previous diastereoselective beta-functionalization reaction of enals to nitroalkenes that was carried out using the same catalyst (Scheme 2.5.5).[19] The mechanism and stereochemical outcome of the nitroalkene coupling was studied computationally and a transition state barrier of 15.3 kcal/mol was calculated for the *syn* product.[20] One possible reason for the high *syn* diastereoselectivity of the reaction results from lowering steric interaction on the enal and nitroalkene substituents in the C-C bond-

forming step. Due to the similarity of these two reactions, these interactions could also be operative in the coupling of enals and pyridiniums.

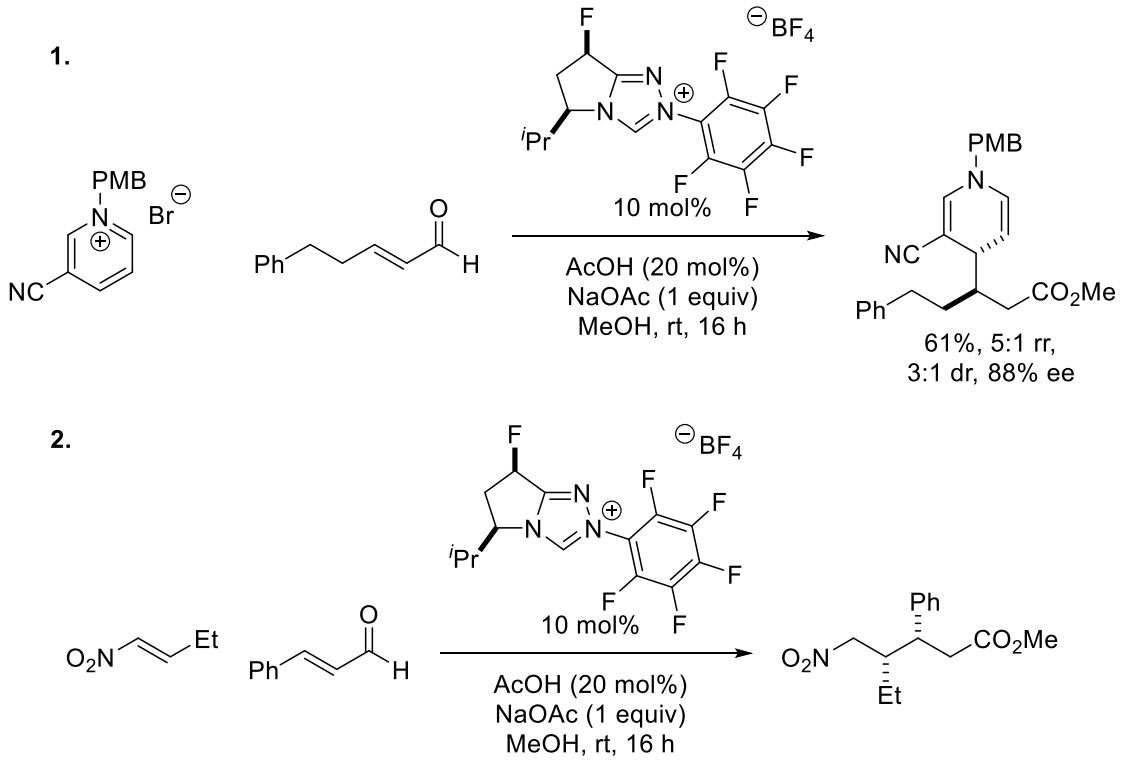

Scheme 2.5.5

2.6 Product Derivatization

The products of these reactions could be further elaborated to other interesting motifs relevant to drug discovery. The *N*-allyl substituted 1,4-dihydropyridine product can be deprotected using palladium (0) and barbituric acid. The deprotected 1,4-dihydropyridine is rapidly oxidized in air to generate the corresponding pyridine (Scheme 2.6.1).

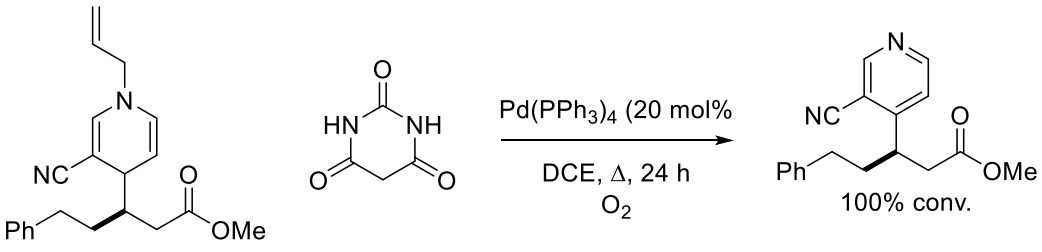

Scheme 2.6.1

Treatment of the 1,4-dihydropyridine with $Pd(OH)_2$ reduces the more electron rich alkene selectively and avoids over-reduction to the piperidine. The piperidine could be accessed by reduction with triethylsilane and TFA in DCM. This gives the expected piperidine in 70% yield and proceeds without eroding the previously generated stereocenters. This could be deprotected using CAN to furnish the piperidine in quantitative yields (Scheme 2.6.2).

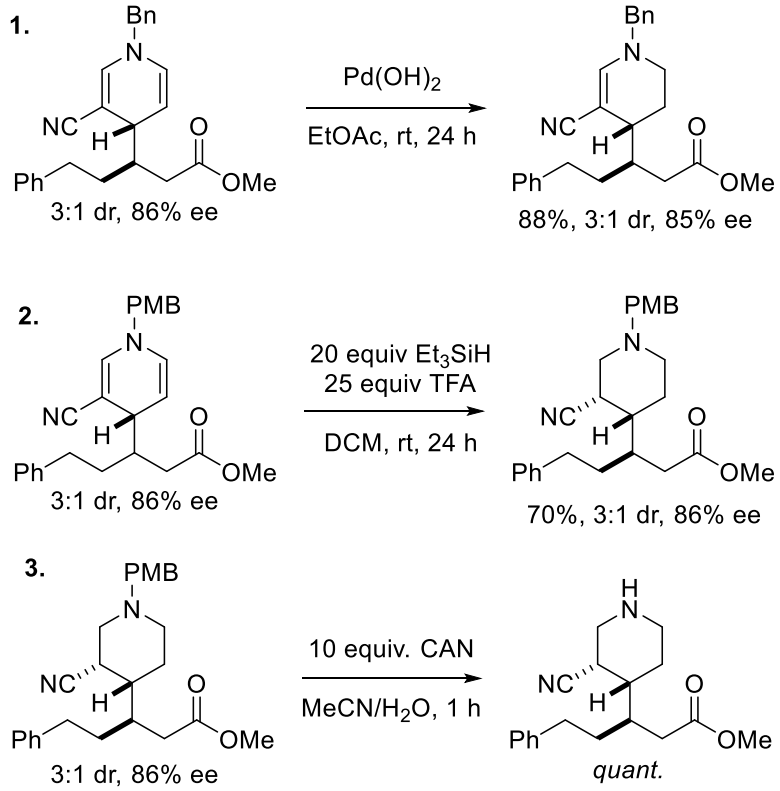

Scheme 2.6.2

2.7 Conclusion

In conclusion, an NHC-catalyzed method of the nucleophilic dearomatization of *N*-alkyl pyridines was developed. This method enables the rapid synthesis of alkyl 1,4-dihydropyridines and the products could be further elaborated to other important scaffolds. The reaction proceeds with high enantioselectivity and favors formation of the 1,4-dihydropyridine over the 1,2-dihydropyridine. The reaction tolerates a range of enals in the reaction; however, selectivity is

lower when conjugated or branched aliphatic enals are used. The pyridinium scope is broad and tolerates many different *N*-substituents along with different electron withdrawing groups at the 3-position, although a 3-cyano group was necessary for high enantioselectivity.

References

[1] (a) McDonald, T. F.; Pelzer, S.; Trautwein, W.; Pelzer, D. J. *Physiol. Rev.* **1994**, *74*, 365. (b) Goldmann, S.; Stoltefuss, J. *Angew. Chem., Int. Ed.* **1991**, *30*, 1559. (c) Gordeev, M. F.; Patel, D. V.; England, B. P.; Jonnalagadda, S.; Combs, J. D.; Gordon, E. M. *Bioorg. Med. Chem.* **1998**, *6*, 883. (d) Burgess, V. A.; Davies, S. G.; Skerlj, R. T. *Tetrahedron: Asymmetry* **1991**, *2*, 299. (e) Sinclair, A.; Stockman, R. A. *Nat. Prod. Reports* **2007**, *24*, 298.

[2] (a) Bosch, J.; Bennasar, M. L. *Synlett* **1995**, *1995*, 587. (b) Stout, D. M.; Meyers, A. I. *Chem. Rev.* **1982**, *82*, 223. (c) Buffat, M. G. P. *Tetrahedron* **2004**, *60*, 1701. (d) Dugger, R. W.; Ragan, J. A.; Ripin, D. H. B. *Org. Proc. Res. Dev.* **2005**, *9*, 253. (e) Hilton, M. C.; Dolewski, R. D.; McNally, A. *J. Am. Chem. Soc.* **2016**, *138*, 13806.

[3] (a) Pajuste, K.; Plotniece, A. *Chem. Heterocyclic Comp.* **2016**, *52*. (b) Yu, J.; Shi, F.; Gong, L. Z. *Acc. Chem. Res.* **2011**, *44*, 1156.

[4] Thu Pham, H.; Chataigner, I.; Renaud, J.-L. *Curr. Org. Chem.* **2012**, *16*, 1754.

[5] Bull, J. A.; Mousseau, J. J.; Pelletier, G.; Charette, A. B. *Chem. Rev.* **2012**, *112*, 2642.

[6] (a) Baraznenok, I. L.; Nenajdenko, V. G.; Balenkova, E. S. *Tetrahedron* **2000**, *56*, 3077. (b) Charette, A. B.; Grenon, M.; Lemire, A.; Pourashraf, M.; Martel, J. *J. Am. Chem. Soc.* **2001**, *123*, 11829. (c) Charette, A. B.; Mathieu, S.; Martel, J. *Org. Lett.* **2005**, *7*, 5401. (d) Charette, A. B.; Grenon, M. *Can. J. Chem.* **2001**, *79*, 1694.

[7] (a) Meyers, A. I. *J. Org. Chem.* **2005**, *70*, 6137. (b) Meyers, A. I.; Oppenlaender, T. *J. Chem. Soc., Chem. Commun.* **1986**, 920. (c) Mangeney, P.; Gosmini, R.; Raussou, S.; Commercon, M.; Alexakis, A. *J. Org. Chem.* **1994**, *59*, 1877.

[8] Ichikawa, E.; Suzuki, M.; Yabu, K.; Albert, M.; Kanai, M.; Shibasaki, M. *J. Am. Chem. Soc.* **2004**, *126*, 11808.

[9] Sun, Z.; Yu, S.; Ding, Z.; Ma, D. *J. Am. Chem. Soc.* **2007**, *129*, 9300.

[10] Fernández-Ibáñez, M. Á.; Maciá, B.; Pizzuti, M. G.; Minnaard, A. J.; Feringa, B. L. *Angew. Chem., Int. Ed.* **2009**, *48*, 9339.

[11] Christian, N.; Aly, S.; Belyk, K. *J. Am. Chem. Soc.* **2011**, *133*, 2878.

[12] Yang, Z.-P.; Wu, Q.-F.; You, S.-L. *Angew. Chem., Int. Ed.* **2014**, *53*, 6986.

[13] García Mancheño, O.; Asmus, S.; Zurro, M.; Fischer, T. *Angew. Chem., Int. Ed.* **2015**, *54*, 8823.

[14] Bertuzzi, G.; Sinisi, A.; Caruana, L.; Mazzanti, A.; Fochi, M.; Bernardi, L. *ACS Catalysis* **2016**, *6*, 6473.

[15] Bertuzzi, G.; Sinisi, A.; Pecorari, D.; Caruana, L.; Mazzanti, A.; Bernardi, L.; Fochi, M. *Org. Lett.* **2017**, *19*, 834.

[16] (a) White, N. A.; Rovis, T. *J. Am. Chem. Soc.* **2015**, *137*, 10112. (b) Zhang, Y.; Du, Y.; Huang, Z.; Xu, J.; Wu, X.; Wang, Y.; Wang, M.; Yang, S.; Webster, R. D.; Chi, Y. R. *J. Am. Chem. Soc.* **2015**, *137*, 2416. (c) White, N. A.; Rovis, T. *J. Am. Chem. Soc.* **2014**, *136*, 14674.

[17] DiRocco, D. A.; Rovis, T. *Angew. Chem., Int. Ed.* **2012**, *51*, 5904.

[18] DiRocco, D. A.; Oberg, K. M.; Rovis, T. *J. Am. Chem. Soc.* **2012**, *134*, 6143.

[19] White, N. A.; DiRocco, D. A.; Rovis, T. *J. Am. Chem. Soc.* **2013**, *135*, 8504.

[20] Zhang, Q.; Yu, H.-Z.; Fu, Y. *Organic Chemistry Frontiers* **2014**, *1*, 614.

Chapter 3. Investigation of N-Heterocyclic Carbene Reactivity

3.1 Asymmetric Intermolecular Stetter Reactions with α,β-unsaturated Ketones

Although there has been a significant amount of work on the asymmetric intermolecular coupling of aldehydes to Michael acceptors, these are generally limited to very activated substrates. The first advances in the asymmetric intermolecular Stetter reaction came in 2007. Enders[1] coupled aryl aldehydes with chalcones and Rovis demonstrated a highly enantioselective coupling of glyoxamides to alkylidene malonates.[2] Since these initial reports, the scope of Michael acceptors in the reaction has been expanded to include nitroalkenes,[3] chalcone derivatives,[4] ketoesters,[5] and enoates (Figure 3.1).[6] The scope of aldehyde coupling partners in the reaction is much more broad and a variety of aryl, heteroaryl, α,β-unsaturated, and aliphatic aldehydes have been successfully employed in the reaction.[6a]

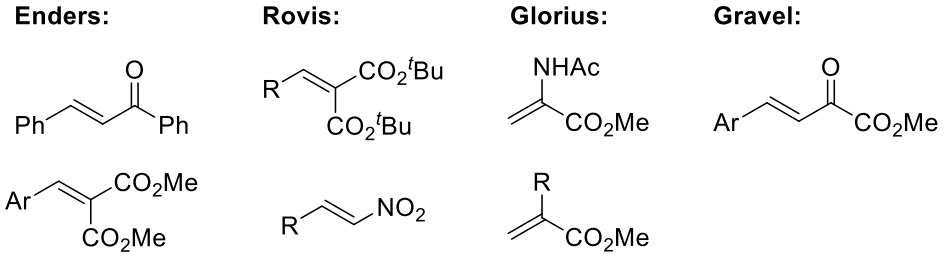

Figure 3.1 Scope of Michael acceptors in the asymmetric Stetter reaction.

Despite the progress expanding the scope of the asymmetric intermolecular Stetter reaction, the use of Michael acceptors lacking aromatic substitution or a second electron-withdrawing group remains an enormous challenge of this methodology, limiting its broad application in synthesis. The use of 1,1-disubstituted enoates has been demonstrated in the reaction and the success of this methodology relies on the use of carbene catalysts with highly donating *N*-aryl substituents to increase the reactivity of the catalyst. Additionally, the reactivity and selectivity

of the reaction depends on the absence of beta substituents on the Michael acceptor. This class of substrates (lacking beta substituents) have been previously demonstrated to be much more reactive in the cyanide and thiazolium-catalyzed reactions.[7] Thus, while these substrates greatly expanded the scope of Michael acceptors, there is still a need for catalysts that can reliably couple aldehydes to less activated Michael acceptors bearing a beta substituent. To date, there has been only one reported example of a simple beta substituted Michael acceptor delivering the Stetter product with appreciable levels of enantioselectivity (Scheme 3.1.1).

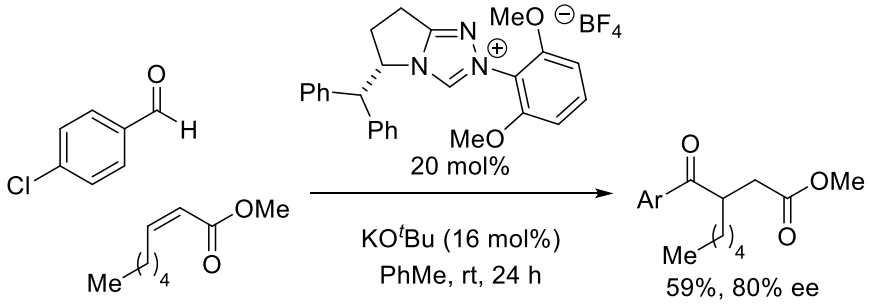

Scheme 3.1.1

Due to the lack of methods for the asymmetric intermolecular Stetter reaction with simple Michael acceptors, we became interested in using beta substituted Michael acceptors with simple enones or equivalents that lack secondary activating groups. The realization of this strategy would significantly expand the scope of this methodology and contribute to its utility in synthesis.

We began our investigation by screening a variety of achiral catalysts in the reaction with furfural and 4-phenylbutenone. (Scheme 3.1.2) Under these initial conditions, the reactivity of these catalysts was highly variable with the tri-halogenated aryl groups as the *N*-substituent providing (**51** and **52**) the product in the highest yield (58% and 73% yield, respectively). Interestingly, the mesityl-substituted catalyst gives the product in 20% yield, much higher than the other carbenes bearing electron-donating groups, and roughly equivalent to the tribromo-difluoro catalyst tested. These results suggest that the steric environment imparted by substituents ortho to

the triazolium impact the reactivity of the carbene. However, the electronics also impact reactivity comparing **51** and **52** which give the product in 58% and 21% yield, respectively, implying that very electron-withdrawing aryl groups on the catalyst inhibit reactivity.

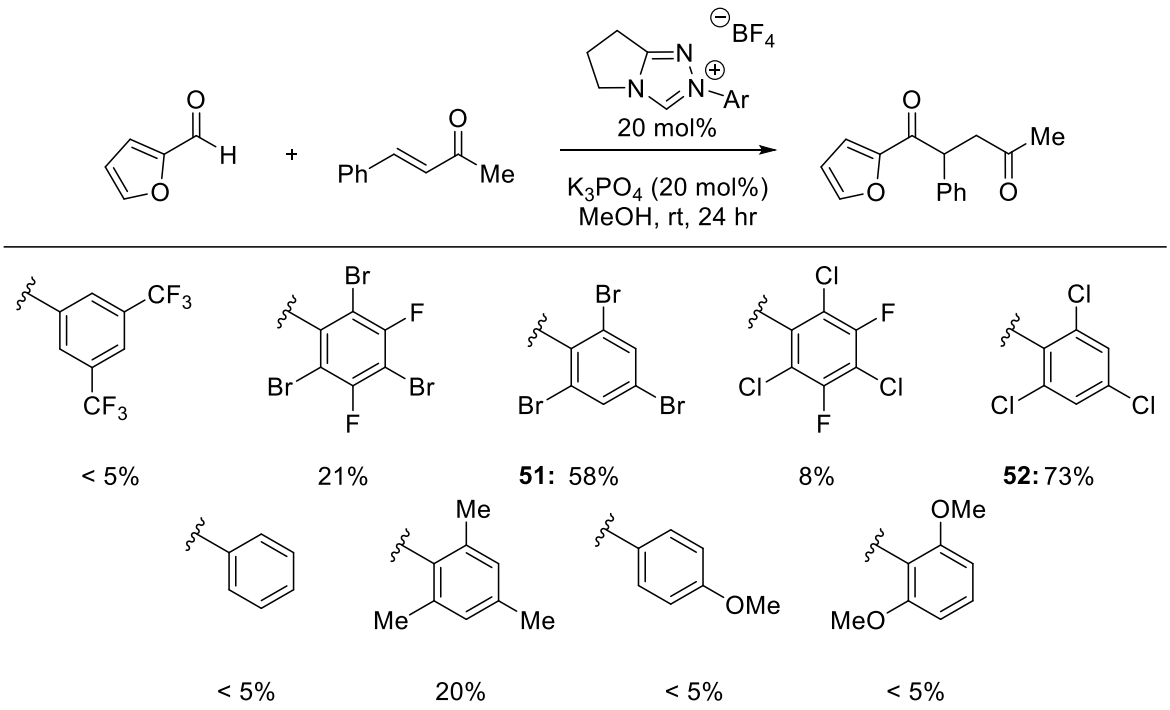

Scheme 3.1.2

Using catalyst **52**, we then screened a variety of aldehydes and enones in the reaction to probe the reactivity. Disappointingly, replacement of the beta phenyl substituent with an aliphatic group completely inhibits reactivity. The only reactivity that was observed in these reactions was with furfural, which selectively forms the benzoin product, but does not add to the Michael acceptor. No reactivity was observed with either enals or aliphatic aldehyde. A variety of bases and solvents were then screened with aliphatic aldehydes coupling to 4-phenylbutenone; however, no desired product was observed (Scheme 3.1.3).

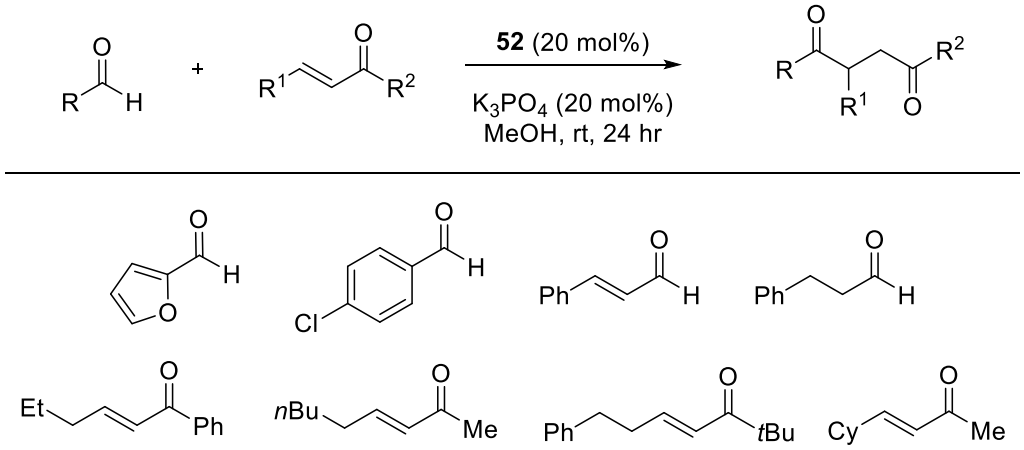

Scheme 3.1.3

With the trends of the racemic reaction in mind, we then turned our attention toward the asymmetric reaction. Due to the much higher reactivity of the trichlorophenyl catalyst in the racemic reaction, we chose to initially screen chiral catalysts bearing the same *N*-substituent. We first attempted the reaction using chiral catalyst **53**. Using this catalyst, the selectivity was improved from an initial 17% ee with furfural to 46% ee with 2-pyridine carboxaldehyde (Scheme 3.1.4).

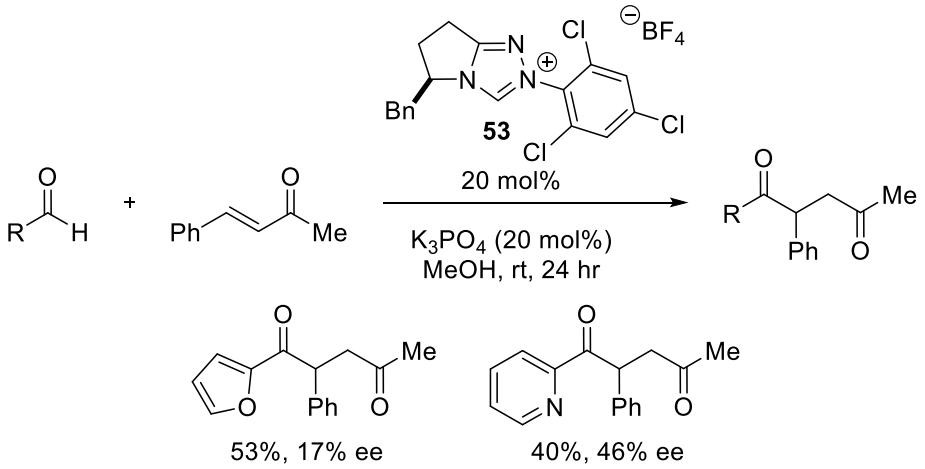

Scheme 3.1.4

Switching to a weaker base in the reaction proved deleterious to reactivity and selectivity. Sodium acetate gives the product in trace amounts, while Cs_2CO_3 gives 22% yield and 15% ee.

Fluorinated catalyst **19** delivers the product with much higher enantioselectivity (80% ee vs 46% ee) than the catalyst lacking a fluorine in the backbone an energy difference of ~0.8 kcal/mol at room temperature. A similar effect was noted in the asymmetric intermolecular Stetter reaction between aryl aldehydes and nitroalkenes where the highest selectivity was achieved using catalyst **19**, which gives the Stetter adduct in 80% ee and 15% yield (Scheme 3.1.5).[3c]

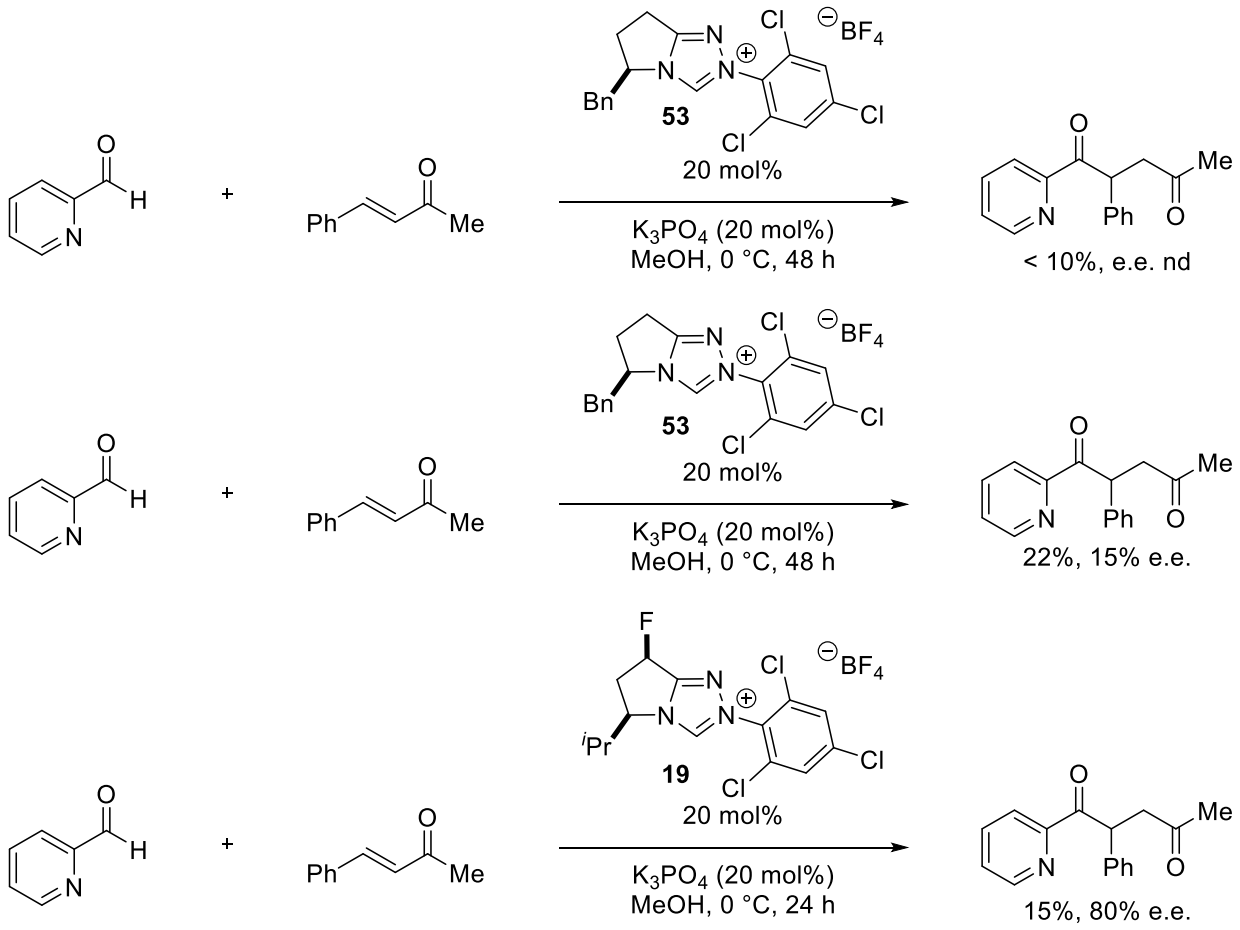

Scheme 3.1.5

In addition to the optimization of the beta aryl enone, we also investigated enones with aliphatic substituents. This substrate class participates in the reaction, but is much less reactive and enantioselectivity is reduced. Switching the solvent from methanol to DMSO increased the yield and selectivity (21%, <5% ee in methanol compared to 40%, 28% ee in DMSO) when aliphatic

enones are used (Scheme 3.1.6). Interestingly, increasing the steric bulk of the substituent alpha to the ketone slightly increases the enantioselectivity of the process, despite being four carbons away from the reactive center.

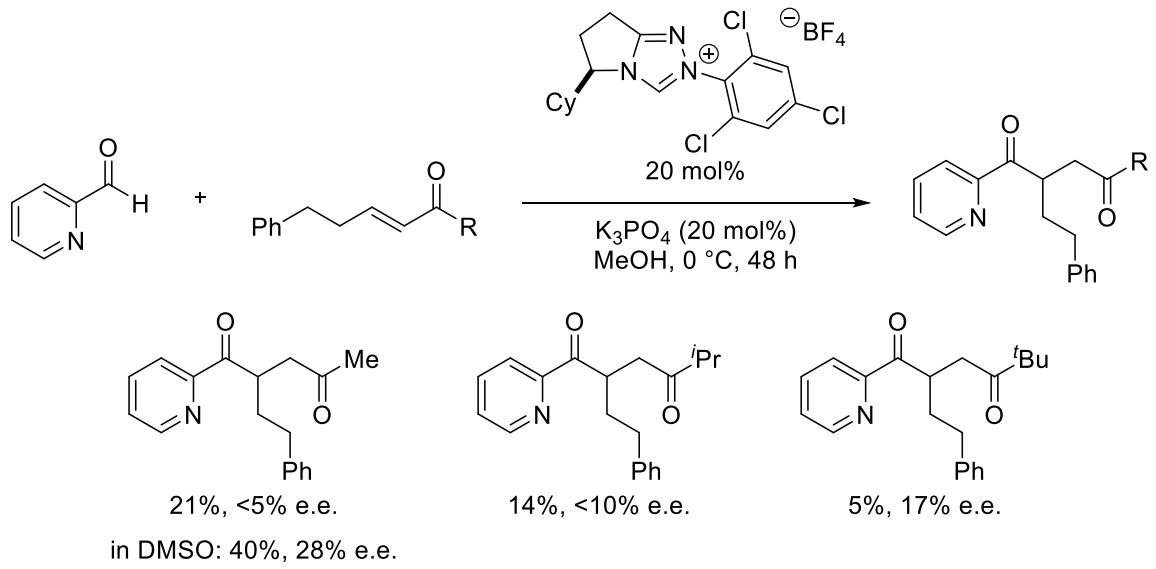

Scheme 3.1.6

Due to the consistently low enantioselectivity of the reaction, we wondered whether the product could be epimerizing under the reaction conditions. To probe this, we ran the reaction in methanol-d_4 and found that there is no deuterium incorporation at the newly generated stereocenter. Another experiment to probe possible epimerization is to add some of the diketone product to the reaction. Diketone **54** was added to the reaction mixture and no erosion of the ee was detected (Scheme 3.1.7). The lack of deuterium incorporation at the methine and complete deuteration at the methyl ketone suggests that deprotonation at this position is heavily favored over the methine stereocenter. Taken together, these experiments demonstrate that the low enantioselectivity of the reaction is not likely a result of epimerization of the methine stereocenter. Rather, we conclude that the stereocenter is controlled by the orientation of the addition of the Breslow intermediate to the Michael acceptor.

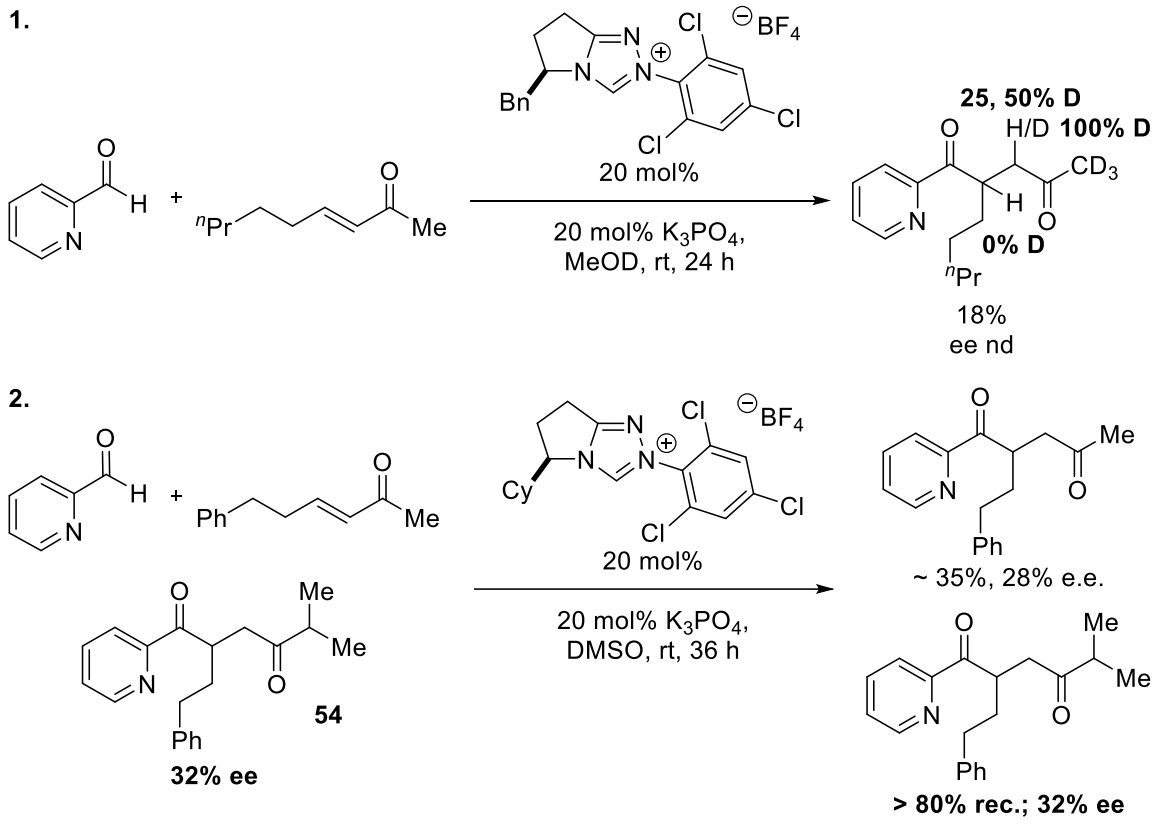

Scheme 3.1.7

In conclusion, the Stetter reactions with simple enones was investigated, and a variety of factors were found to influence the selectivity and reactivity of these substrates. The *N*-substituent appears to have a profound effect on the reactivity of the process with 2,4,6-trichlorophenyl substituted catalysts delivering product in higher yields. Epimerization studies demonstrated that the products are not racemizing under the reaction conditions despite the low enantioselectivity of the process across a range of catalysts and substrates. As noted in the case of nitroalkenes, backbone fluorination of the catalyst drastically boosts selectivity, but in the case of enones did not increase the yield. Despite the challenges associated with the reaction, we isolated the product in a promising 80% ee.

3.2 Investigation of Electronic Effects of Triazolylidene Boryl Radicals

Boranes bearing an NHC ligand have become important reagents for organic chemistry as replacements for tin hydrides in free radical reactions.[8] Applying this strategy, NHC-boranes have been used to effect a variety of transformations including hydroxymethylation with carbon monoxide,[9] xanthate reduction,[10] and reductive cyclizations.[11] Additionally, they have been shown to be efficient co-initiators in the radical photopolymerization of acrylates.[12]

Previous studies have investigated the relationship between the sterics of the NHC-borane and their reactivity.[13] These studies clearly demonstrate that the reactivity of the NHC-borane can be attenuated by increasing the steric bulk of the NHC on the NHC-borane radical complex in H-atom and halogen extraction reactions. Our group developed a modular synthesis of triazolium pre-catalysts for NHC catalysis that allows for the rapid synthesis of a variety of catalysts ranging from strongly electron-donating to heavily electron-withdrawing.[14] Thus, these NHCs could be complexed to boranes to generate a library of NHC-boranes to probe the electronic effects on reactivity. In terms of organocatalysis, the *N*-aryl substituent has a recognized impact on reactivity due to a variety of steric or electronic factors.[15]

In collaboration with the Emmanuel Lacôte research group, a small library of NHC-boranes was prepared with varying electronics of the *N*-aryl substituent (Scheme 3.2.1). As my contribution, I synthesized trimethoxyphenyl triazolium that was converted to the NHC-Borane for use in this study. The rate constant of hydrogen abstraction with oxygen radicals using di-*tert*-butyl peroxide or benzophenone as the radical source were then measured, along with the B-H bond-dissociation energies, and the rate of addition of the NHC-borane radical. These three parameters showed no correlation between the electronics of the *N*-aryl substituent and reactivity. In contrast, the addition of the NHC-boryl radical to acrylates was found to have a linear

correlation to the calculated electronegativity of the NHC-boryl radicals. As the electronegativity of the boryl radical decreases, the faster the addition to methyl acrylate.

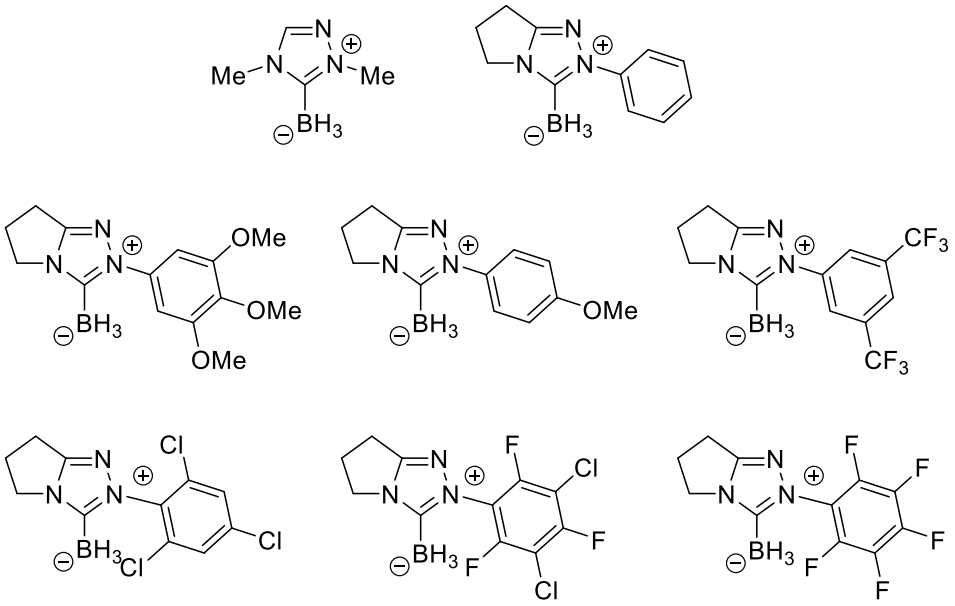

Scheme 3.2.1

While the rate of addition of NHC-boryl radicals to methyl methacrylate showed a strong linear correlation, this did not translate to the efficiency of the boryl radical as a co-initiator in the radical photopolymerization of trimethylolpropane triacylate. N-Pentafluorophenyl triazolium outperformed the other co-initiators, except for the dimethyl triazolium, despite having the slowest rate of addition to methyl methacrylate. This suggests that the rate-limiting step of the reaction is not the addition of the NHC-boryl radical to the acrylate.

3.3 Synthesis of (–)-Paroxetine and (–)-Femoxitine

The rapid and stereodefined synthesis of piperidines is a topic that has had much attention from the synthetic community.[16] Our group previously reported the highly enantio- and diastereoselective coupling of enals with nitroalkenes to give δ-nitroesters with high enantio- and diastereoselectivity.[17] Using this methodology, a one-pot procedure was also developed for the *in-situ* conversion of these δ-nitroesters into the corresponding δ-lactam, which proceeded without

eroding the newly defined stereocenters. The rapid access to *trans* 3,4-disubstituted piperidones enabled by this process inspired us to the synthesize the common selective serotonin reuptake inhibitors (SSRIs) Paroxetine and Femoxetine (Figure 3.3.1). Paroxetine (Paxil) and Femoxetine were discovered in 1970 as a treatment for depression, anxiety, and panic disorder. While Femoxetine was not pursued, Paroxetine was introduced to the market in 1992.[18]

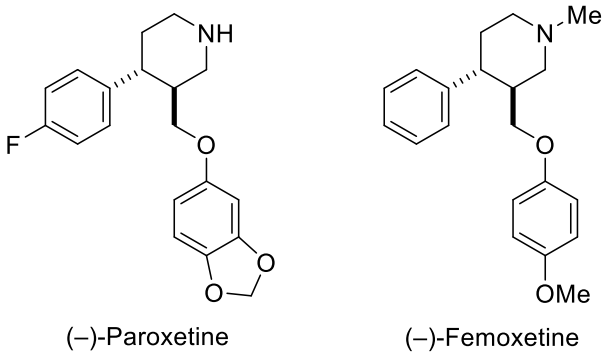

Figure 3.3.1 Structures of Paroxetine and Femoxitine.

The synthesis of Paroxetine began by generating nitroalkene **56** from commercially available aldehyde **55** using a Henry reaction with nitromethane, followed by elimination with trifluoroacetic acid to give **56** in 68% yield over two steps. My contribution to the synthesis of Paroxetine was the synthesis of aldehyde **55**, which is commercially available from Aurora Building Blocks, but we chose to make it via a two-step process starting from sesamol. To synthesize **55**, sesamol was first treated with 3-chloro-1,2-propane diol in the presence of sodium hydroxide to give the corresponding diol. This diol was then treated with sodium periodate (1.3 equiv) to cleave the diol and generate **55** in 82% yield.Aldehyde **55** was then converted to the corresponding nitroalkene (**56**) in a two-step sequence to setup the NHC-catalyzed δ-lactam synthesis to complete the core of Paroxetine. Using triazolium **19**, the one pot procedure for the synthesis of the 3,4-disubstituted piperidone was carried out, delivering 1.8 g of the product in 58% yield, 10:1 dr, and 82% ee. Reduction of the δ-lactam to the corresponding piperidine

completes the synthesis, giving Paroxetine in 88% yield (35% over four steps), 10:1 dr, and 82% ee (Scheme 3.3.2).

Scheme 3.3.2

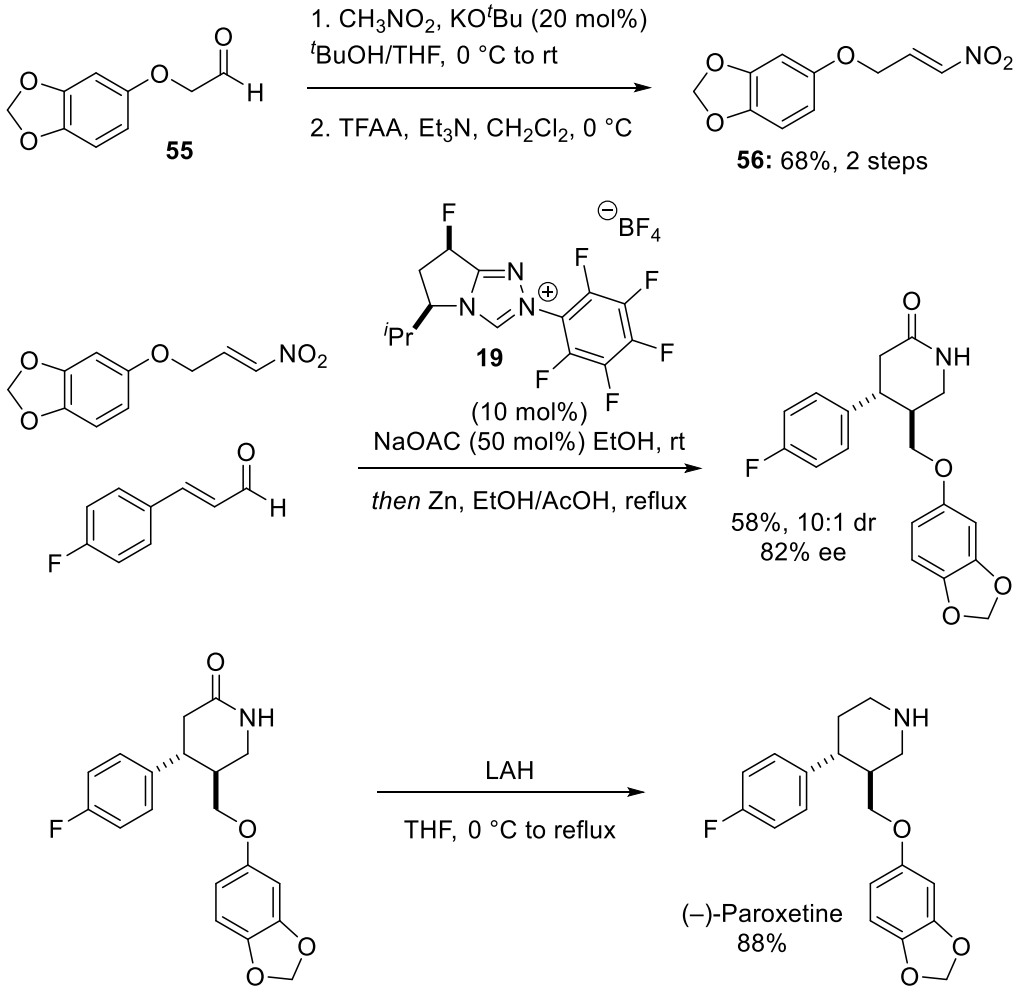

This synthetic sequence could also be applied to the synthesis of Femoxetine, which was completed in 5% yield over 5 steps, 7:1 dr, and 82% ee (Scheme 3.3.3).[19] The starting aldehyde was generated similarly by treatment of mequinol with 3-chloro-1,2-propane and sodium hydroxide, followed by sodium periodate to generate the corresponding aldehyde. This was then converted to the nitroalkene following two-step Henry reaction and elimination sequence to set up the NHC-catalyzed lactam synthesis. The lactam was then reduced to the piperidine with lithium

aluminum hydride. Finally, the *N*-methyl piperidine was generated using methyl iodide to complet the synthesis of Femoxetine.

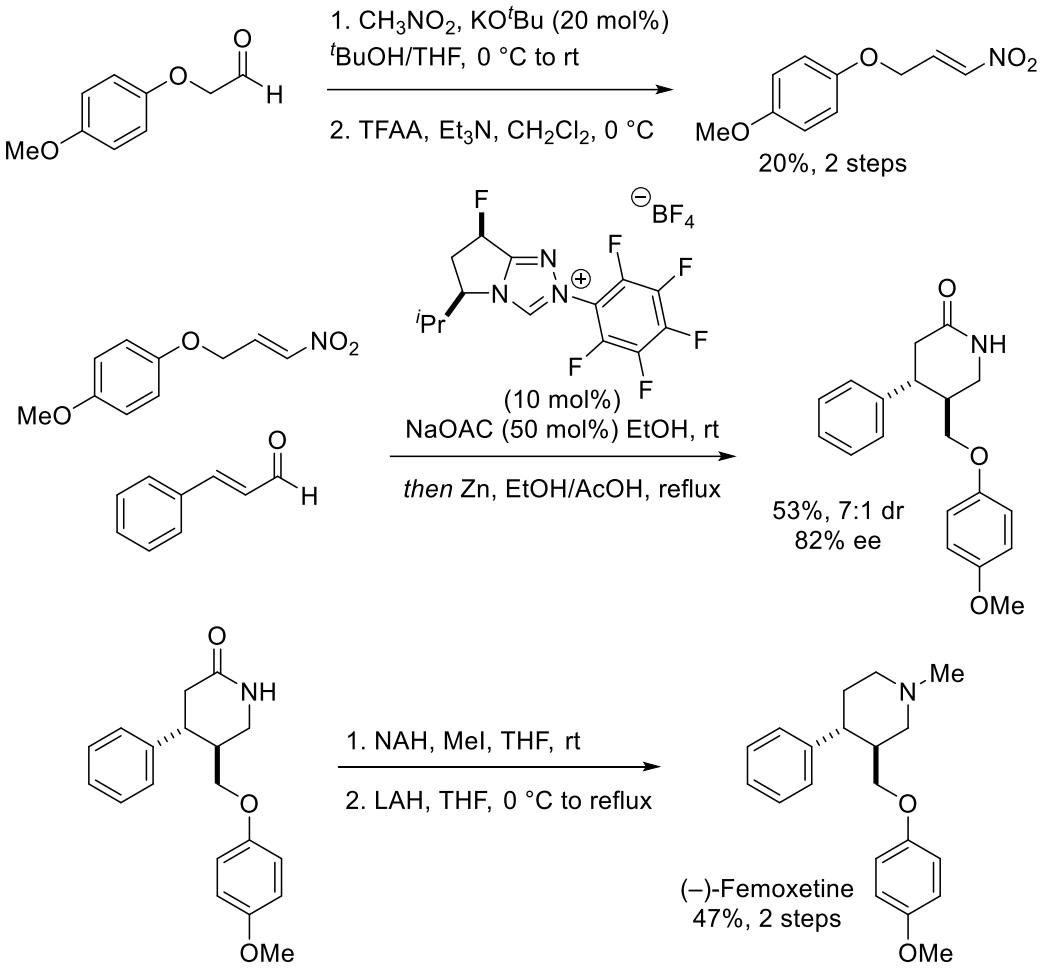

Scheme 3.3.3

References

[1] Enders, D.; Han, J.; Henseler, A. *Chem. Commun.* **2008**, 3989.

[2] Liu, Q.; Perreault, S.; Rovis, T. *J. Am. Chem. Soc.* **2008**, *130*, 14066.

[3] (a) DiRocco, D. A.; Noey, E. L.; Houk, K. N.; Rovis, T. *Angew. Chem., Int. Ed.* **2012**, *51*, 2391. (b) DiRocco, D. A.; Rovis, T. *J. Am. Chem. Soc.* **2011**, *133*, 10402. (c) DiRocco, D. A.; Oberg, K. M.; Dalton, D. M.; Rovis, T. *J. Am. Chem. Soc.* **2009**, *131*, 10872.

[4] Fang, X.; Chen, X.; Lv, H.; Chi, Y. R. *Angew. Chem., Int. Ed.* **2011**, *50*, 11782.

[5] Sánchez-Larios, E.; Thai, K.; Bilodeau, F.; Gravel, M. *Org. Lett.* **2011**, *13*, 4942.

[6] (a) Wurz, N. E.; Daniliuc, C. G.; Glorius, F. *Chem. Euro. J.* **2012**, *18*, 16297. (b) Jousseaume, T.; Wurz, N. E.; Glorius, F. *Angew. Chem., Int. Ed.* **2011**, *50*, 1410.

[7] Stetter, H.; Kuhlmann, H., The Catalyzed NucleophilicAddition of Aldehydes to Electrophilic Double Bonds. In *Organic Reactions*, John Wiley & Sons, Inc.: 2004; Vol. 40, pp 407-496.

[8] (a) Yeh, E. A. H.; Kumli, E.; Damodaran, K.; Curran, D. P. *J. Am. Chem. Soc.* **2013**, *135*, 1577. (b) Ueng, S.-H.; Makhlouf Brahmi, M.; Derat, É.; Fensterbank, L.; Lacôte, E.; Malacria, M.; Curran, D. P. *J. Am. Chem. Soc.* **2008**, *130*, 10082.

[9] Kawamoto, T.; Okada, T.; Curran, D. P.; Ryu, I. *Org. Lett.* **2013**, *15*, 2144.

[10] Ueng, S.-H.; Fensterbank, L.; Lacôte, E.; Malacria, M.; Curran, D. P. *Org. Lett.* **2010**, *12*, 3002.

[11] Pan, X.; Lacôte, E.; Lalevée, J.; Curran, D. P. *J. Am. Chem. Soc.* **2012**, *134*, 5669.

[12] (a) Telitel, S.; Vallet, A.-L.; Schweizer, S.; Delpech, B.; Blanchard, N.; Morlet-Savary, F.; Graff, B.; Curran, D. P.; Robert, M.; Lacôte, E.; Lalevée, J. *J. Am. Chem. Soc.* **2013**, *135*, 16938. (b) Telitel, S.; Schweizer, S.; Morlet-Savary, F.; Graff, B.; Tschamber, T.; Blanchard, N.; Fouassier, J. P.; Lelli, M.; Lacôte, E.; Lalevée, J. *Macromolecules* **2013**, *46*, 43. (c) Lalevée, J.; Telitel, S.; Tehfe, M. A.; Fouassier, J. P.; Curran, D. P.; Lacôte, E. *Angew. Chem., Int. Ed.* **2012**, *51*, 5958. (d) Tehfe, M.-A.; Monot, J.; Malacria, M.; Fensterbank, L.; Fouassier, J.-P.; Curran, D. P.; Lacôte, E.; Lalevée, J. *ACS Macro Letters* **2012**, *1*, 92. (e) Tehfe, M.-A.; Monot, J.; Brahmi, M. M.; Bonin-Dubarle, H.; Curran, D. P.; Malacria, M.; Fensterbank, L.; Lacote, E.; Lalevee, J.; Fouassier, J.-P. *Polym. Chem.* **2011**, *2*, 625. (f) Tehfe, M.-A.; Makhlouf Brahmi, M.; Fouassier, J.-P.; Curran, D. P.; Malacria, M.; Fensterbank, L.; Lacôte, E.; Lalevée, J. *Macromolecules* **2010**, *43*, 2261.

[13] (a) Walton, J. C.; Brahmi, M. M.; Monot, J.; Fensterbank, L.; Malacria, M.; Curran, D. P.; Lacôte, E. *J. Am. Chem. Soc.* **2011**, *133*, 10312. (b) Walton, J. C.; Brahmi, M. M.; Fensterbank, L.; Lacôte, E.; Malacria, M.; Chu, Q.; Ueng, S.-H.; Solovyev, A.; Curran, D. P. *J. Am. Chem. Soc.* **2010**, *132*, 2350.

[14] (a) Vora, H. U.; Lathrop, S. P.; Reynolds, N. T.; Kerr, M. S.; Read de Alaniz, J.; Rovis, T. *Organic Syntheses* **2010**, *87*, 362. (b) Kerr, M. S.; Read de Alaniz, J.; Rovis, T. *J. Am. Chem. Soc.* **2002**, *124*, 10298.

[15] (a) Tucker, D. E.; Quinn, P.; Massey, R. S.; Collett, C. J.; Jasiewicz, D. J.; Bramley, C. R.; Smith, A. D.; O'Donoghue, A. C. *J. Phys. Org. Chem.* **2015**, *28*, 108. (b) Collett, C. J.; Massey, R. S.; Taylor, J. E.; Maguire, O. R.; O'Donoghue, A. C.; Smith, A. D. *Angew. Chem., Int. Ed.* **2015**, *54*, 6887. (c) Collett, C. J.; Massey, R. S.; Maguire, O. R.;

Batsanov, A. S.; O'Donoghue, A. C.; Smith, A. D. *Chem. Sci.* **2013**, *4*, 1514. (d) Mahatthananchai, J.; Bode, J. W. *Chem. Sci.* **2012**, *3*, 192. (e) Vora, H. U.; Lathrop, S. P.; Reynolds, N. T.; Kerr, M. S.; Read de Alaniz, J.; Rovis, T. *Org. Synth.* **2010**, *87*, 362. (f) Rovis, T. *Chem. Lett.* **2007**, *37*, 2.

[16] (a) Chen, W.; Wilde, R. G.; Seidel, D. *Org. Lett.* **2014**, *16*, 730. (b) Peng, Z.; Wong, J. W.; Hansen, E. C.; Puchlopek-Dermenci, A. L. A.; Clarke, H. J. *Org. Lett.* **2014**, *16*, 860. (c) Wang, S.-G.; You, S.-L. *Angew. Chem., Int. Ed.* **2014**, *53*, 2194. (d) Huy, P. H.; Koskinen, A. M. P. *Org. Lett.* **2013**, *15*, 5178. (e) Martin, T. J.; Rovis, T. *Angew. Chem., Int. Ed.* **2013**, *52*, 5368. (f) Kumar, P.; Louie, J. *Org. Lett.* **2012**, *14*, 2026. (g) Duttwyler, S.; Lu, C.; Rheingold, A. L.; Bergman, R. G.; Ellman, J. A. *J. Am. Chem. Soc.* **2012**, *134*, 4064. (h) Roughley, S. D.; Jordan, A. M. *J. Med. Chem.* **2011**, *54*, 3451.

[17] White, N. A.; DiRocco, D. A.; Rovis, T. *J. Am. Chem. Soc.* **2013**, *135*, 8504.

[18] (a) Bourin, M.; Chue, P.; Guillon, Y. *CNS Drug Reviews* **2001**, *7*, 25. (b) Gunasekara, N. S.; Noble, S.; Benfield, P. *Drugs* **1998**, *55*, 85. (c) Barnes, R. D.; Wood-Kaczmar, M. W.; Curzons, A. D.; Lynch, I. R.; Richardson, J. E.; Buxton, P. C., Anti-depressant crystalline paroxetine hydrochloride hemihydrate. Google Patents: **1988**.

[19] White, N. A.; Ozboya, K. E.; Flanigan, D. M.; Rovis, T. *Asian J. Org. Chem.* **2014**, *3*, 442.

Appendix I. Supplementary Information for Chapter 2

Materials and Methods

All reactions were carried out with magnetic stirring under an atmosphere of argon in oven-dried glassware. Methanol was purchased from Sigma-Aldrich and stored in an anhydrous atmosphere. Sodium acetate was purchased from Aldrich and stored under anhydrous atmosphere. ^{1}H NMR spectra were recorded on Varian 400 MHz spectrometer at ambient temperature or a Bruker Avance III 500 (500 MHz). Data is reported as follows: chemical shift in parts per million (δ, ppm) from $CDCl_3$ (7.26 ppm) or acetone-D6 (2.03 ppm), multiplicity (s = singlet, bs = broad singlet, d = doublet, t = triplet, q = quartet, and m = multiplet), coupling constants (Hz). ^{13}CNMR were recorded on Varian 400 MHz (at 100 MHz) spectrometer or a Bruker Avance III 500 (125 MHz) at ambient temperature. Chemical shifts are reported in ppm from $CDCl_3$ (77.36 ppm) or acetoneD-6 (205.87, 30.6 ppm). Mass spectra were recorded on an Agilent 6130 Quadrupole LC/MS. HPLC spectra were obtained on an Agilent 1100 series system. Optical rotations were obtained on an Autopol - III automatic polarimeter or a Jasco DIP - 1000 digital polarimeter. Infrared spectra were recorded on a Perkin - Elmer Spectrum Two (Diamond ATR) IR or a Nicolet iS-50 FT-IR spectrometer. Thin layer chromatography was performed on SiliCycle® 250μm 60A plates. Visualization was accomplished with UV light or $KMnO_4$ stain followed by heating.

General Procedure for the synthesis of dihydropyridine derivatives

The 1,4-dihydropyridines were synthesized by combining 0.2 mmol of enal, 0.30 mmol pyridinium salt, 0.02 mmol NHC (10 mol%) and 0.2 mmol NaOAc in a vial equipped with a stir bar and Teflon cap. This mixture was then placed in an inert atmosphere (glove box) and diluted with 2 mL of methanol (0.1 M) along with 0.02 mmol acetic acid (20 mol%). The vial was then sealed and stirred at room temperature for 24 h. After this time, the solvent was evaporated and the crude reaction mixture was purified by silica chromatography (dry loading on celite) to afford the title compounds.

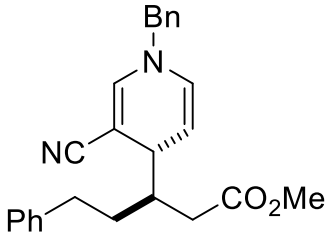

methyl 3-(1-benzyl-3-cyano-1,4-dihydropyridin-4-yl)-5-phenylpentanoate (**33**): Pale yellow oil. 61% yield, 5:1 rr, 3:1 dr, 88% ee. R_f = 0.3 (4:1 Hexanes:EtOAc); $[\alpha]_D^{21}$ = -32.8 (c = 0.136 g/mL); **HPLC analysis:** Chiralpak IA column, 80:20 hexanes/iso-propanol, 0.5 mL/min. Major: 18.1 min, minor: 16.8. **^{1}HNMR**: (500 MHz, Chloroform-d) δ 7.31 (dd, J = 4.7, 2.5 Hz, 5H), 7.23 (d, J = 6.0 Hz, 3H), 7.17 – 7.14 (m, 2H), 6.74 (d, J = 1.5 Hz, 1H), 5.89 (d, J = 8.1 Hz, 1H), 4.63 (ddd, J = 7.2, 4.4, 2.7 Hz, 1H), 4.29 (s, 2H), 3.69 (s, 3H), 3.48 (t, J = 3.7 Hz, 1H), 2.69 – 2.65 (m, 2H), 2.41 (dd, J = 7.1, 4.1 Hz, 2H), 2.13 – 1.98 (m, 2H), 1.62 (qd, J = 5.5, 2.8 Hz, 2H). **^{13}CNMR:** (101 MHz, Chloroform-d) δ 173.51, 144.24, 142.21, 136.07, 129.55, 129.02, 128.41, 127.12, 121.23, 103.51, 57.55, 51.68,

51.62, 41.73, 36.37, 35.66, 33.87, 33.04. **IR** (ATR, neat) 3026, 2923, 2856, 2191, 1730, 1672, 1590, 1412, 1181, 735, 701 cm^{-1} **LRMS** (ESI + APCI) *m/z* [M+H] calcd 387.2, found 387.2

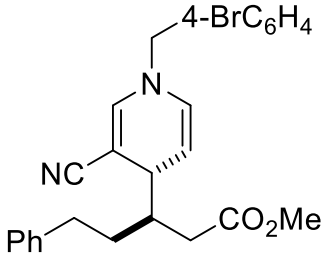

methyl 3-(1-benzyl-3-cyano-1,4-dihydropyridin-4-yl)-5-methylhexanoate (**34**): Pale yellow oil. 71% yield, 3:1 rr, 2:1 dr, 87% ee. R_f = 0.35 (4:1 Hexanes:EtOAc); $[\alpha]_D^{21}$ = -12.2 (c = 0.01 g/mL); **HPLC analysis:** Chiralpak IA column, 90:10 hexanes/iso-propanol, 1.0 mL/min. Major: 11.2 min, minor: 10.8 min. **^{1}HNMR:** (400 MHz, Chloroform-d) δ 7.33 (dd, J = 25.5, 7.9 Hz, 3H), 7.25 – 7.04 (m, 3H), 6.99 (d, J = 8.4 Hz, 2H), 6.69 (d, J = 1.6 Hz, 1H), 5.91 – 5.76 (m, 1H), 4.61 (dd, J = 8.1, 4.4 Hz, 1H), 4.21 (s, 2H), 3.67 (s, 3H), 3.52 – 3.40 (m, 1H), 2.80 – 2.56 (m, 2H), 2.42 – 2.27 (m, 2H), 2.21 – 1.92 (m, 2H), 1.76 – 1.47 (m, 2H). **^{13}CNMR:** (101 MHz, Chloroform-d) δ 173.33, 143.92, 142.15, 129.30, 128.36, 125.91, 122.19, 120.89, 103.67, 103.01, 81.70, 81.22, 56.91, 51.67, 41.57, 41.21, 36.40, 35.57, 33.86, 33.16. **IR** (ATR, neat) 3060, 3025, 2923, 2857, 2191, 1729, 1672, 1591, 1435, 1404, 1178, 1010 cm^{-1} **LRMS** (ESI + APCI) *m/z* [M+H] calcd 465.1, found 465.1

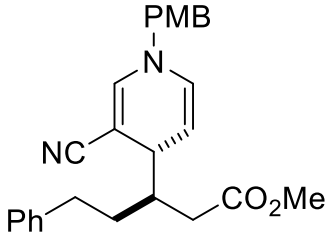

methyl 3-(3-cyano-1-(4-methoxybenzyl)-1,4-dihydropyridin-4-yl)-5-phenylpentanoate (**35**): Pale yellow oil. 50% yield, 6:1 rr, 3:1 dr, 85% ee. R_f = 0.3 (4:1 Hexanes:EtOAc); $[\alpha]_D^{21}$ = -22.2 (c = 0.01 g/mL); **HPLC analysis:** Chiralpak IA column, 90:10 hexanes/iso-propanol, 1.0 mL/min. Major: 12.0 min, minor: 10.8 min. **^{1}HNMR**: ^{1}H NMR (400 MHz, Chloroform-d) δ 7.33 – 7.27 (m, 3H), 7.23 – 7.15 (m, 5H), 7.09 (d, J = 8.8 Hz, 2H), 7.05 (d, J = 8.8 Hz, 2H), 6.86 (d, J = 8.7 Hz, 2H), 6.79 (d, J = 8.7 Hz, 2H), 6.70 (d, J = 1.6 Hz, 1H), 5.86 (ddd, J = 8.2, 1.7, 0.9 Hz, 1H), 4.59 (dd, J = 8.1, 4.4 Hz, 1H), 4.19 (s, 2H), 3.79 (s, 3H), 3.66 (s, 3H), 3.46 – 3.41 (m, 1H), 2.80 – 2.59 (m, 4H), 2.34 – 2.22 (m, 1H), 2.15 – 1.94 (m, 3H), 1.74 – 1.50 (m, 3H). **^{13}CNMR:** (101 MHz; CDCl3): δ 173.5, 159.5, 144.1, 142.2, 129.4, 128.5, 128.4, 128.4, 127.9, 121.3, 114.4, 103.4, 80.4, 57.1, 55.3, 51.6, 41.8, 41.3, 36.4, 35.6, 33.9, 33.0 **IR** (ATR, neat) 3061, 3026, 2925, 2856, 2191, 1731, 1672, 1588, 1513, 1412, 1248, 1175 cm^{-1} **LRMS** (ESI + APCI) *m/z* [M+H] calcd 417.2, found 417.2

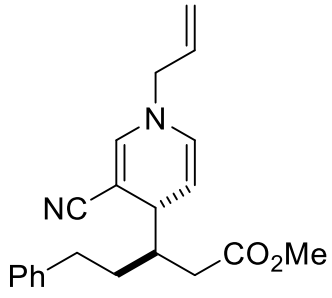

methyl 3-(1-allyl-3-cyano-1,4-dihydropyridin-4-yl)-5-phenylpentanoate (**36**): Pale yellow oil. 45% yield, 3:1 rr, 3:1 dr, 86% ee. R_f = 0.2 (4:1 Hexanes:EtOAc); $[\alpha]_D^{21}$ = -19.3 (c = 0.01 g/mL); **HPLC analysis:** Chiralpak IA column, 90:10 hexanes/iso-propanol, 1.0 mL/min. Major: 16.0 min, minor: 14.5. **^{1}HNMR:** ^{1}H NMR (400 MHz, Chloroform-d) δ 7.30 – 7.28 (m, 3H), 7.21 – 7.16 (m, 2H), 6.64 (d, J = 4 Hz, 1H), 5.71 – 5.68 (m, 1H), 5.84 – 5.82 (m, 1H), 5.25 – 5.17 (m, 2H), 4.58 (dd, J = 4, 8 Hz, 1H), 3.66 (s, 3H), 3.47 – 3.43 (m, 1H), 2.75 – 2.62 (m, 3H), 2.45 – 2.25 (m, 2H), 2.05 – 1.96 (m, 2H), 1.68 – 1.56 (m, 2H); **^{13}CNMR:** (101 MHz; CDCl3): δ 171 **IR** (ATR, neat) 3061, 3025, 2925, 2860, 2192, 1673, 1591, 1412, 1218, 1189 cm^{-1} **LRMS** (ESI + APCI) *m/z* [M+H] calcd 337.2, found 337.2

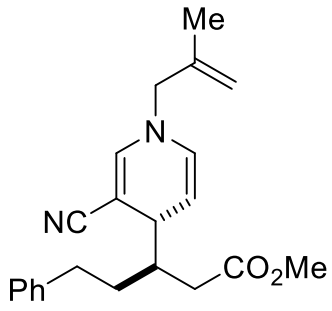

methyl 3-(3-cyano-1-(3-methylbut-3-en-1-yl)-1,4-dihydropyridin-4-yl)-5-phenylpentanoate (**37**): Pale yellow oil. 38% yield, 4:1 rr, 2:1 dr, 89% ee. R_f = 0.3 (4:1 Hexanes:EtOAc); $[\alpha]_D^{21}$ = 23.1 (c = 0.009 g/mL); **HPLC analysis:** Chiralpak OC column, 90:10 hexanes/iso-propanol, 1.0 mL/min. Major: 40.0 min, minor: 37.8 min. **1HNMR:** (400 MHz, Chloroform-d) δ 7.25 (d, J = 3.1 Hz, 1H), 7.23 – 7.12 (m, 4H), 6.59 (dd, J = 10.7, 1.6 Hz, 1H), 5.90 – 5.80 (m, 1H), 4.86 – 4.63 (m, 3H), 4.57 (dd, J = 8.1, 4.4 Hz, 1H), 3.66 (s, 3H), 3.48 – 3.40 (m, 1H), 3.20 (td, J = 7.1, 4.4 Hz, 2H), 2.66 – 2.57 (m, 2H), 2.37 (dd, J = 17.3, 7.0 Hz, 1H), 2.23 – 2.15 (m, 3H), 2.06 – 1.94 (m, 2H), 1.70 (d, J = 12.7 Hz, 4H); **13CNMR:** (101 MHz, Chloroform-d) δ 173.55, 144.01, 142.19, 140.81, 129.14, 128.37, 125.77, 123.61, 121.49, 113.57, 109.19, 103.32, 79.47, 52.42, 51.60, 42.01, 41.30, 37.92, 36.15, 35.65, 33.82, 33.62, 32.97, 32.46, 22.18. **IR** (ATR, neat) 3061, 3026, 2925, 2857, 1731, 1672, 1625, 1588, 1414, 1170 cm^{-1}; **LRMS** (ESI + APCI) *m/z* [M+H] calcd 365.2, found 365.2

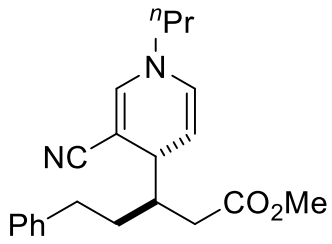

methyl 3-(3-cyano-1-propyl-1,4-dihydropyridin-4-yl)-5-phenylpentanoate (**38**): Pale yellow oil. 46% yield, 3:1 rr, 3:1 dr, 88% ee. R_f = 0.3 (4:1 Hexanes:EtOAc); $[\alpha]_D^{21}$ = -34.0 (c = 0.01 g/mL); **HPLC analysis:** Chiralpak IA column, 90:10

hexanes/iso-propanol, 1.0 mL/min. Major: 13.0 min, minor: 11.7 min. **^{1}HNMR**: (400 MHz, Chloroform-d) δ 7.33 – 7.27 (m, 1H), 7.23 – 7.11 (m, 3H), 6.63 (d, J = 1.6 Hz, 1H), 5.90 – 5.80 (m, 1H), 4.60 – 4.53 (m, 1H), 3.66 (s, 3H), 3.48 – 3.40 (m, 1H), 3.08 – 2.98 (m, 2H), 2.67 – 2.56 (m, 2H), 2.48 – 2.30 (m, 2H), 2.08 – 1.92 (m, 2H), 1.57 – 1.49 (m, 2H), 0.86 (t, J = 7.4 Hz, 3H).**^{13}CNMR:** (101 MHz; CDCl3): δ 173.56, 144.17, 142.17, 129.31, 128.34, 123.61, 121.59, 101.85, 79.13, 55.86, 51.60, 42.02, 41.29, 36.19, 35.65, 33.78, 32.89, 23.14, 10.79 **IR** (ATR, neat) 3061, 3026, 2930, 2876, 2190, 1731, 1671, 1587, 1414, 1133 cm^{-1} **LRMS** (ESI + APCI) *m/z* [M+H] calcd 339.2, found 339.2.

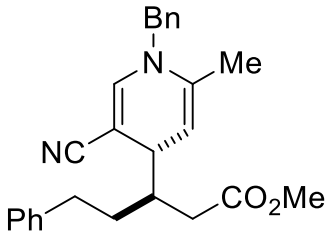

methyl 3-(1-benzyl-5-cyano-2-methyl-1,4-dihydropyridin-4-yl)-5-methylhexanoate (**39**): Pale yellow oil. 46% yield, >20:1 rr, 4:1 dr, 91% ee. R_f = 0.3 (4:1 Hexanes:EtOAc); $[\alpha]_D^{21}$ = -11.6 (c = 0.01 g/mL); **HPLC analysis:** Chiralpak IA column, 90:10 hexanes/iso-propanol, 1.0 mL/min. Major: 15.0 min, minor: 13.6 min. **^{1}HNMR**: (400 MHz, Chloroform-d) δ 7.36 – 7.27 (m, 3H), 7.26 – 7.14 (m, 6H), 7.11 (dd, J = 6.5, 3.1 Hz, 1H), 6.73 (s, 1H), 4.53 – 4.32 (m, 3H), 3.67 (s, 3H), 3.51 – 3.42 (m, 1H), 2.78 – 2.58 (m, 3H), 2.40 (dd, J = 7.0, 2.5 Hz, 1H), 2.16 – 1.95 (m, 2H), 1.75 (s, 3H), 1.65 – 1.51 (m, 1H). **^{13}CNMR:** (101 MHz, Chloroform-d) δ 173.57, 145.89, 142.27, 137.40, 135.40, 128.42, 128.38, 127.76, 125.99, 121.20, 101.60, 81.05, 53.98, 51.61, 41.81, 37.40, 35.81, 33.94, 33.20, 18.72. **IR** (ATR, neat) 3061, 3027, 2922, 2853, 2191, 1731, 1679, 1603, 1435, 1407, 1179, 1155 cm^{-1}; **LRMS** (ESI + APCI) *m/z* [M+H] calcd 401.2, found 401.2

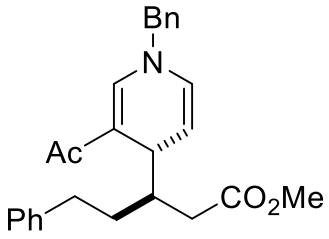

methyl 3-(3-acetyl-1-benzyl-1,4-dihydropyridin-4-yl)-5-phenylpentanoate (**40**): Pale yellow oil. 46% yield, 4:1 rr, 5:1 dr, 50% ee. R_f = 0.2 (4:1 Hexanes:EtOAc); $[\alpha]_D^{21}$ = -52.7 (c = 0.008 g/mL); **HPLC analysis:** Chiralpak IA column, 93:7 hexanes/iso-propanol, 1.0 mL/min. Major: 71.8 min, minor: 78.2. **^{1}HNMR**: (500 MHz, Chloroform-d) δ 7.3a2 – 7.27 (m, 4H), 7.24 – 7.21 (m, 3H), 7.16 (d, J = 6.7 Hz, 4H), 5.98 (d, J = 7.8 Hz, 1H), 4.96 – 4.87 (m, 1H), 4.41 (s, 2H), 3.71 (s, 3H), 2.70 – 2.54 (m, 2H), 2.34 (d, J = 7.3 Hz, 2H), 2.19 (s, 4H), 2.10 (dd, J = 10.2, 6.0 Hz, 1H), 1.80 – 1.63 (m, 3H), 1.52 – 1.39 (m, 1H). **^{13}CNMR:** (126 MHz; CDCl3): δ 195.27, 173.97, 143.48, 142.86, 136.52, 129.20, 128.94, 128.39, 128.30, 128.00, 127.02, 125.61, 111.66, 106.15, 58.01, 51.55, 40.87, 36.00, 33.92, 32.64, 24.65. **IR** (ATR, neat) 3026, 2923, 2856, 1730, 1667, 1574, 1454, 1434, 1387, 1177 cm^{-1}. **LRMS** (ESI + APCI) *m/z* [M+H] calcd 404.2, found 404.3

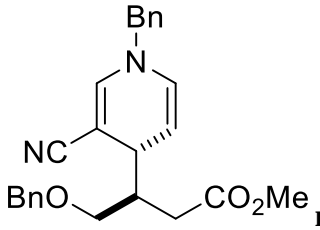

methyl 3-(1-benzyl-3-cyano-1,4-dihydropyridin-4-yl)-4-(benzyloxy)butanoate (**41**): Pale yellow oil. 63% yield, 3:1 rr, 4:1 dr, 81% ee. R_f = 0.3 (4:1 Hexanes:EtOAc); $[\alpha]_D^{21}$ = -8.0 (c = 0.005 g/mL); **HPLC analysis:** Chiralpak IA column, 95:5 hexanes/iso-propanol, 1.0 mL/min. Major: 35.6 min, minor: 44.2 min. **^{1}HNMR**: (400 MHz, Chloroform-d) δ 7.33 (q, J = 4.1, 3.5 Hz, 9H), 7.24 – 7.21 (m, 2H), 7.18 – 7.15 (m, 2H), 6.71 (d, J = 1.6 Hz, 1H), 6.05 – 5.97 (m, 1H), 5.87 (d, J = 8.9 Hz, 1H), 4.62 (dd, J = 8.0, 4.6 Hz, 1H), 4.28 (s, 2H), 3.67 (s, 3H), 3.60 (s, 3H), 3.55 – 3.51 (m, 2H), 3.51 – 3.46 (m, 1H), 2.69 – 2.62 (m, 1H), 2.45 – 2.39 (m, 2H), 2.38 – 2.33 (m, 1H). **^{13}CNMR:** (101 MHz; CDCl3): 13C NMR (101 MHz, Chloroform-d) δ 173.31, 148.32, 144.17, 138.34, 135.97, 129.05, 128.26, 127.70, 127.22, 123.34, 121.40, 110.04, 104.09, 73.10, 70.42, 68.08, 57.89, 57.57, 56.76, 51.55, 42.64, 39.52, 34.24, 33.23, 31.23, 29.68. **IR** (ATR, neat) 3062, 3030, 2950, 2855, 2193, 1732, 1625, 1453, 1246, 1103 cm^{-1}; **LRMS** (ESI + APCI) *m/z* [M+H] calcd 403.2, found 403.2

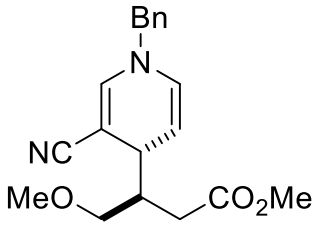

methyl 3-(1-benzyl-3-cyano-1,4-dihydropyridin-4-yl)-4-methoxybutanoate (**42**): Pale yellow oil. 63% yield, 5:1 rr, 2:1 dr, 84% ee. R_f = 0.2 (4:1 Hexanes:EtOAc); $[\alpha]_D^{21}$ = -33.6 (c = 0.005 g/mL); **HPLC analysis:** Chiralpak IA column, 80:20 hexanes/iso-propanol, 1.0 mL/min. Major: 8.1 min, minor: 9.8 min. **1H NMR:** (400 MHz, Chloroform-d) δ 7.36 (dt, J = 13.0, 6.8 Hz, 5H), 7.18 (d, J = 6.6 Hz, 2H), 6.72 (d, J = 1.6 Hz, 1H), 5.89 (d, J = 8.0 Hz, 1H), 4.63 (dd, J = 8.1, 4.5 Hz, 1H), 4.30 (s, 2H), 3.69 (t, J = 4.2 Hz, 2H), 3.65 (s, 2H), 3.55 (dd, J = 9.6, 6.6 Hz, 1H), 3.52 – 3.48 (m, 1H), 3.37 (dd, J = 9.6, 7.4 Hz, 1H), 3.31 (s, 2H), 2.43 – 2.35 (m, 1H), 2.25 (dd, J = 6.9, 3.2 Hz, 1H); **13C NMR:** (101 MHz, Chloroform-d) δ 173.35, 148.35, 144.19, 135.98, 129.29, 129.05, 128.29, 127.23, 123.36, 121.37, 104.12, 79.78, 72.63, 58.77, 58.35, 57.60, 51.58, 42.59, 41.01, 39.46, 34.15, 33.03, 31.45, 31.14. **IR** (ATR, neat) 2950, 2925, 2192, 1730, 1672, 1589, 1413, 1179, 1118 cm^{-1} **LRMS** (ESI + APCI) *m/z* [M+H] calcd 327.2, found 327.2

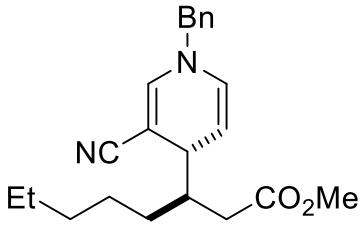

methyl 3-(1-benzyl-3-cyano-1,4-dihydropyridin-4-yl)octanoate (**43**): Pale yellow oil. 63% yield, 4:1 rr, 3:1 dr, 84% ee. R_f = 0.2 (4:1 Hexanes:EtOAc); $[\alpha]_D^{21}$ = -23.7 (c = 0.01 g/mL); **HPLC analysis:** Chiralpak IA column, 90:10 hexanes/iso-propanol, 1.0

mL/min. Major: 6.4 min, minor: 5.8 min. **^{1}HNMR**: (400 MHz, Chloroform-d) δ 7.40 – 7.29 (m, 3H), 7.22 – 7.16 (m, 2H), 6.70 (d, J = 1.6 Hz, 1H), 5.87 (d, J = 8.8 Hz, 1H), 4.60 (dd, J = 8.2, 4.4 Hz, 1H), 4.28 (s, 2H), 3.65 (s, 3H), 3.38 (t, J = 3.7 Hz, 1H), 2.30 (dd, J = 7.2, 2.9 Hz, 2H), 1.99 – 1.91 (m, 1H), 1.69 – 1.60 (m, 1H), 1.38 – 1.16 (m, 9H), 0.92 – 0.85 (m, 4H). **^{13}CNMR:** (101 MHz, Chloroform-d) δ 173.70, 161.51, 144.08, 136.18, 128.99, 128.19, 127.16, 122.89, 121.22, 110.47, 103.75, 102.63, 92.89, 80.85, 57.52, 55.30, 51.53, 41.78, 36.39, 35.60, 33.30, 32.01, 30.77, 28.49, 27.00, 22.55, 14.06. **IR** (ATR, neat) 2952, 2927, 2856, 2192, 1731, 1673, 1591, 1411, 1204, 1151 cm^{-1}; **LRMS** (ESI + APCI) *m/z* [M+H] calcd 353.2, found 353.3

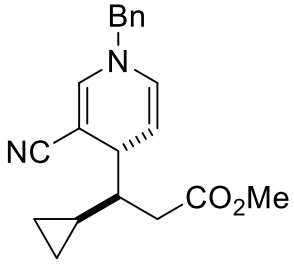

methyl 3-(1-benzyl-3-cyano-1,4-dihydropyridin-4-yl)-3-cyclopropylpropanoate (**44**): Pale yellow oil. 31% yield, 3:1 rr, 3:1 dr, 85% ee. R_f = 0.4 (4:1 Hexanes:EtOAc); $[\alpha]_D^{21}$ = -60.0 (c = 0.01 g/mL); **HPLC analysis:** Chiralpak IA column, 90:10 hexanes/iso-propanol, 1.0 mL/min. Major: 14.3 min, minor: 16.2 min. **^{1}HNMR**: (400 MHz, Chloroform-d) δ 7.35 (d, J = 7.1 Hz, 4H), 7.21 – 7.17 (m, 2H), 6.71 (d, J = 1.6 Hz, 1H), 5.91 (d, J = 10.2 Hz, 1H), 4.62 (dd, J = 8.1, 4.6 Hz, 1H), 4.29 (s, 3H), 3.66 – 3.64 (m, 3H), 3.46 – 3.41 (m, 1H), 2.42 (dd, J = 24.9, 7.4 Hz, 3H), 1.24 – 1.17 (m, 1H), 0.94 – 0.82 (m, 2H), 0.50 – 0.47 (m, 1H), 0.45 – 0.41 (m, 1H), 0.32 (dt, J = 9.0, 4.5 Hz, 1H), 0.08 (tt, J = 9.5, 4.6 Hz, 2H). **^{13}CNMR:** (101 MHz; CDCl3): δ 173.59, 148.79, 144.05, 136.16, 128.98, 127.19, 123.45, 121.54, 110.13, 81.01, 59.04, 47.88, 45.35, 37.85, 36.50, 34.53, 13.18, 11.62, 4.58, 3.57. **IR** (ATR, neat) 3064, 3002, 2923, 2851, 2192, 1673, 1591, 1437, 1414, 1245, 1180 cm^{-1} **LRMS** (ESI + APCI) *m/z* [M+H] calcd 323.2, found 323.2

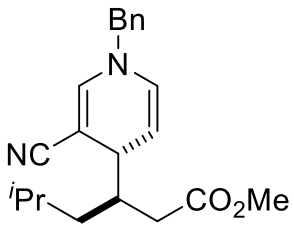

methyl 3-(1-benzyl-3-cyano-1,4-dihydropyridin-4-yl)-5-methylhexanoate (**45**): Pale yellow oil. 52% yield, 3:1 rr, 2:1 dr, 58% ee. R_f = 0.2 (4:1 Hexanes:EtOAc); $[\alpha]_D^{21}$ = -18.9 (c = 0.010 g/mL); **HPLC analysis:** Chiralpak IE column, 90:10 hexanes/iso-propanol, 1.0 mL/min. Major: 38.1 min, minor: 33.8 min. **^{1}HNMR**: (400 MHz, Chloroform-d) δ 7.35 (dq, J = 11.9, 6.6, 5.2 Hz, 4H), 7.21 – 7.19 (m, 1H), 6.71 (d, J = 1.6 Hz, 1H), 5.88 (d, J = 8.2 Hz, 1H), 4.60 (dd, J = 8.1, 4.3 Hz, 1H), 4.28 (s, 2H), 3.66 (d, J = 6.9 Hz, 3H), 3.38 (s, 1H), 2.28 (t, J = 6.9 Hz, 2H), 1.60 (ddd, J = 19.8, 14.2, 6.6 Hz, 2H), 1.49 – 1.43 (m, 1H), 1.18 – 1.07 (m, 1H), 0.91 (d, J = 6.5 Hz, 6H). **^{13}CNMR:** (101 MHz, Chloroform-d) δ 173.60, 161.51, 148.80, 136.20, 129.59, 129.42, 128.99, 128.20, 127.22, 127.14, 122.98, 121.13, 103.61, 102.61, 92.90, 57.53, 55.31, 51.53, 40.04, 39.21, 36.33, 35.74, 25.19, 23.30, 22.10. **IR** (ATR, neat) 2926, 2867, 2193, 1733, 1674, 1593, 1454, 1206, 1194, 1152 cm^{-1} **LRMS** (ESI + APCI) *m/z* [M+H] calcd 339.2, found 339.2

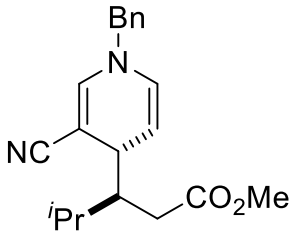

methyl (S)-3-((S)-1-benzyl-3-cyano-1,4-dihydropyridin-4-yl)-4-methylpentanoate (**46**): Pale yellow oil. 54% yield, 5:1 rr, 3:1 dr, 42% ee. R_f = 0.2 (4:1 Hexanes:EtOAc); $[\alpha]_D^{21}$ = 0.5699 (c = 0.011 g/mL); **HPLC analysis:** Chiralpak IA column, 90:10 hexanes/iso-propanol, 1.0 mL/min. Major: 14.6 min, minor: 10.2 min. **^{1}HNMR**: (500 MHz, Chloroform-d) δ 7.46 – 7.32 (m, 8H), 7.23 (q, J = 8.2, 7.0 Hz, 4H), 6.67 (d, J = 1.5 Hz, 1H), 5.91 – 5.85 (m, 1H), 4.59 (dd, J = 8.2, 4.3 Hz, 1H), 4.31 (d, J = 3.9 Hz, 3H), 3.68 (s, 3H), 3.54 (t, J = 3.7 Hz, 1H), 3.36 (d, J = 5.9 Hz, 1H), 2.60 (dd, J = 15.8, 5.8 Hz, 1H), 2.37 – 2.31 (m, 1H), 1.94 (qd, J = 7.1, 3.2 Hz, 1H), 1.77 – 1.69 (m, 2H), 0.96 (dd, J = 6.6, 5.1 Hz, 8H). **^{13}CNMR:** (126 MHz, Chloroform-d) δ 174.40, 143.73, 136.06, 129.61, 129.03, 128.24, 127.92, 127.30, 120.88, 102.91, 82.59, 57.44, 51.56, 47.66, 35.24, 34.24, 28.80, 20.59. **IR** (ATR, neat) 2958, 2192, 1732, 1672, 1627, 1592, 1367, 1413 1181, 1118, 703 cm^{-1} **LRMS** (ESI + APCI) *m/z* [M+H] calcd 325.4, found 325.1

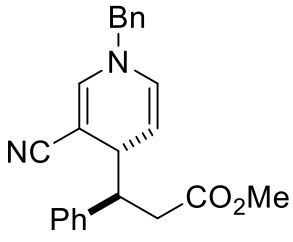

methyl (R)-3-((S)-1-benzyl-3-cyano-1,4-dihydropyridin-4-yl)-3-phenylpropanoate (**47**): Pale yellow oil. 40.5 mg, 57% yield, 8:1 rr, 1:1 dr, 24% ee. R_f = 0.2 (4:1 Hexanes:EtOAc); $[\alpha]_D^{21}$ = -20.0 (c = 0.017 g/mL); **HPLC analysis:** Chiralpak IE column, 70:30 hexanes/iso-propanol, 1.0 mL/min. Major: 14.3 min, minor: 16.2 min. **^{1}HNMR**: (500 MHz, Chloroform-d) δ 7.42 – 7.29 (m, 12H), 7.28 – 7.24 (m, 3H), 7.21 (d, J = 7.2 Hz, 2H), 7.09 (d, J = 6.9 Hz, 2H), 6.82 (dd, J = 6.5, 2.8 Hz, 2H), 6.68 (d, J = 1.5 Hz, 1H), 6.48 (d, J = 1.5 Hz, 1H), 5.88 (d, J = 8.1 Hz, 1H), 5.78 (d, J = 8.1 Hz, 1H), 4.70 (dd, J = 8.1, 4.7 Hz, 1H), 4.54 (dd, J = 8.1, 4.5 Hz, 1H), 4.26 (s, 2H), 4.12 (s, 2H), 3.61 (dd, J = 6.4, 3.8 Hz, 1H), 3.59 (s, 3H), 3.59 (s, 3H), 3.55 (t, J = 4.1 Hz, 1H), 3.43 – 3.35 (m, 2H), 3.00 – 2.74 (m, 4H). **^{13}CNMR:** (126 MHz, Chloroform-d) δ 172.91, 172.35, 144.05, 143.71, 139.89, 139.52, 129.76, 129.56, 129.17, 129.06, 128.93, 128.35, 128.26, 128.24, 127.97, 127.95, 127.17, 126.88, 126.80, 121.28, 120.99, 81.11, 57.47, 57.21, 51.70, 51.66, 47.68, 40.22, 39.14, 35.88, 34.92. **IR** (ATR, neat) 3029, 2949, 2910, 2191, 1733, 1673, 1591, 1453, 1413, 1184, 1160, 740, 702 cm^{-1} **LRMS** (ESI) *m/z* [M+H] calcd 359.2, found 359.2

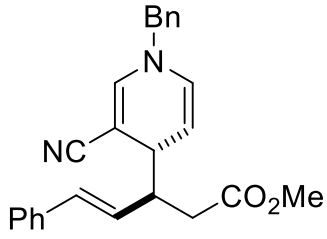

methyl (S,E)-3-((S)-1-benzyl-3-cyano-1,4-dihydropyridin-4-yl)-5-phenylpent-4-enoate (48): Pale yellow oil. 38% yield, 5:1 rr, 1:1 dr, 24% ee. R_f = 0.2 (4:1 Hexanes:EtOAc); $[\alpha]_D^{21}$ = -91.8 (c = 0.006 g/mL); **HPLC analysis:** Chiralpak IE column, 80:20 hexanes/iso-propanol, 1.0 mL/min. Major: 36.4 min, minor: 32.9 min. **^{1}HNMR**: (500 MHz, Chloroform-d) δ 7.36 (dd, J = 12.3, 7.8 Hz, 4H), 7.34 – 7.30 (m, 4H), 7.26 (dd, J = 7.6, 3.4 Hz, 2H), 7.21 (d, J = 7.8 Hz, 1H), 7.09 (dd, J = 7.5, 2.7 Hz, 2H), 6.68 (t, J = 1.8 Hz, 1H), 6.18 (dd, J = 15.8, 9.4 Hz, 1H), 5.94 (dt, J = 8.2, 2.2 Hz, 1H), 4.77 – 4.68 (m, 1H), 4.27 (s, 2H), 3.66 (s, 3H), 3.59 (s, 1H), 3.50 (dt, J = 12.8, 4.1 Hz, 1H), 2.90 (dt, J = 10.2, 4.7 Hz, 1H), 2.84 – 2.73 (m, 1H), 2.60 – 2.49 (m, 1H).**^{13}CNMR:** (126 MHz, Chloroform-d) δ 172.46, 143.83, 133.09, 132.32, 129.95, 129.08, 129.02, 128.57, 128.28, 127.36, 127.19, 127.05, 126.50, 103.25, 102.21, 57.53, 51.74, 47.70, 40.23, 39.16, 38.78, 38.45, 35.91. **IR** (ATR, neat) 3026, 2954, 2923, 2856, 2191, 1732, 1672, 1590, 1412, 1182, 747, 701 cm^{-1} **LRMS** (ESI) *m/z* [M+H] calcd 385.2, found 385.

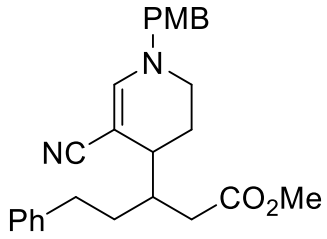

methyl 3-(5-cyano-1-(4-methoxybenzyl)-1,2,3,4-tetrahydropyridin-4-yl)-5-phenylpentanoate: Palladium hydroxide (XX mg, XX mmol) was added to a vial containing dihydropyridine **3i** (42.3 mg, 0.1 mmol) and methanol (2 mL) at room temperature under argon. The vial was then placed under vacuum and back-filled with Argon two times. After removal of the argon atmosphere a third time with vacuum, a hydrogen balloon was placed in the vial and the reaction stirred was stirred for 12 h. After this time, celite is added to the reaction mixture, and the solids were removed by filtration through celite to give 37.4 mg (88%, 3:1 dr, 86% ee) of a yellow oil. R_f = 0.2 (4:1 Hexanes:EtOAc); $[\alpha]_D^{21}$ = -35.2 (c = 0.125 g/mL); **HPLC analysis:** Chiralpak IB column, 85:15 hexanes/iso-propanol, 1.0 mL/min. Major: 31.2 min, minor: 29.0 min. **^{1}HNMR**: (500 MHz, Chloroform-d) δ 7.32 – 7.27 (m, 2H), 7.23 – 7.17 (m, 3H), 7.14 – 7.09 (m, 2H), 6.98 (dd, J = 11.3, 1.2 Hz, 1H), 6.93 – 6.87 (m, 2H), 4.17 (d, J = 7.4 Hz, 2H), 3.83 (s, 3H), 3.71 (s, 3H), 3.01 (dt, J = 12.3, 5.5 Hz, 2H), 2.74 – 2.63 (m, 2H), 2.57 (dd, J = 15.2, 6.3 Hz, 1H), 2.47 (d, J = 7.9 Hz, 1H), 2.34 – 2.21 (m, 1H). **^{13}CNMR:** (101 MHz, Chloroform-d) δ 173.41, 159.47, 142.24, 128.91, 128.38, 125.84, 122.88, 114.29, 58.95, 55.33, 51.65, 43.85, 38.51, 37.83, 36.73, 35.86, 34.48, 33.98, 29.70, 22.53. **IR** (ATR, neat) 2927, 2855, 2180, 1732, 1617, 1512, 1248, 1175, 1031 cm^{-1} **LRMS** (ESI) *m/z* [M+H] calcd 419.2, found 419.2

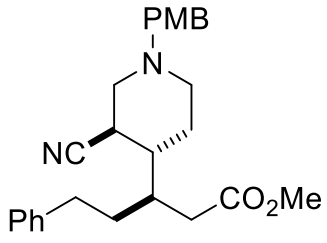

methyl (R)-3-((3R,4R)-3-cyano-1-(4-methoxybenzyl)piperidin-4-yl)-5-phenylpentanoate: A solution of dihydropyridine **3i** (44.3 mg, 0.11 mmol) in CH_2Cl_2 (2 mL) was cooled to -10℃, and triethylsilane (340 uL, 20 equiv) was added along with trifluoracetic acid (204 uL, 25 equiv). This mixture was then allowed to stir while warming to room temperature. After 12 h, volatiles were removed under reduced pressure. The resulting crude oil was purified by column chromatography (DCM/MeOH) to give **10** (51%, 22.8 mg, 0.054 mmol, 3:1 dr, 84% ee) as an off-white solid. R_f = 0.2 (98:2 DCM:MeOH); $[\alpha]_D^{21}$ = -37.8 (c = 0.008 g/mL); **HPLC analysis:** Chiralpak IB column, 85:15 hexanes/iso-propanol, 1.0 mL/min. Major: 10.6 min, minor: 11.6 min. **^{1}HNMR**: (500 MHz, Chloroform-d) δ 7.34 – 7.26 (m, 4H), 7.22 (d, J = 7.3 Hz, 1H), 7.18 (d, J = 7.2 Hz, 2H), 6.96 (d, J = 8.4 Hz, 2H), 4.11 (dd, J = 64.4, 13.0 Hz, 2H), 3.85 (s, 3H), 3.70 (s, 3H), 3.57 (d, J = 11.6 Hz, 1H), 3.48 – 3.38 (m, 1H), 2.80 – 2.66 (m, 2H), 2.60 (dt, J = 15.2, 7.5 Hz, 3H), 2.44 – 2.31 (m, 1H), 2.25 (dd, J = 15.2, 9.9 Hz, 1H), 1.89 (dd, J = 26.0, 10.7 Hz, 3H), 1.81 – 1.71 (m, 1H), 1.42 (dtd, J = 14.4, 9.5, 5.2 Hz, 1H). **^{13}CNMR:** (126 MHz, Chloroform-d) δ 172.46, 140.59, 128.60, 128.25, 126.26, 119.17, 116.76, 114.90, 60.42, 55.43, 51.92, 51.70, 51.51, 39.71, 36.06, 35.90, 33.72, 30.50, 29.07, 21.82. **IR** (ATR, neat) 2925, 1734, 1673, 1612, 1514, 1454, 1251, 1180, 1032, 830 cm^{-1} **LRMS** (ESI) *m/z* [M+H] calcd 421.2, found 421.3

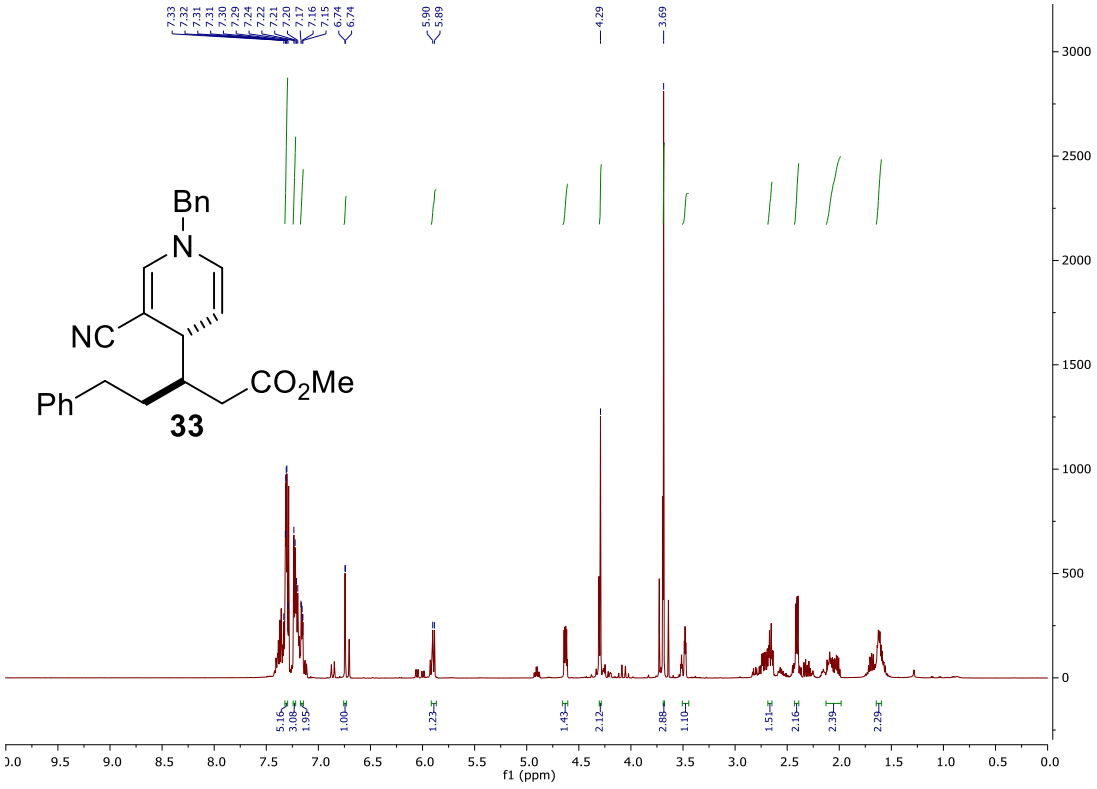
7.33
7.32
7.31
7.31
7.30
7.29
7.24
7.22
7.21
7.20
7.17
7.16
7.15
6.74
6.74
5.90
5.89
4.29
3.69
Bn
N
NC
CO2Me
Ph
33
5.16
3.08
1.95
1.00
1.23
1.43
2.12
2.88
1.10
1.51
2.16
2.39
2.29
f1 (ppm)

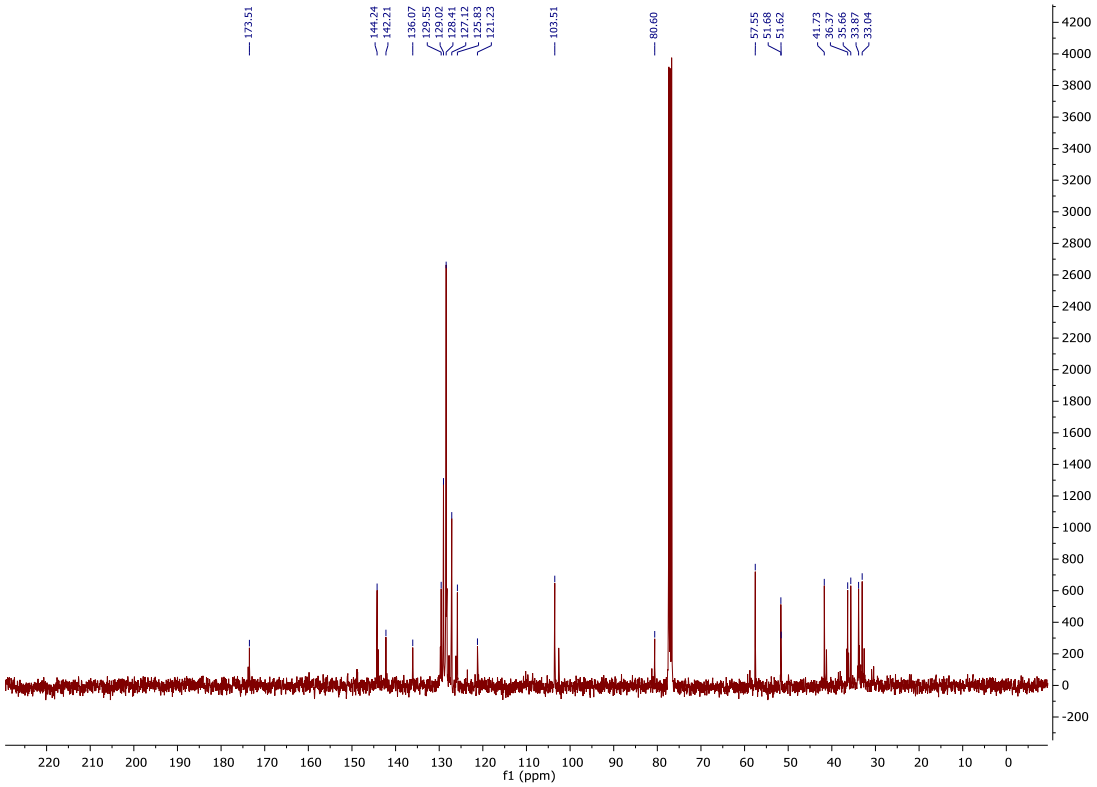
173.51
144.24
142.21
136.07
129.55
129.02
128.41
127.12
125.83
121.23
103.51
80.60
57.55
51.68
51.62
41.73
36.37
35.66
33.87
33.04
f1 (ppm)

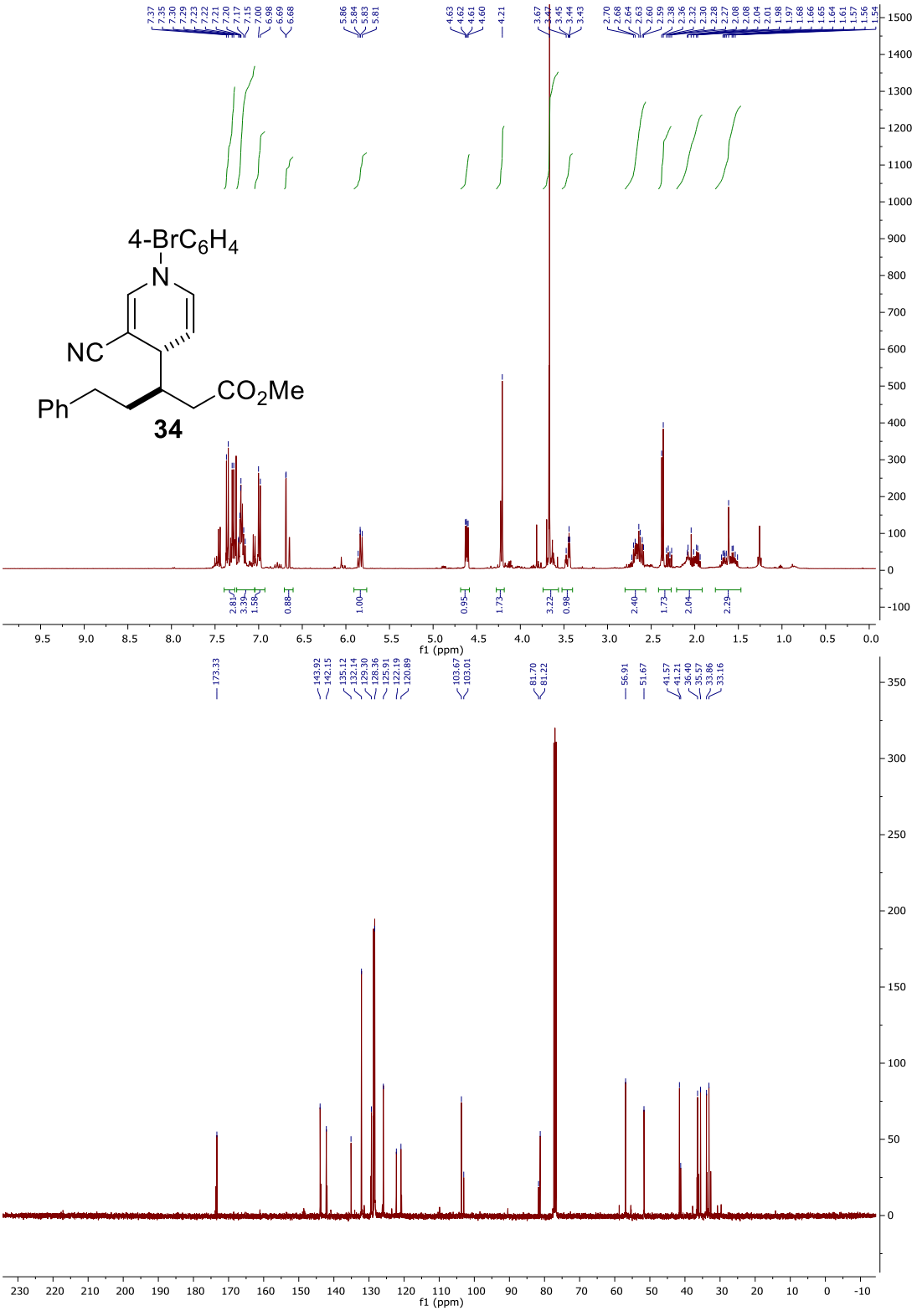
4-BrC6H4
N
NC
CO2Me
Ph
34
f1 (ppm)
f1 (ppm)

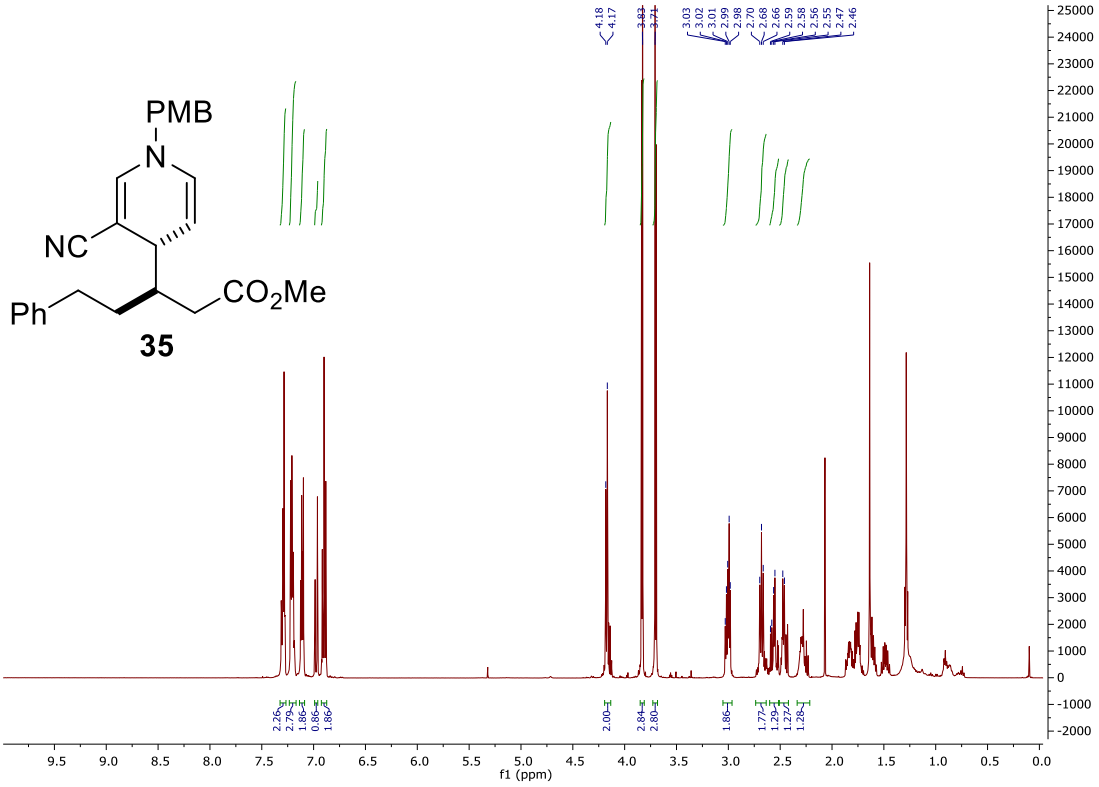
PMB
N
NC
CO2Me
Ph
35
f1 (ppm)

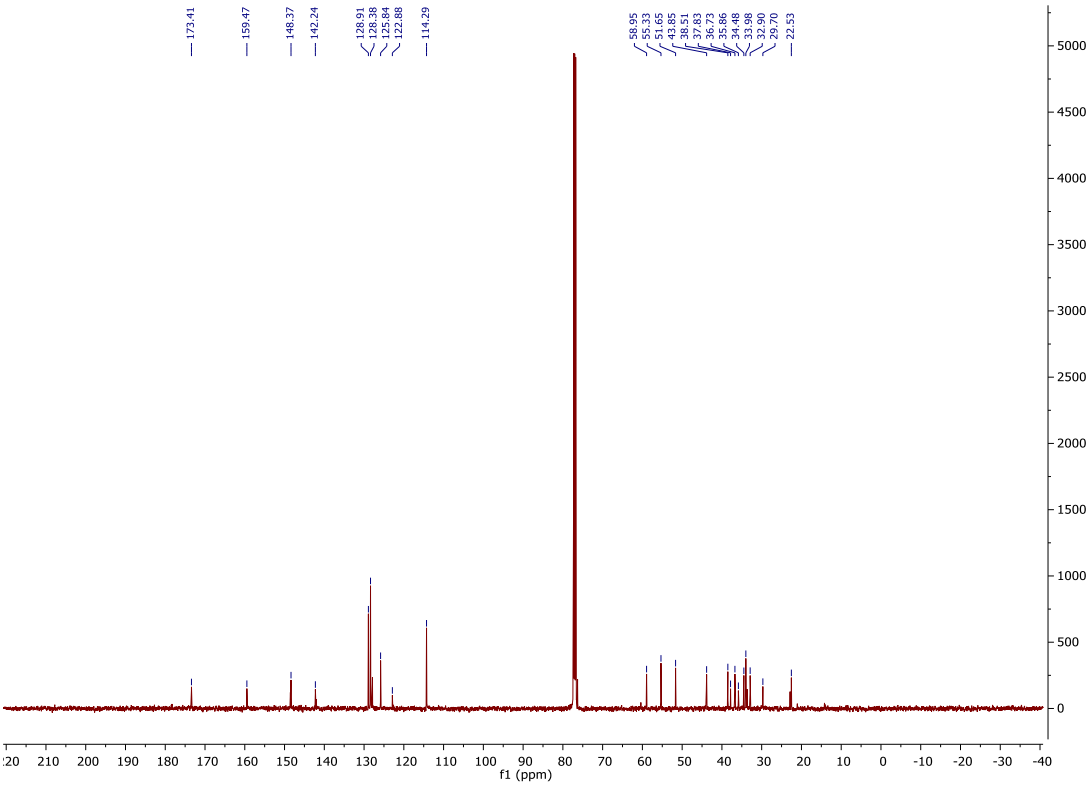
f1 (ppm)

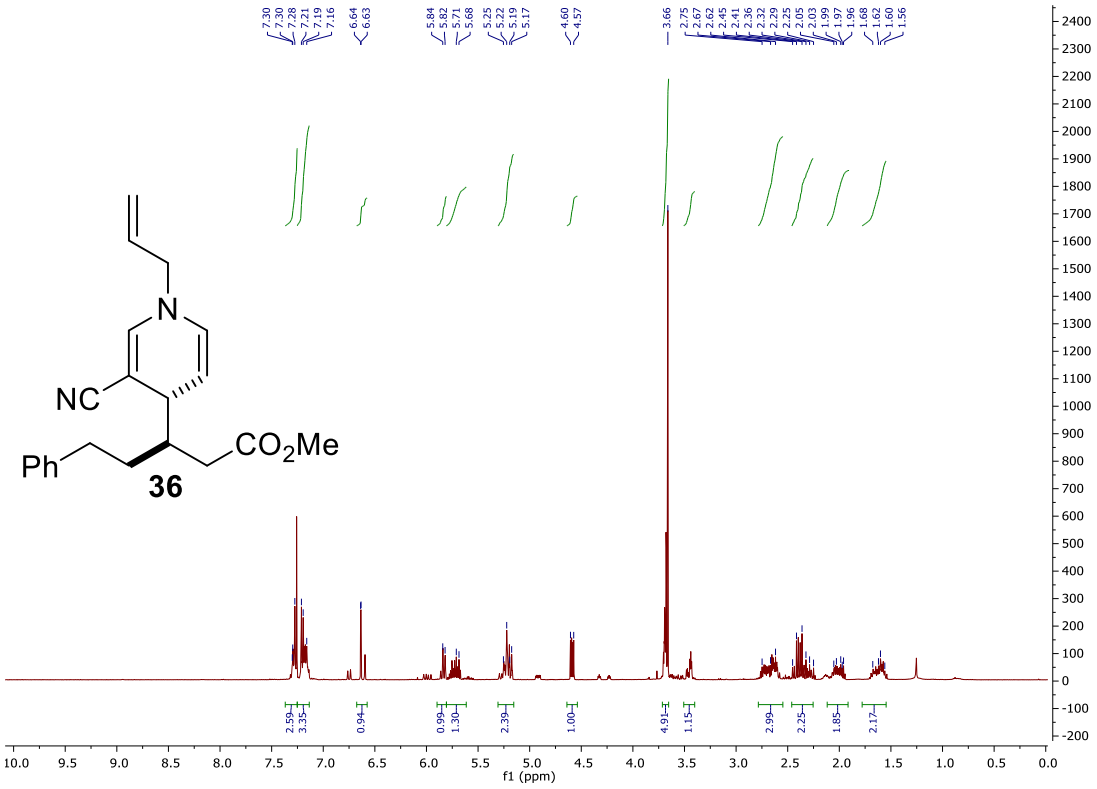
7.30
7.30
7.28
7.21
7.19
7.16
6.64
6.63
5.84
5.82
5.71
5.68
5.25
5.22
5.19
5.17
4.60
4.57
3.66
2.75
2.67
2.62
2.45
2.41
2.36
2.32
2.29
2.25
2.05
2.03
1.99
1.97
1.96
1.68
1.62
1.60
1.56
N
NC
CO2Me
Ph
36
2.59
3.35
0.94
0.99
1.30
2.39
1.00
4.91
1.15
2.99
2.25
1.85
2.17
f1 (ppm)

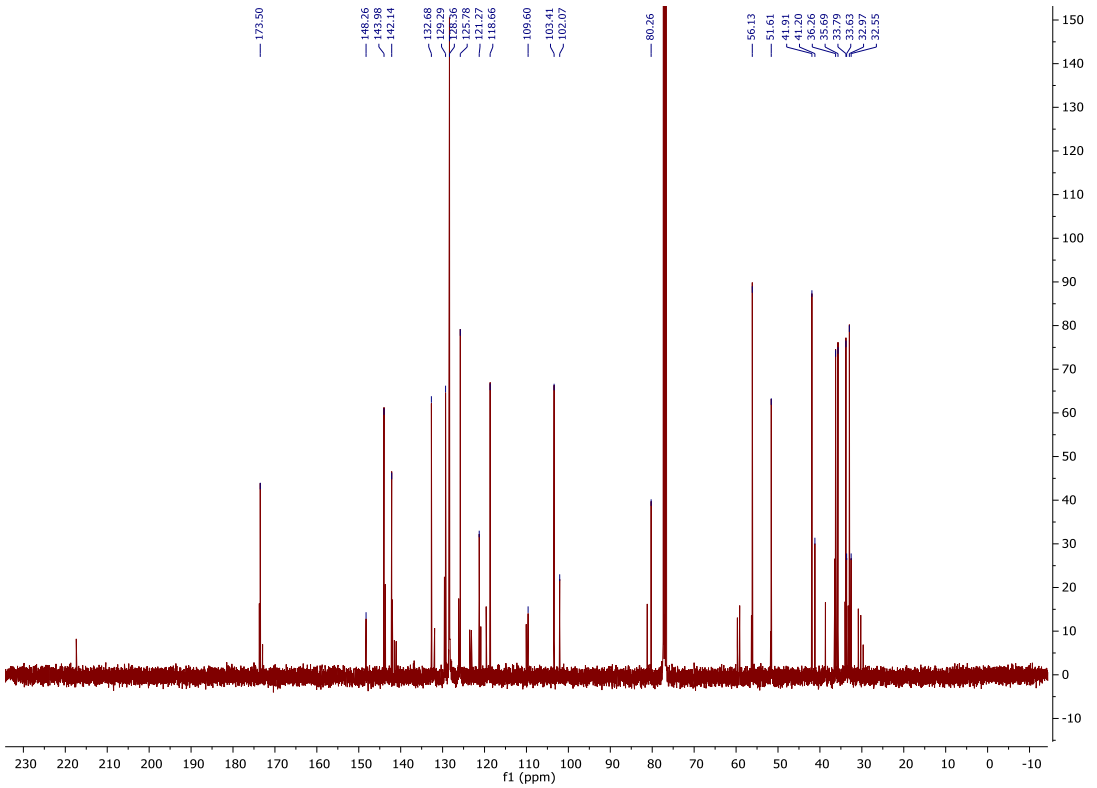
173.50
148.26
143.98
142.14
132.68
129.29
128.36
125.78
121.27
118.66
109.60
103.41
102.07
80.26
56.13
51.61
41.91
41.20
36.26
35.69
33.79
33.63
33.27
32.55
f1 (ppm)

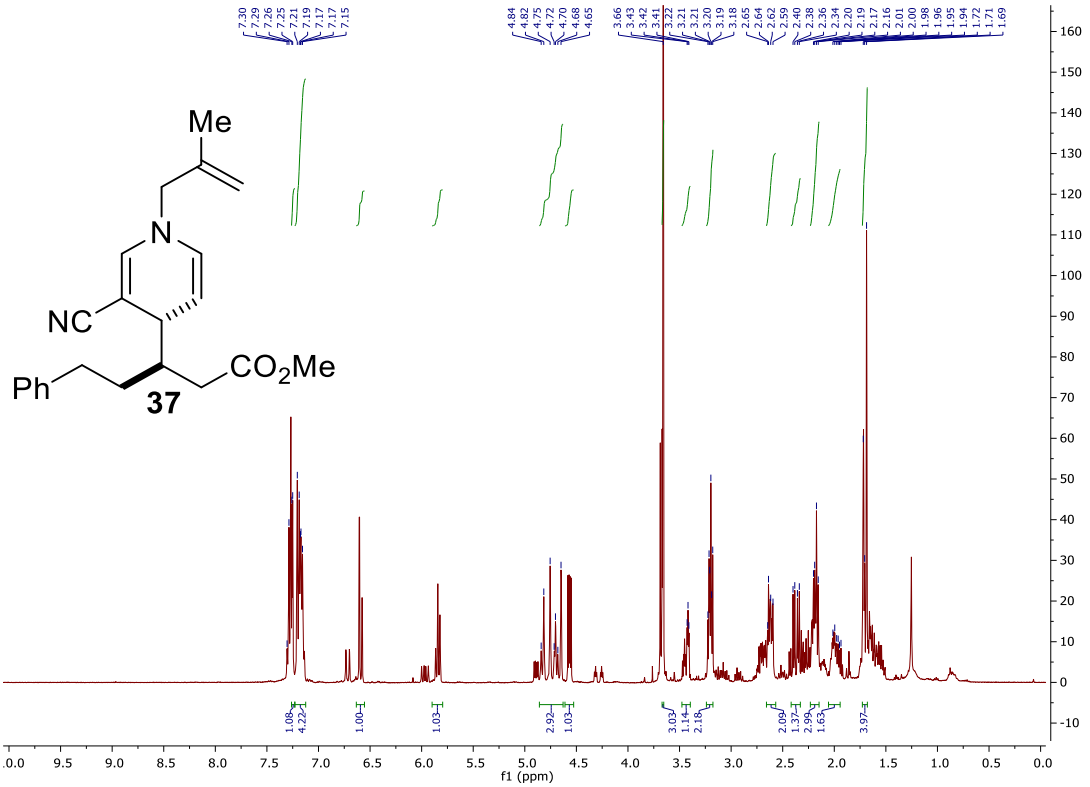
Me
N
NC
Ph
CO2Me
37
f1 (ppm)

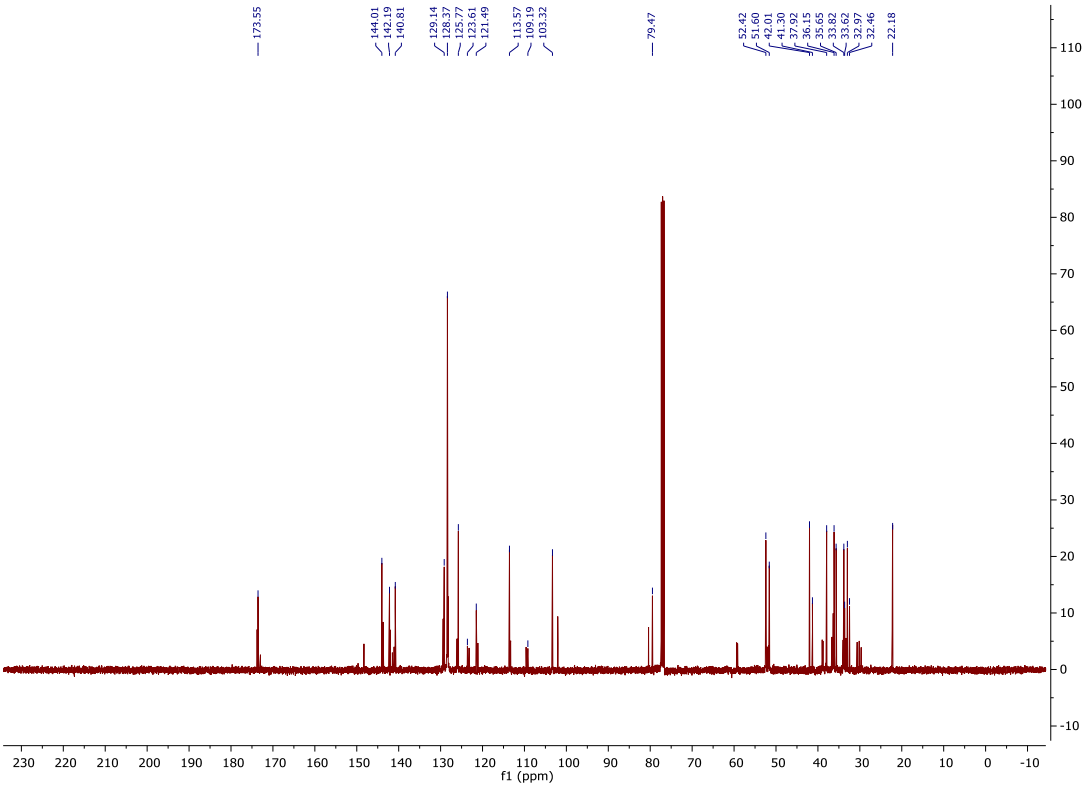
f1 (ppm)

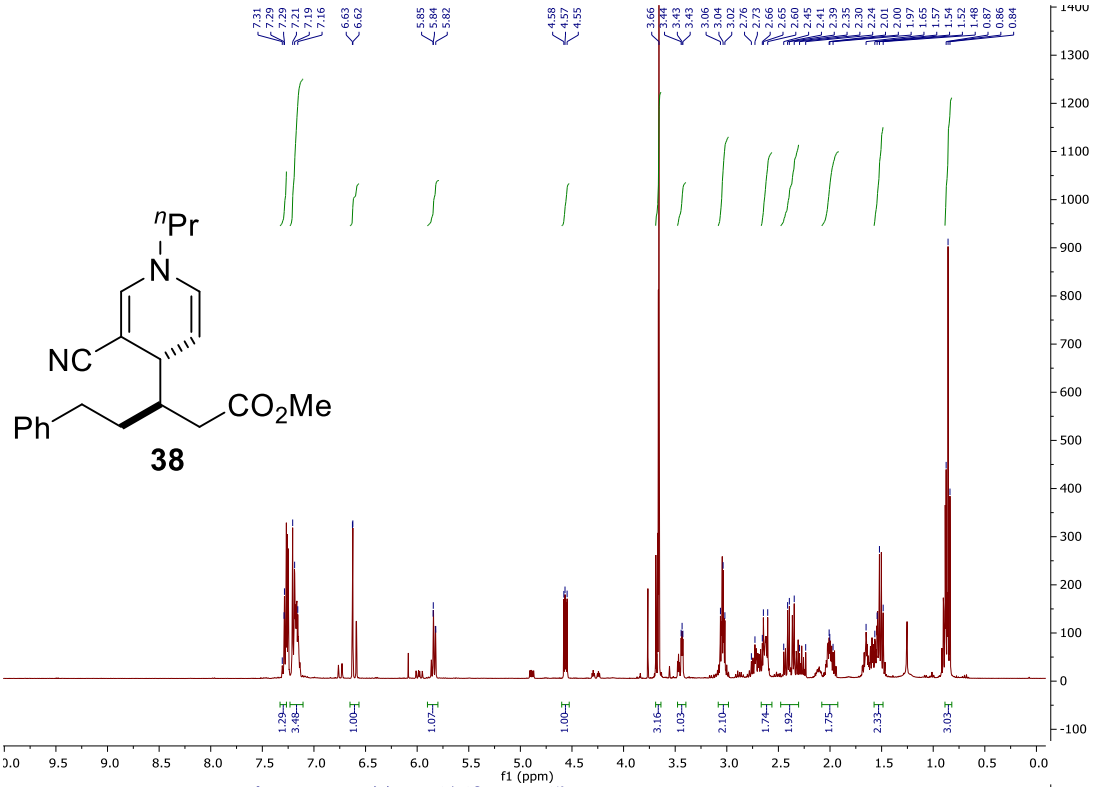
nPr
N
NC
CO2Me
Ph
38
f1 (ppm)

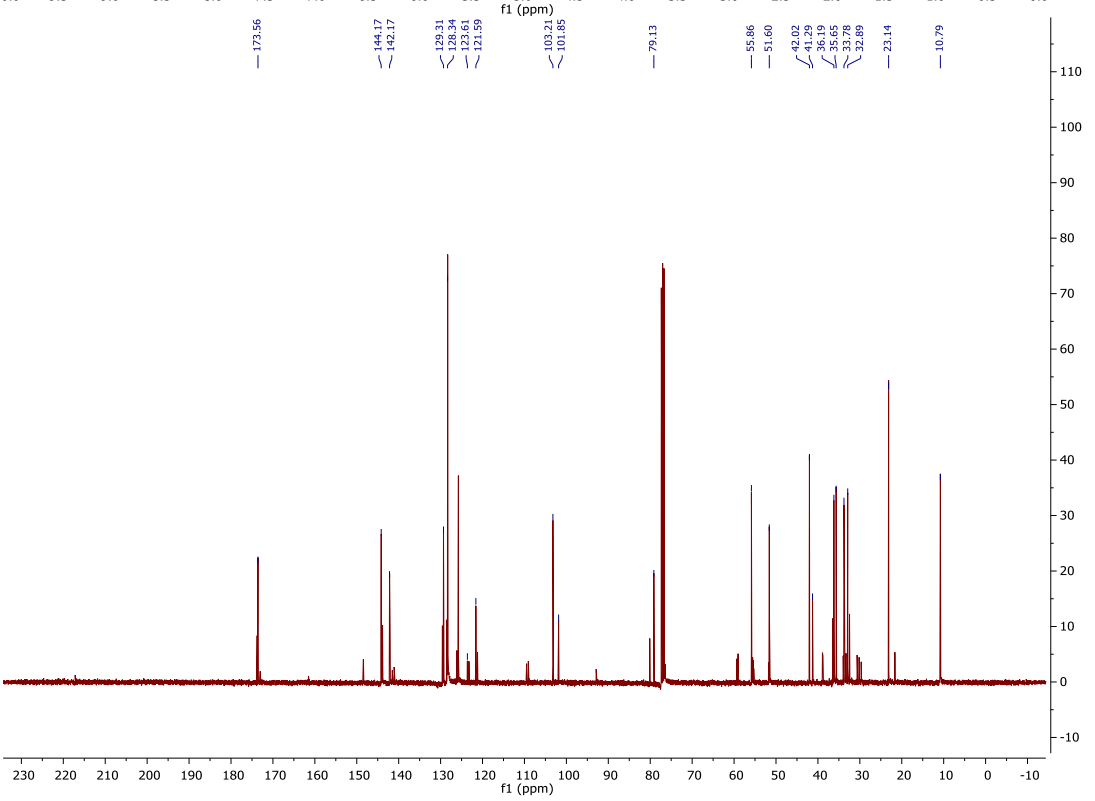
f1 (ppm)

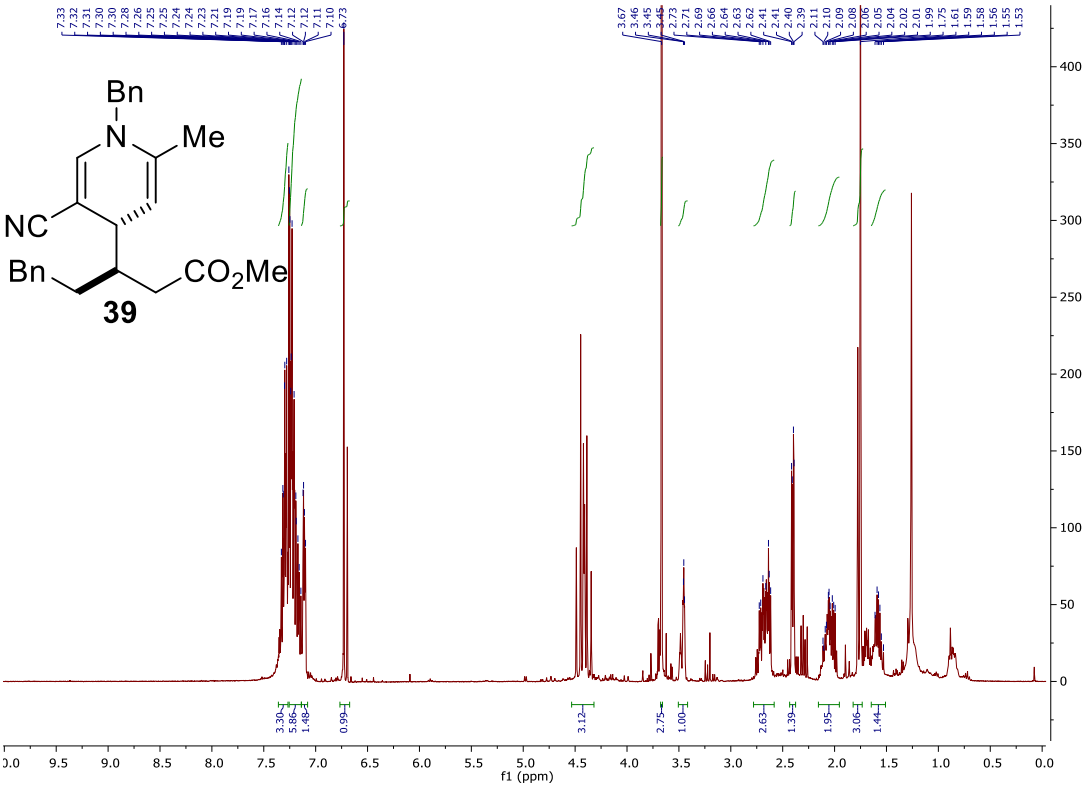
Bn
N
Me
NC
Bn
CO2Me
39
f1 (ppm)

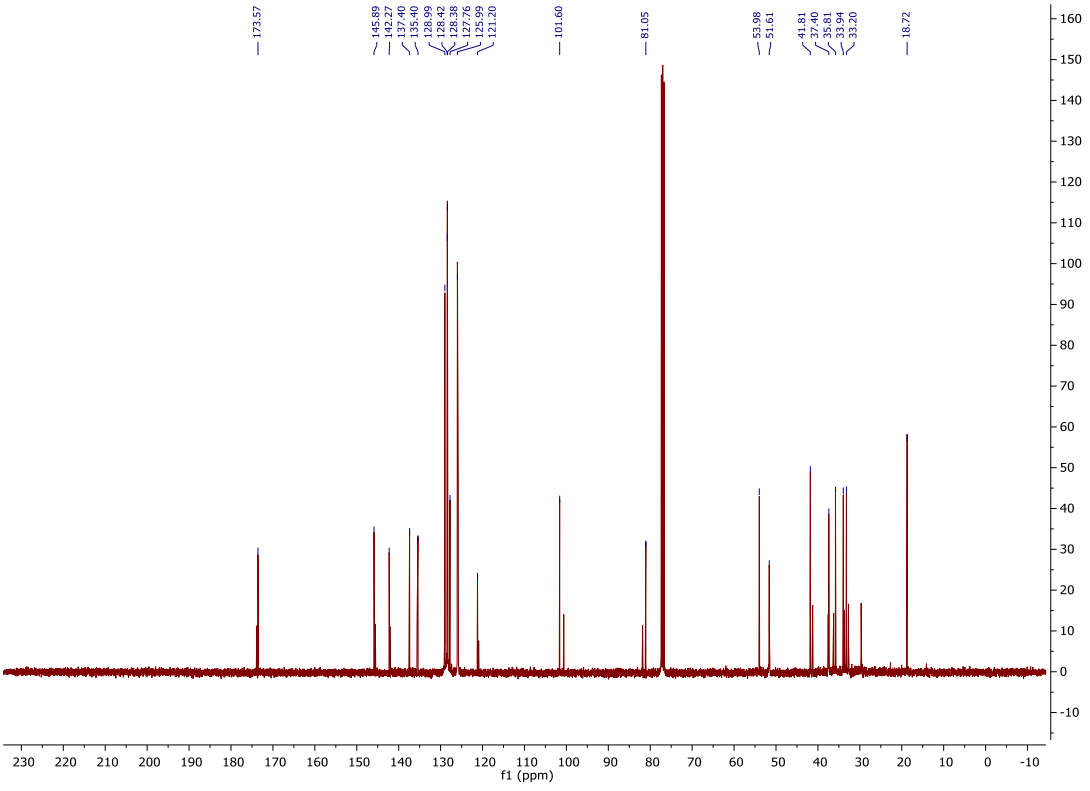
f1 (ppm)

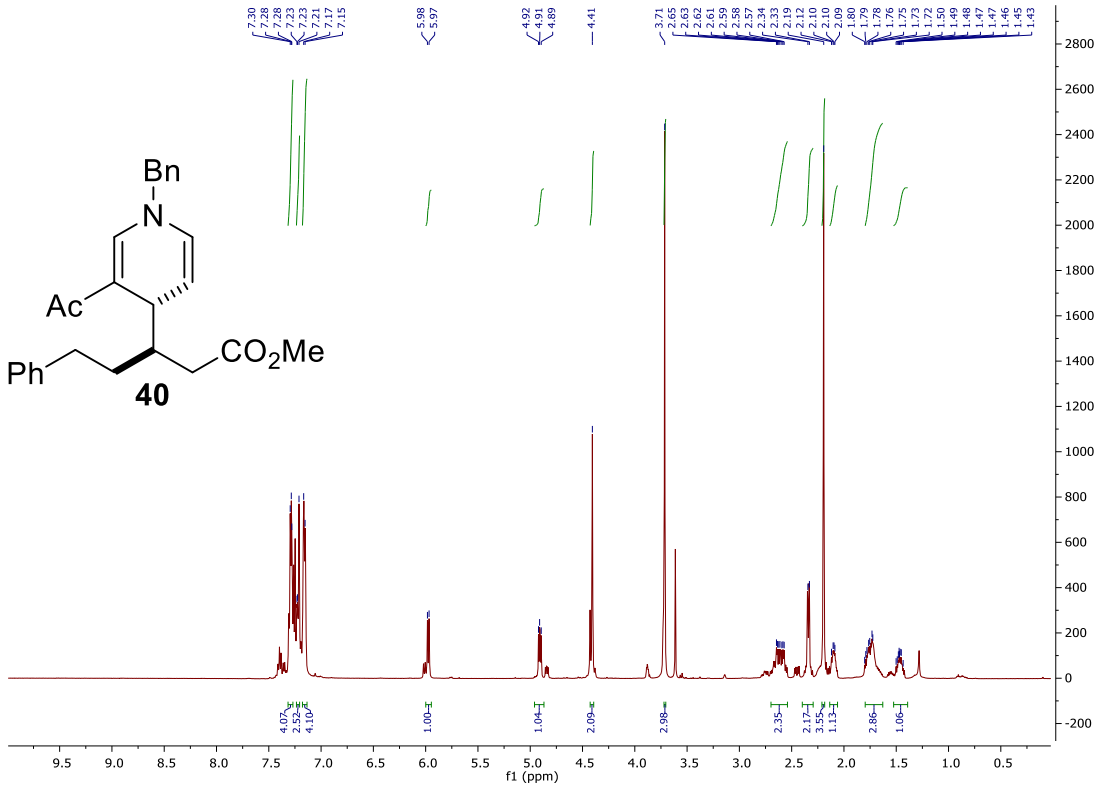
Bn
N
Ac
Ph
CO2Me
40
f1 (ppm)

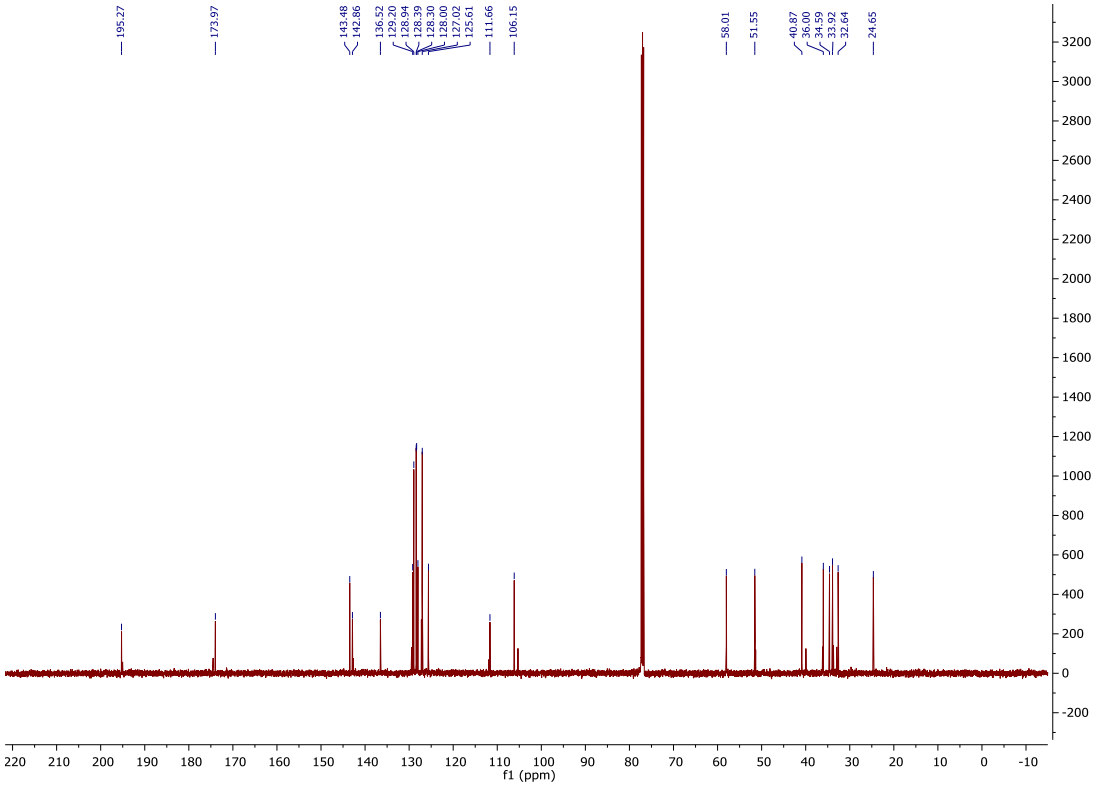
f1 (ppm)

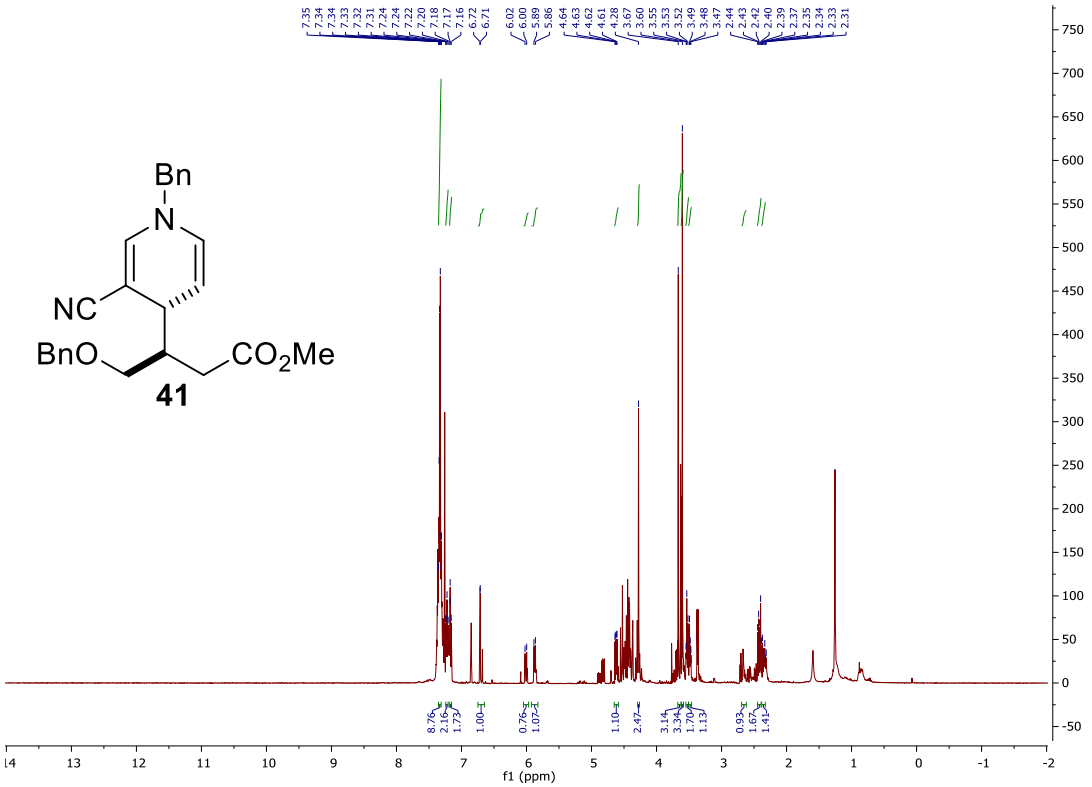
Bn
N
NC
BnO
CO2Me
41
f1 (ppm)

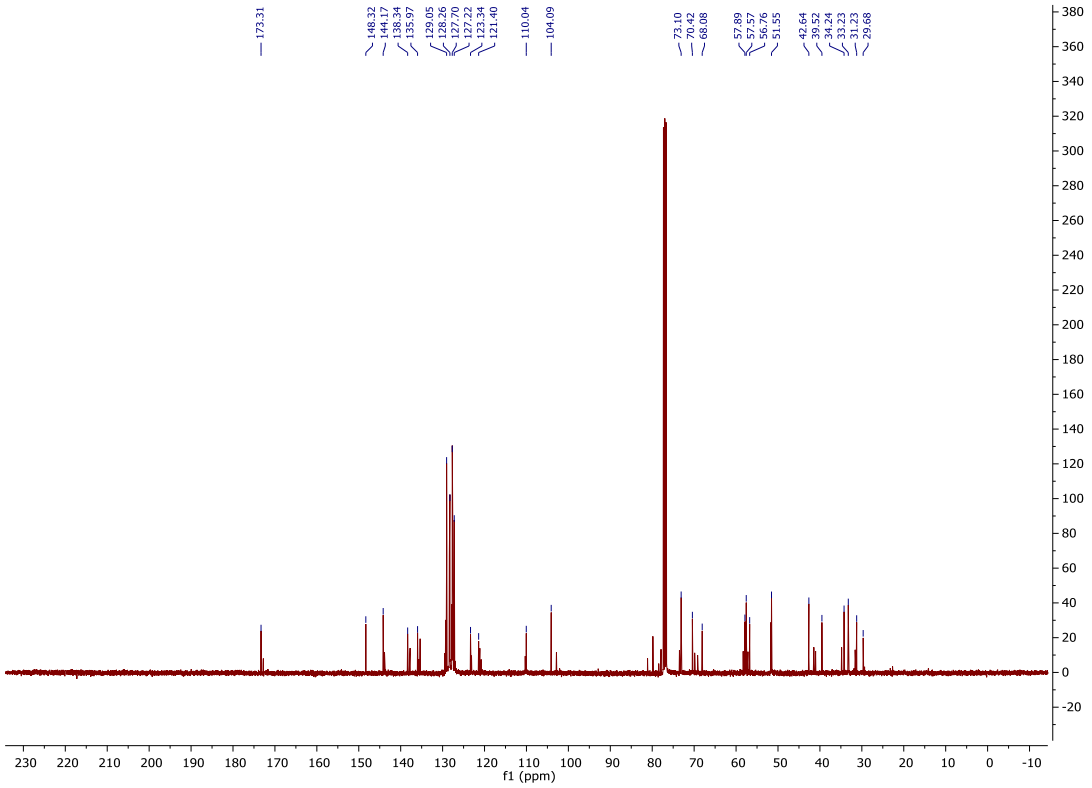
f1 (ppm)

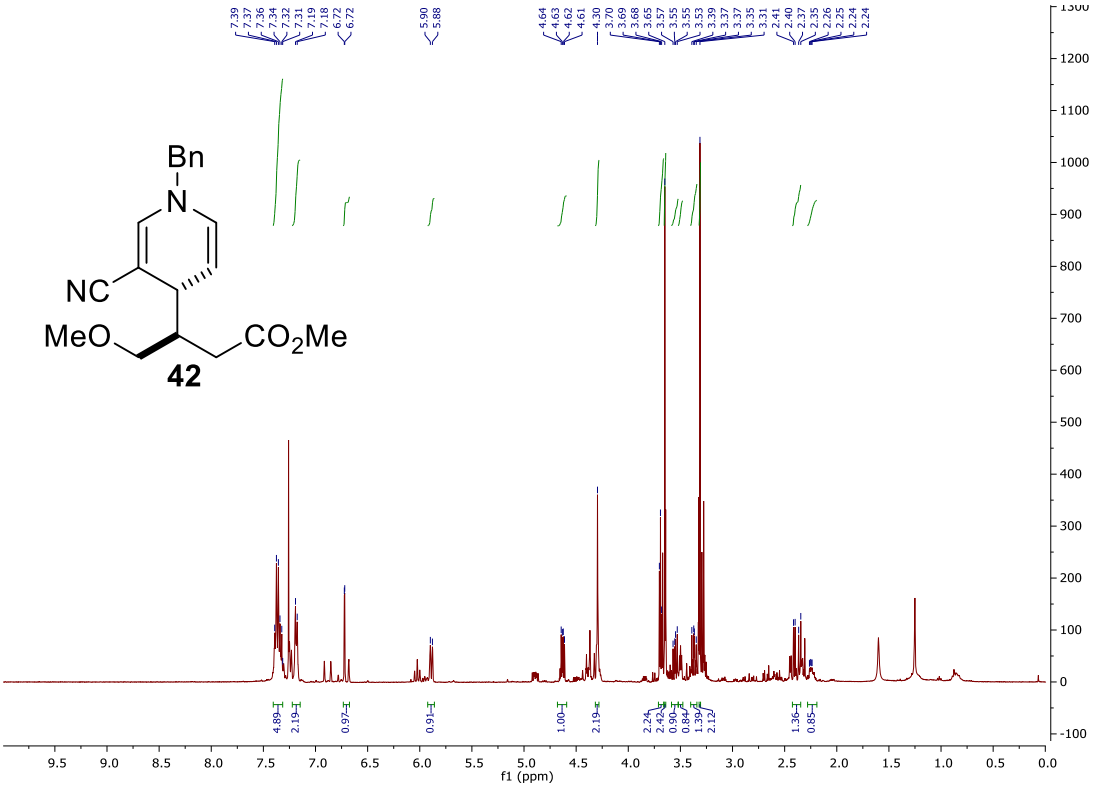
Bn
N
NC
MeO
CO2Me
42
f1 (ppm)

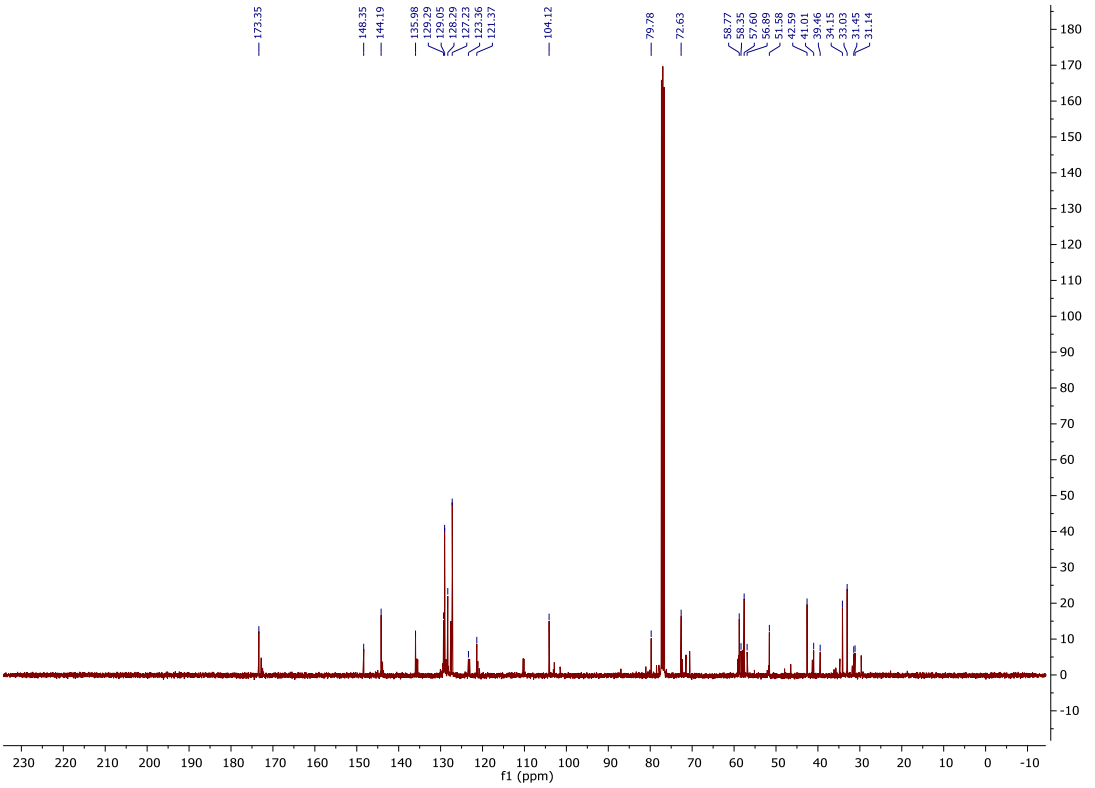
f1 (ppm)

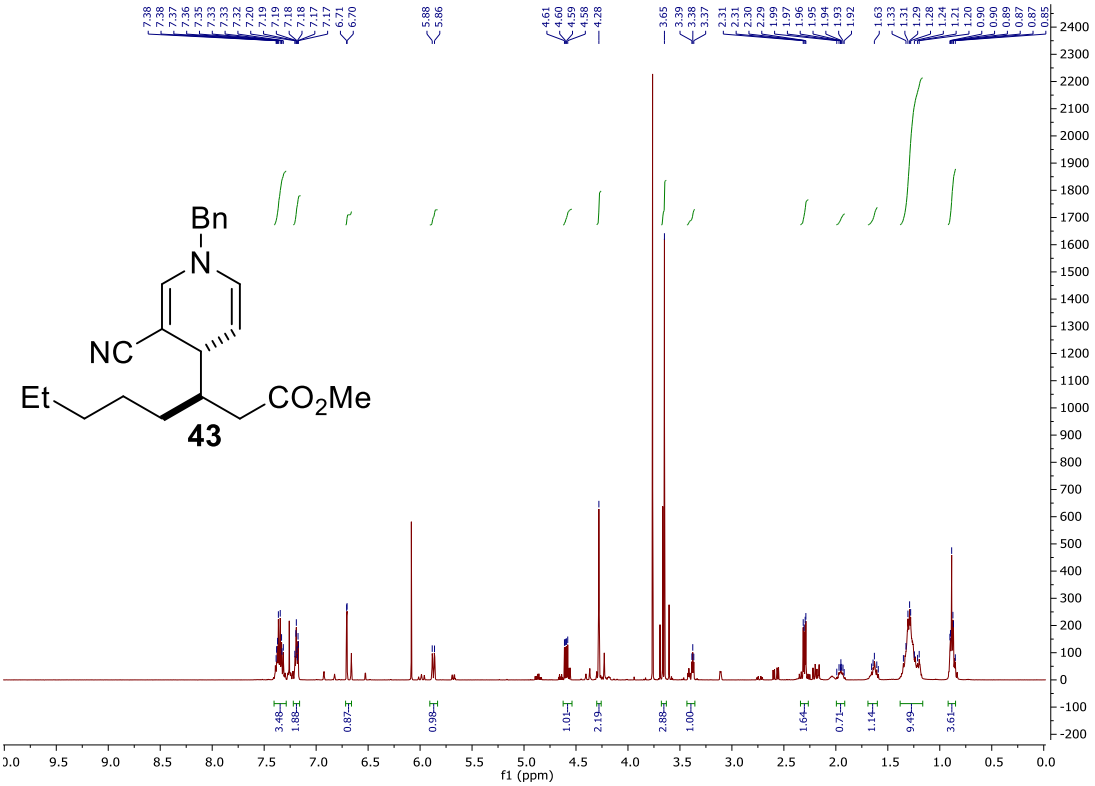
Bn
N
NC
Et
CO2Me
43
f1 (ppm)

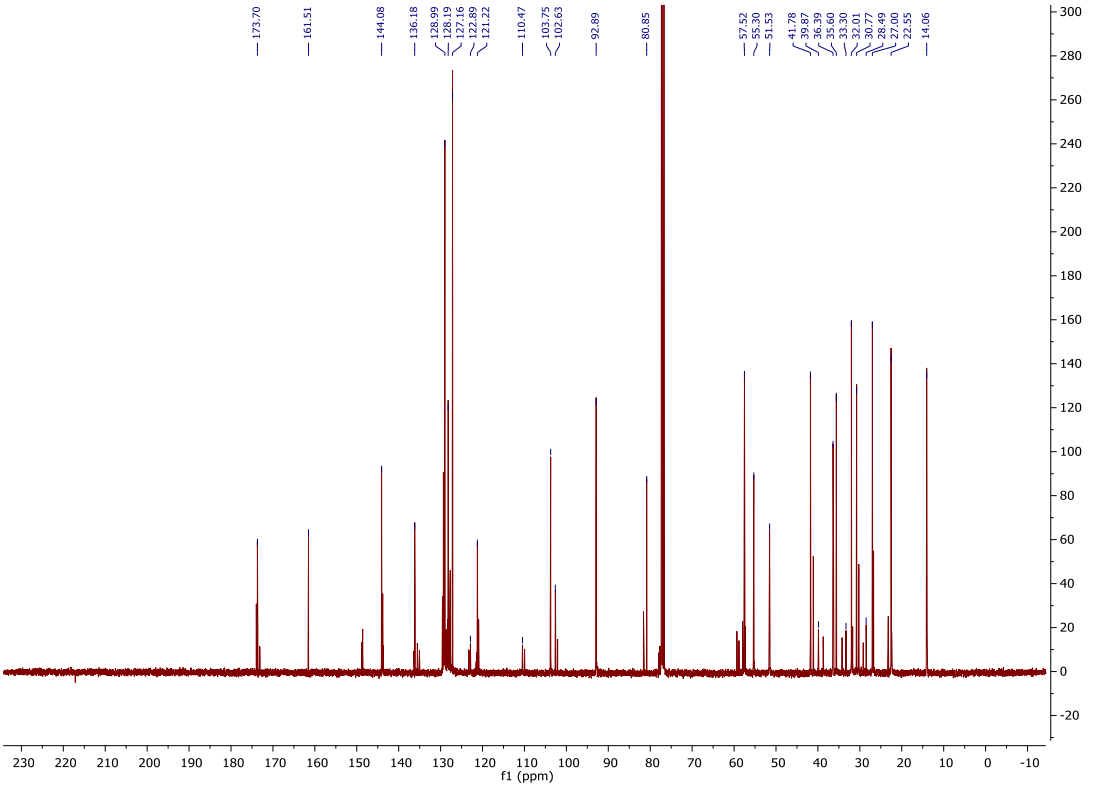
f1 (ppm)

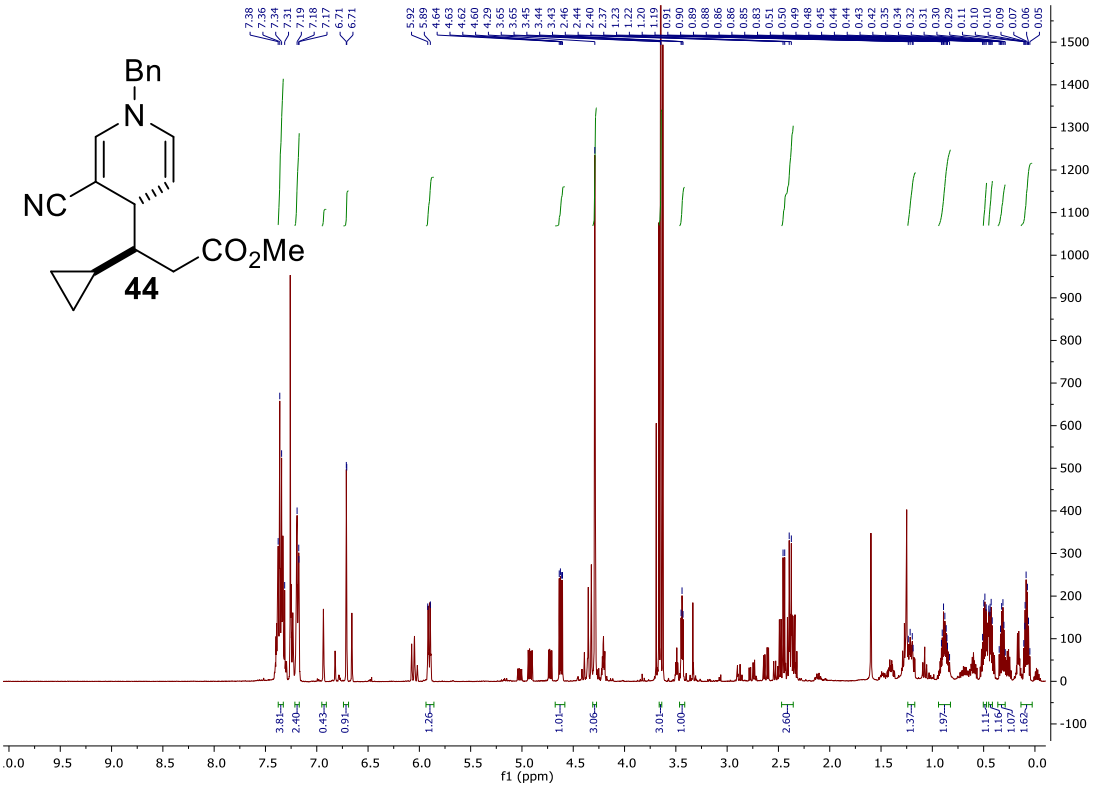
Bn
N
NC
CO2Me
44
f1 (ppm)

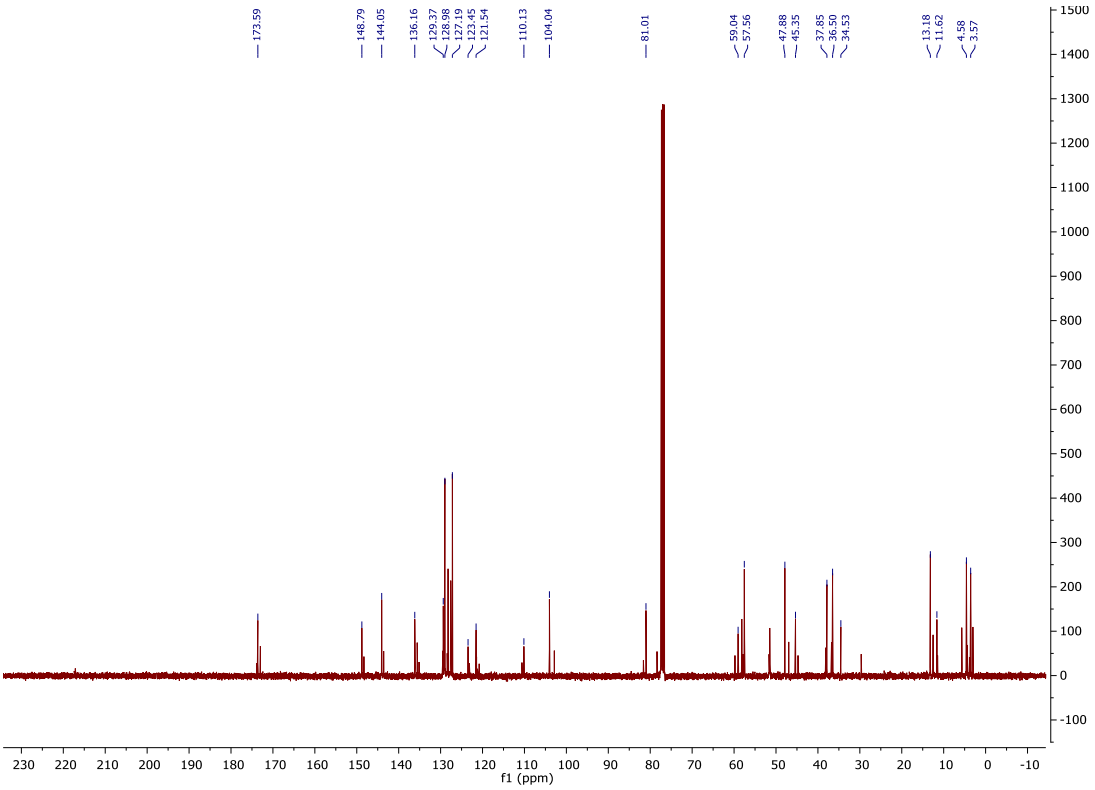
f1 (ppm)

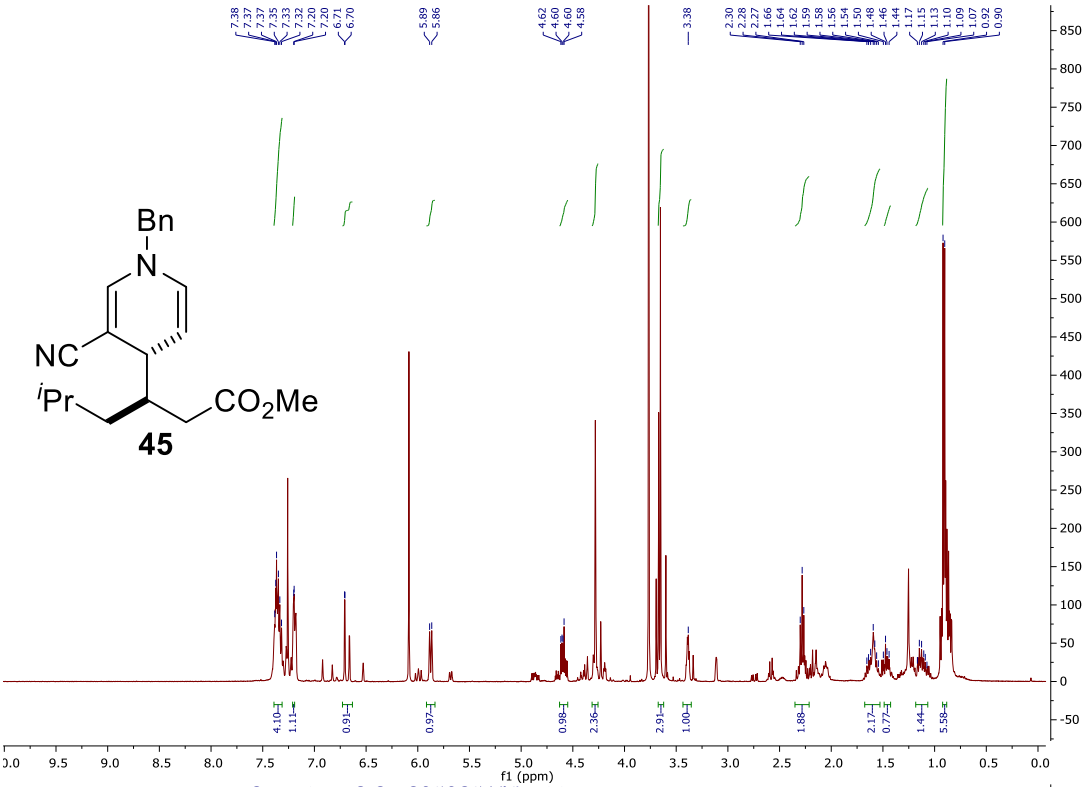
Bn
N
NC
iPr
CO2Me
45
f1 (ppm)

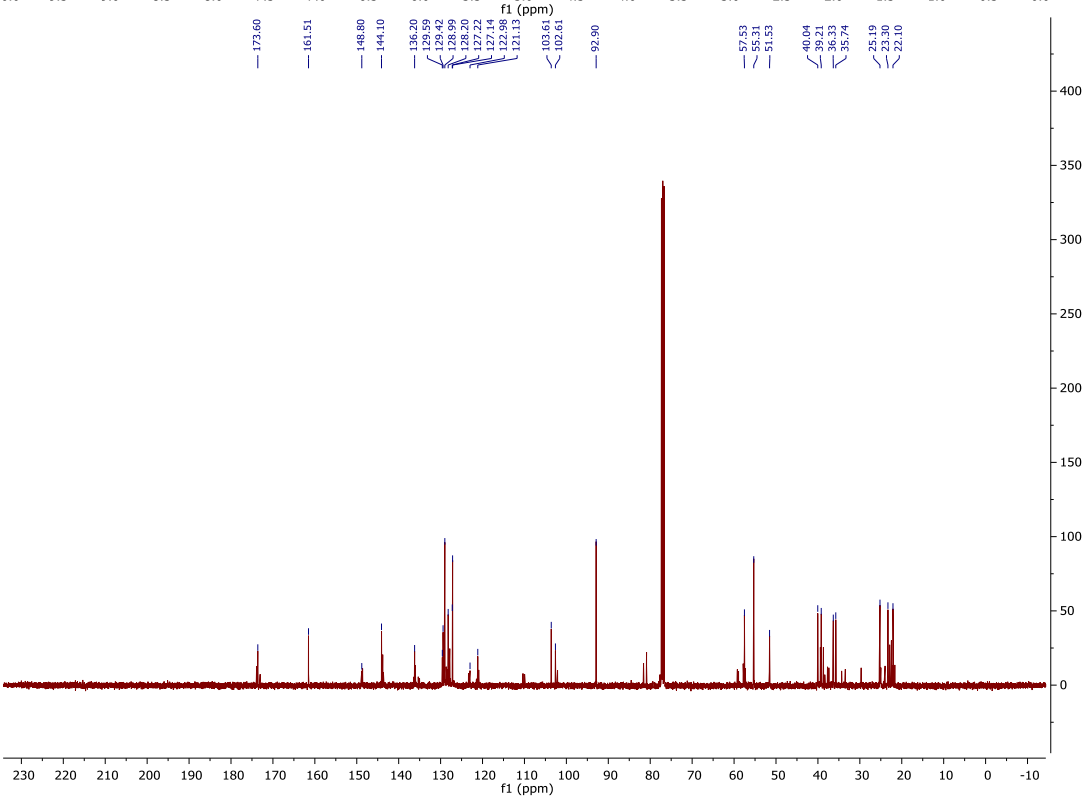
f1 (ppm)

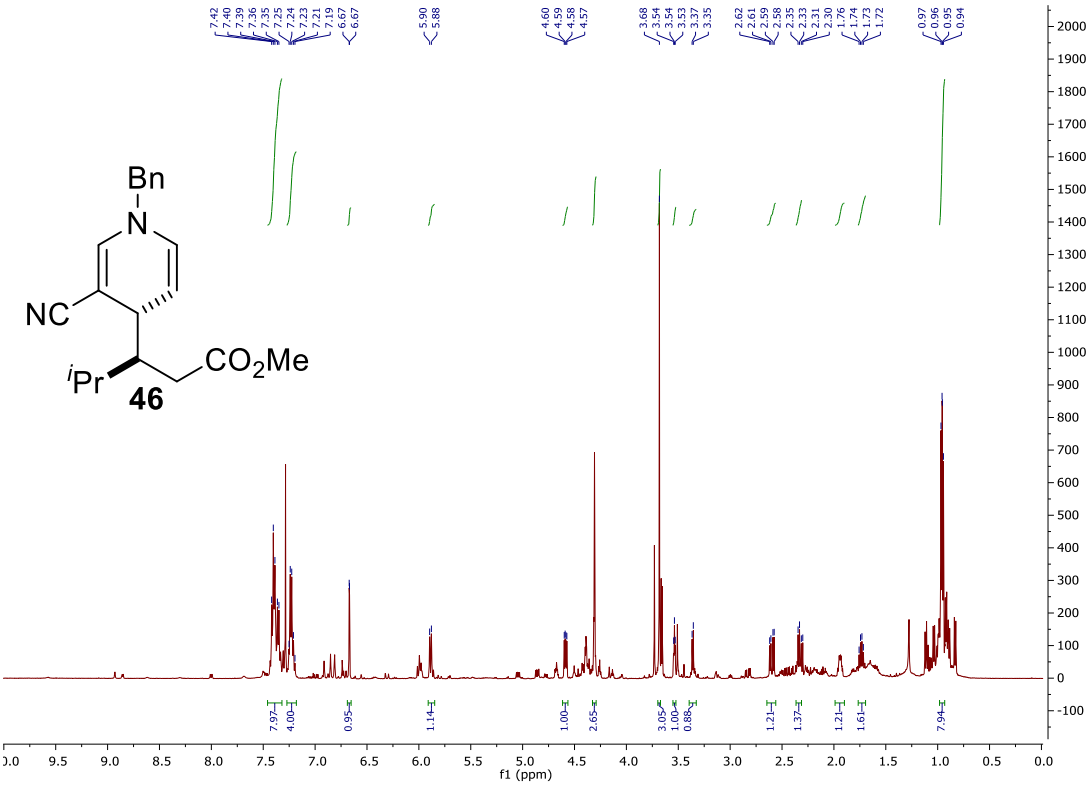
Bn
N
NC
^{i}Pr
CO_2Me
46
f1 (ppm)

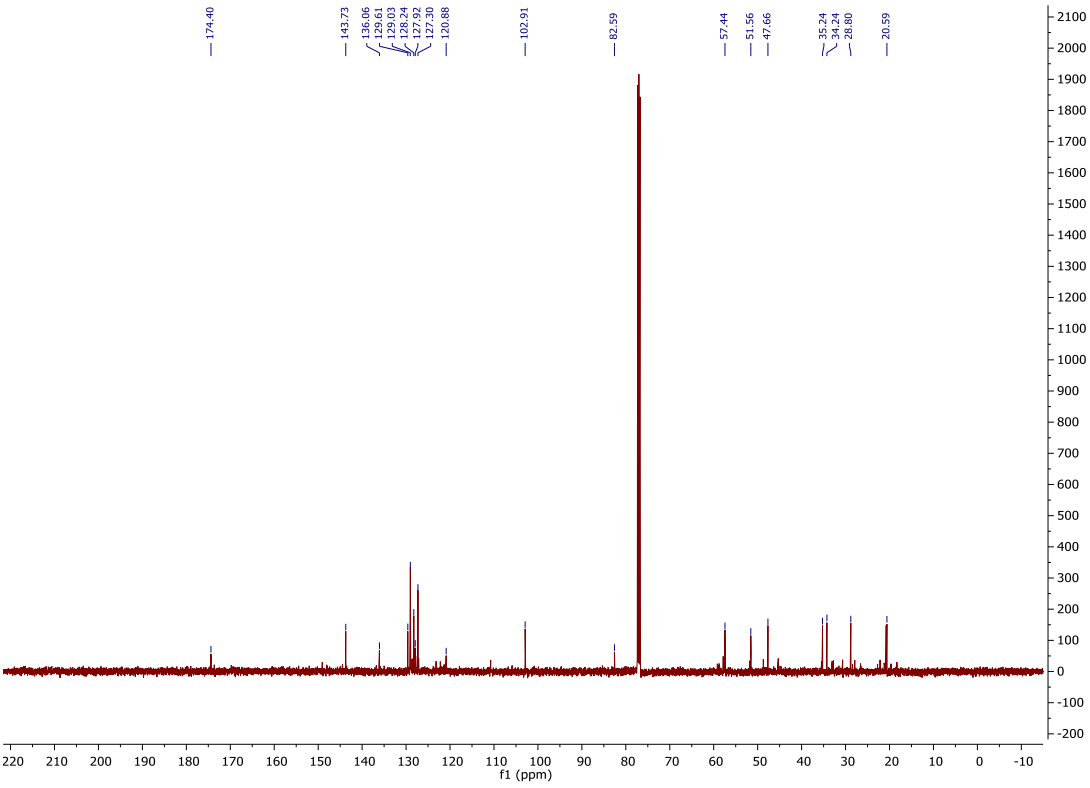
f1 (ppm)

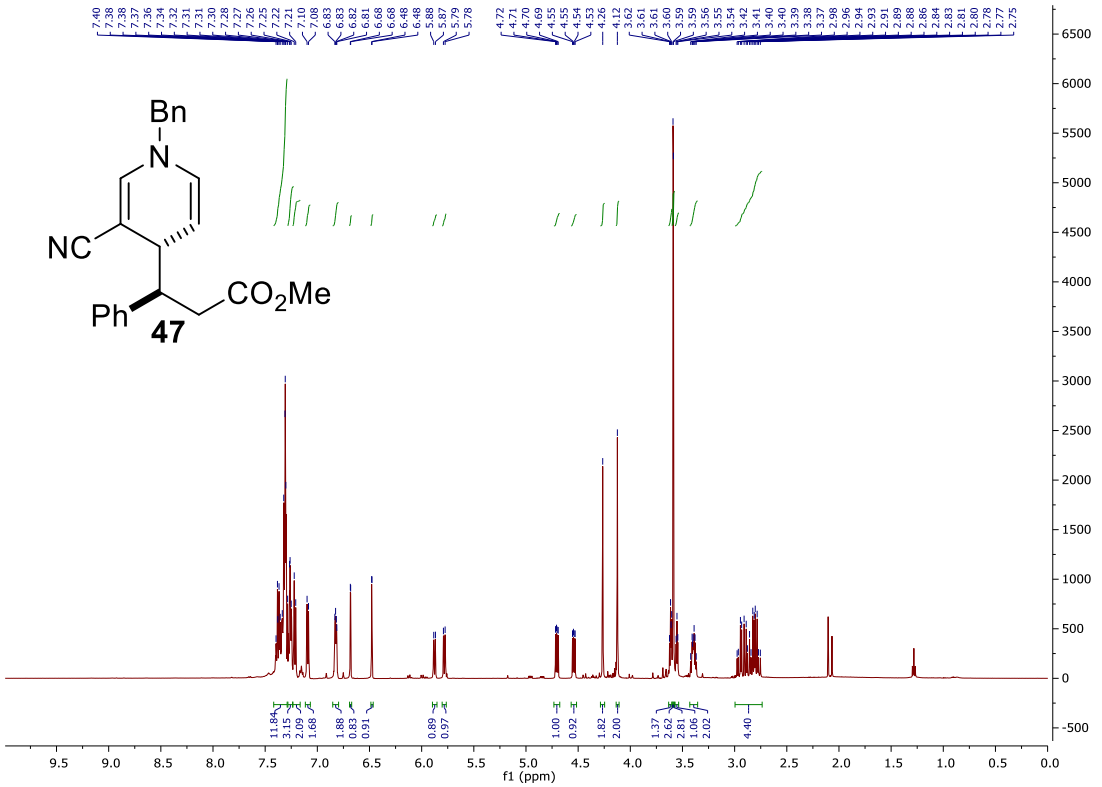
Bn
N
NC
CO2Me
Ph
47
f1 (ppm)

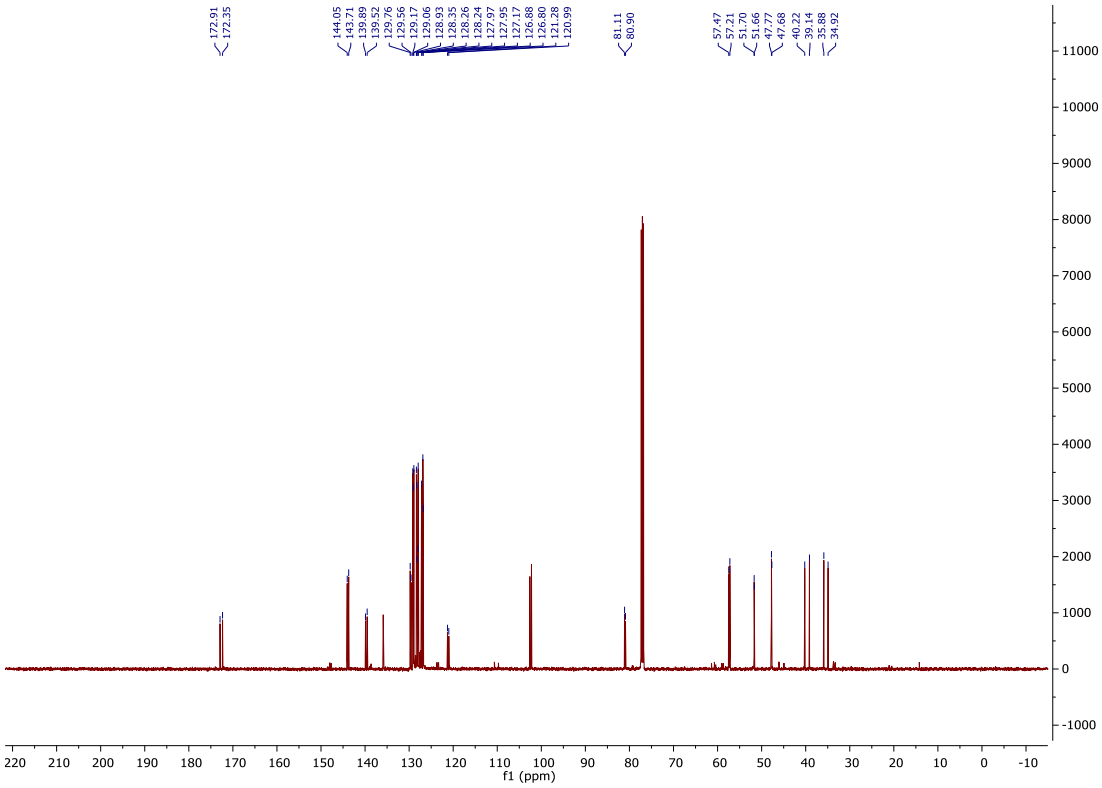
f1 (ppm)

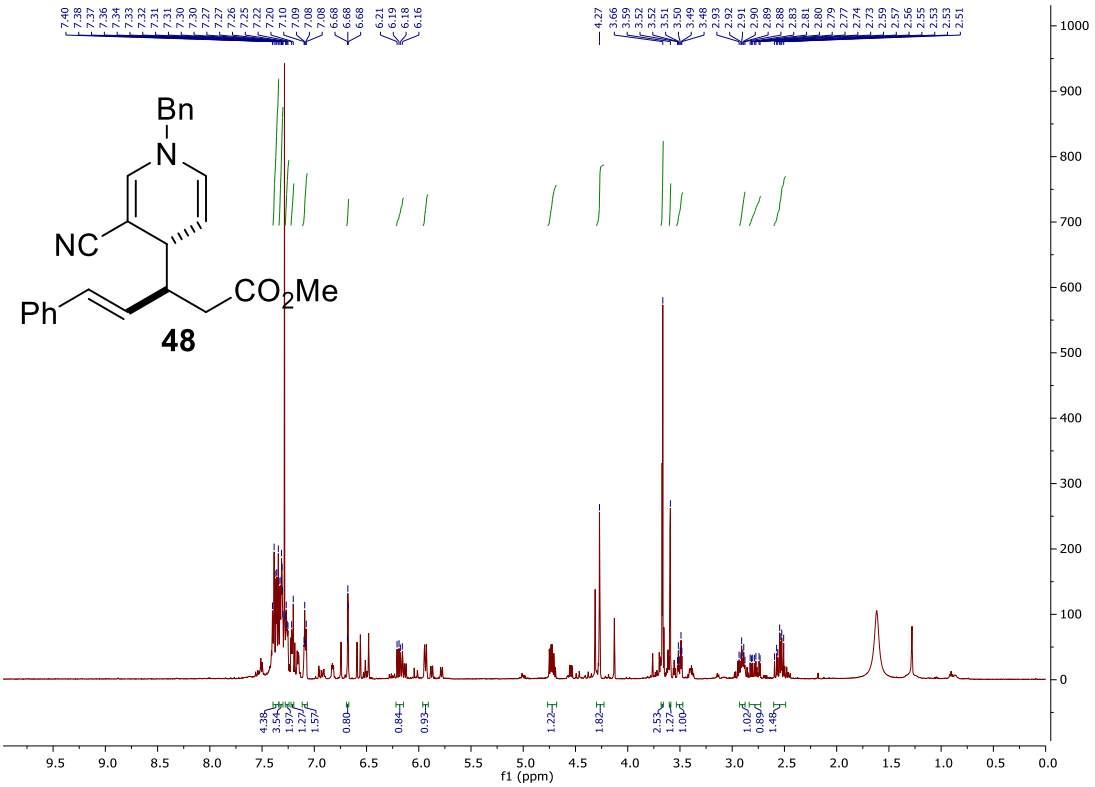
Bn
N
NC
CO2Me
Ph
48
f1 (ppm)

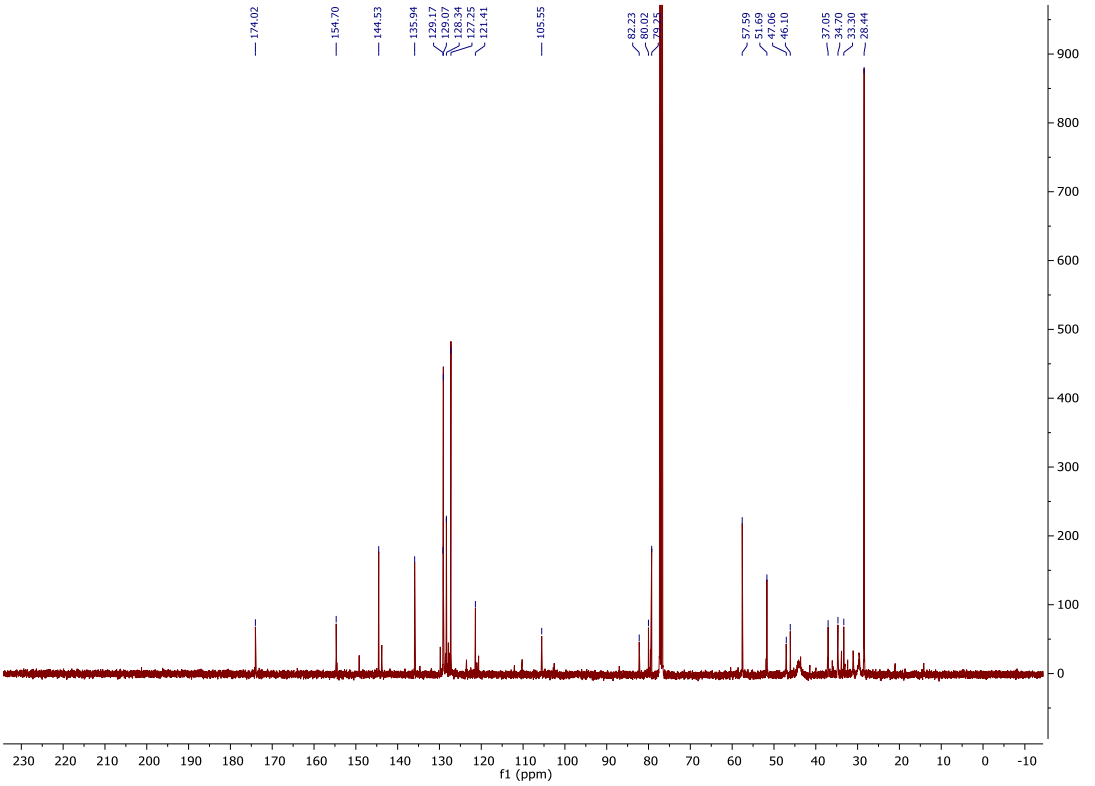
f1 (ppm)

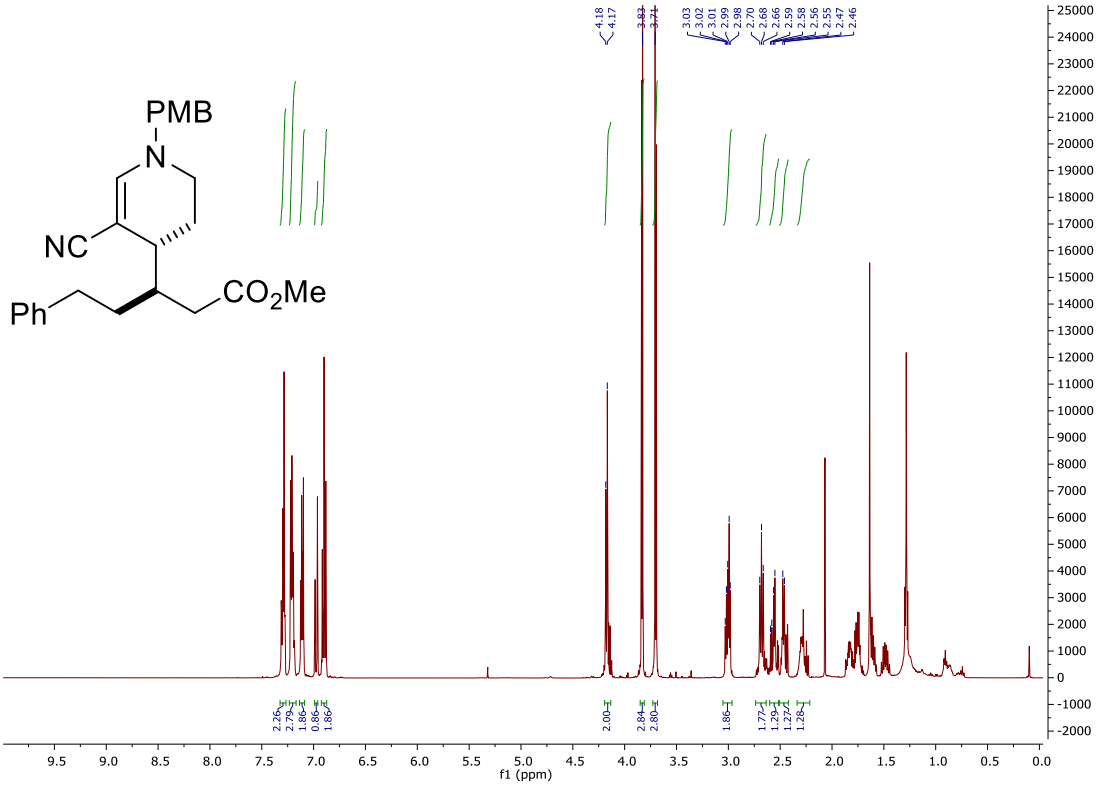
PMB
N
NC
CO2Me
Ph
f1 (ppm)

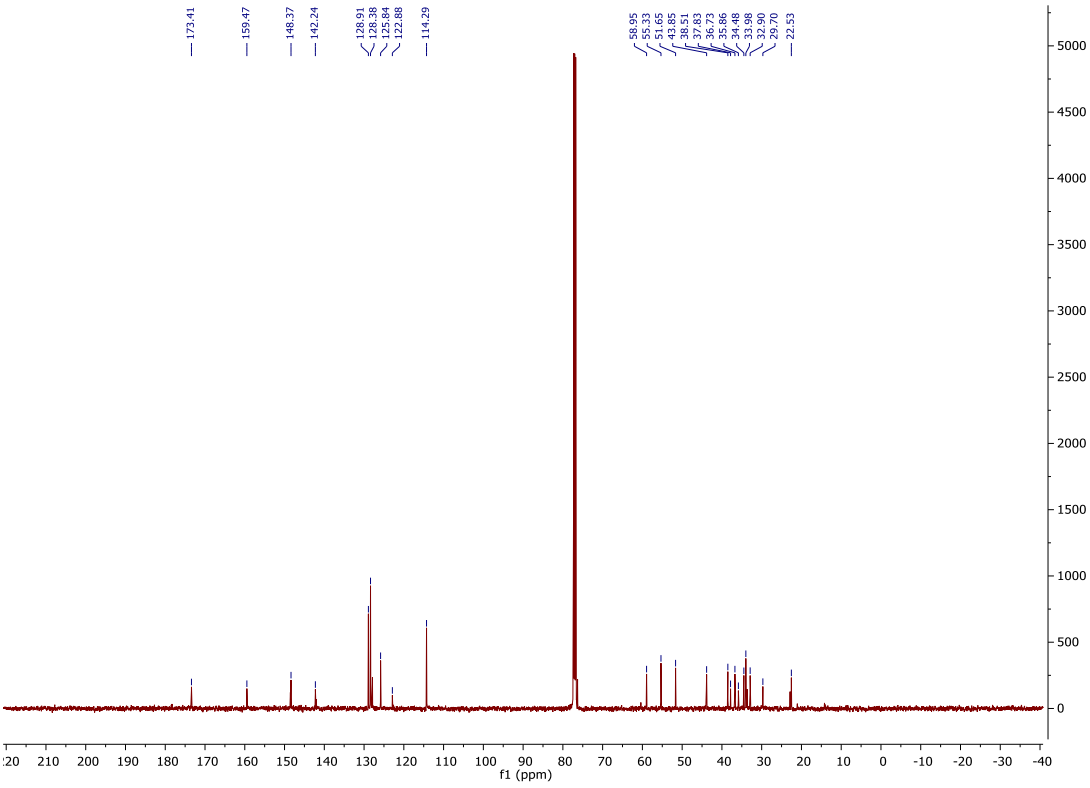
f1 (ppm)

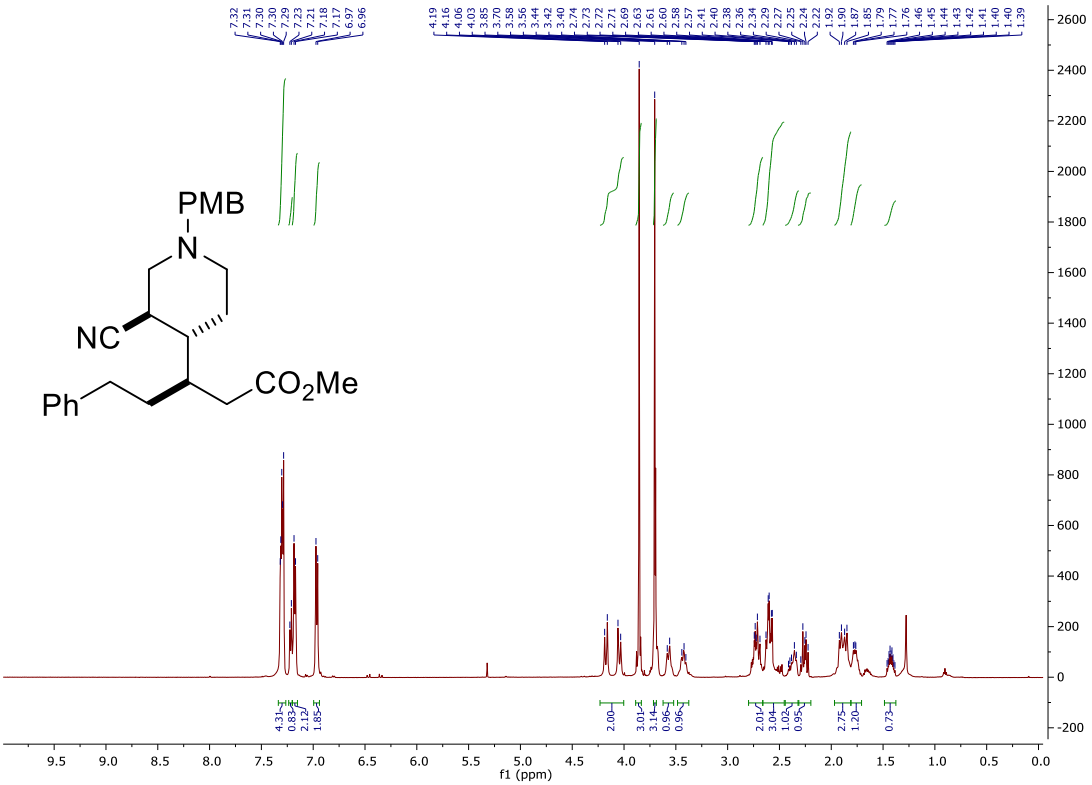
PMB
N
NC
Ph
CO2Me
f1 (ppm)

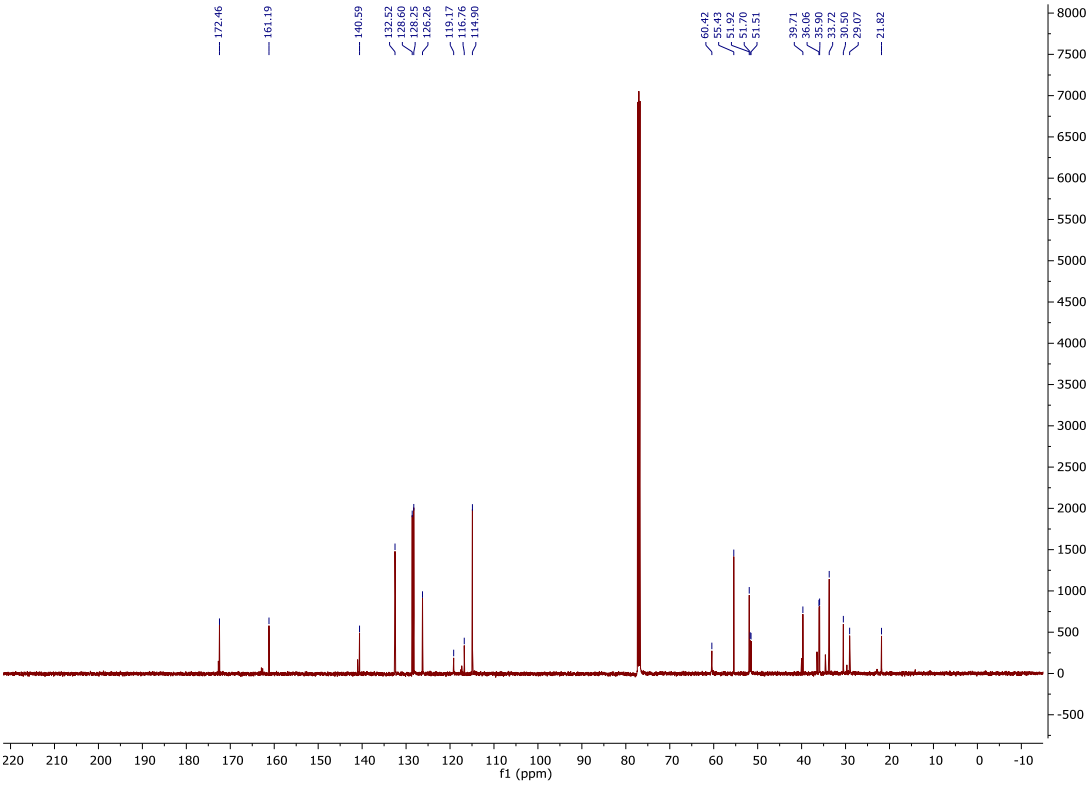
172.46
161.19
140.59
132.52
128.60
128.25
126.26
119.17
116.76
114.90
60.42
55.43
51.92
51.70
51.51
39.71
36.06
35.90
33.72
30.50
29.07
21.82
f1 (ppm)

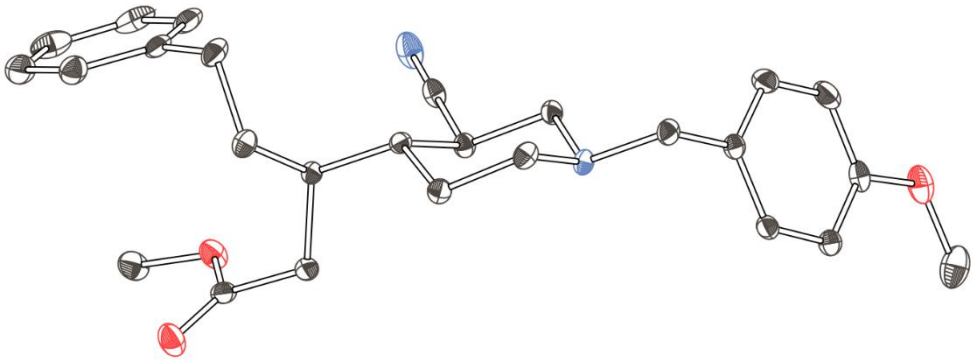

Single crystal X-ray diffraction.[1] Data for all compounds was collected on an Agilent SuperNova diffractometer using mirror-monochromated Cu Kα. Data collection, integration, scaling (ABSPACK) and absorption correction (face-indexed Gaussian integration[2] or numeric analytical methods[3]) were performed in CrysAlisPro.[4] Structure solution was performed using ShelXT.[5] Subsequent refinement was performed by full-matrix least-squares on F^2 in ShelXL.**Error! Bookmark not defined.** Olex2[6] was used for viewing and to prepare CIF files. PLATON[7] was used for Bijvoet difference analysis of absolute structure (further details within). ORTEP graphics were prepared in CrystalMaker.[8] Thermal ellipsoids are rendered at the 50% probability level.

A single crystal of **Darrin1** was grown from a sample of 94% enantiomeric purity as determined by chiral HPLC. A dichloromethan solution was diluted with pentane by vapor diffusion to afford apque, colorless blades. Part of a crystal (.20 x .05 x .05 mm) was separated carefully, mounted with STP oil treatment, and cooled to 100 K on the diffractometer. A full sphere of data were collected to 0.800 Å resolution. 43306 reflections were collected (4462 unique, 4366 observed) with R(int) 4.2% and R(sigma) 2.0% after Gaussian absorption and beam profile correction (Tmin .910, Tmax .977).

The space group was assigned as $P2_12_12_1$ based on the systematic absences. The structure solved routinely in ShelXT with 1 molecule in the asymmetric unit. All non-H atoms were located in the initial solution and refined anisotropically with no restraints. C-H hydrogens were placed in calculated positions and refined with riding coordinates and ADPs.

The final refinement (462 data, 0 restraints, 282 parameters) converged with R_1 ($F_o > 4\sigma(F_o)$) = 2.9%, wR_2 = 7.4%, S = 1.05. The largest Fourier features were 0.16 and -0.15 $e^- A^{-3}$.

1 Single crystal X-ray diffraction was performed at the Shared Materials Characterization Laboratory at Columbia University. Use of the SMCL was made possible by funding from Columbia University.
2 Blanc, E.; Schwarzenbach, D.; Flack, H. D. *J. Appl. Cryst.* **24** (1991), 1035-1041.
3 Clark. R. C.; Reid, J. S. *Acta Cryst.* **A51** (1995), 887-897.
4 Version 1.171.37.35 (2014). Oxford Diffraction /Agilent Technologies UK Ltd, Yarnton, England.
5 Sheldrick, G. M. *Acta Cryst.* **A71** (2015), 3-8.
6 Dolomanov, O. V.; Bourhis, L. J.; Gildea, R. J.; Howard, J. A. K.; Puschmann, H. *J. Appl. Cryst*. **42** (2009), 339-341.
7 Spek, A. *Acta Cryst*. **D65** (2009), 148-155.
8 CrystalMaker Software Ltd, Oxford, England *(www.crystalmaker.com)*.

A crystal with molecular formula $C_{26}H_{32}N_2O_3$ is a reasonable target for absolute structure determination using Cu Kα radiation.[9] The Flack x parameter was 0.07(6) by the Parsons selected quotients method implemented in ShelXL. For confirmation of the absolute structure, the data set was analyzed by the probabilistic approach of Hooft, Straver, and Spek[10] as implemented in PLATON. Errors were assumed to be Gaussian; a normal probabilities plot was linear with correlation coefficient 0.999 and slope 0.956. Using an outlier criterion of 79.66 and sigma criterion of 0.25, 404 Bijvoet pairs were selected for analysis. The Hooft y parameter was 0.06(6) using these parameters. The probability of a racemic twin, P3(rac-twin), was calculated as 4×10^{-14} and the probability of an incorrect absolute structure, P3(false), was 4×10^{-63}. Therefore, we state with high confidence that the absolute structure is correctly assigned.

Figure Sx. Molecular structure of **Darrin1**.

Compound	**Darrin1**
Formula	$C_{26}H_{32}N_2O_3$
MW	420.53
Space group	$P2_12_12_1$
***a* (Å)**	6.27180(10)
***b* (Å)**	14.71860(10)
***c* (Å)**	24.2813(2)
***α* (°)**	90
***β* (°)**	90
***γ* (°)**	90
V (Å^3)	2241.46(4)
Z	4
ρ_{calc} (g cm^{-3})	1.246
T (K)	100
λ (Å)	1.54184
$2\theta_{min}$, $2\theta_{max}$	7, 146
Nref	43306
R(int), R(σ)	.0424, .0200
μ(mm^{-1})	0.645
Size (mm)	.20 x .05 x .05
T_{max}, T_{min}	.977, .910
Data	4462

[9] Parsons, S.; Flack, H. D.; Wagner, T. *Acta Cryst.* **B69** (2013), 249-259.
10 Hooft, R. W. W.; Straver, L. H.; Spek, A. L. *J. Appl. Cryst.* **41** (2008), 96-103.

Restraints	0
Parameters	282
R_1(obs)	0.0288
wR_2(all)	0.0743
S	1.045
Peak, hole (e^- Å^{-3})	0.16, -0.15
Hooft y	0.06(6)

Table 1 Crystal data and structure refinement for bcorr_a.

Identification code	bcorr_a
Empirical formula	$C_{26}H_{32}N_2O_3$
Formula weight	420.53
Temperature/K	100.01(10)
Crystal system	orthorhombic
Space group	$P2_12_12_1$
a/Å	6.27180(10)
b/Å	14.71860(10)
c/Å	24.2813(2)
α/°	90
β/°	90
γ/°	90
Volume/Å^3	2241.46(4)
Z	4
ρ_{calc}g/cm^3	1.246
μ/mm^{-1}	0.645
F(000)	904.0
Crystal size/mm^3	0.196 × 0.049 × 0.048
Radiation	CuKα (λ = 1.54184)
2Θ range for data collection/°	7.022 to 145.98
Index ranges	$-7 \leq h \leq 7$, $-18 \leq k \leq 18$, $-29 \leq l \leq 30$
Reflections collected	43306
Independent reflections	4462 [R_{int} = 0.0424, R_{sigma} = 0.0200]
Data/restraints/parameters	4462/0/282
Goodness-of-fit on F^2	1.045
Final R indexes [I>=2σ (I)]	R_1 = 0.0288, wR_2 = 0.0737
Final R indexes [all data]	R_1 = 0.0296, wR_2 = 0.0743
Largest diff. peak/hole / e Å^{-3}	0.16/-0.15
Flack parameter	0.07(6)

Table 2 Fractional Atomic Coordinates ($\times 10^4$) and Equivalent Isotropic Displacement Parameters ($Å^2 \times 10^3$) for bcorr_a. U_{eq} is defined as 1/3 of of the trace of the orthogonalised U_{IJ} tensor.

Atom	*x*	*y*	*z*	U(eq)
N1	119(2)	6276.2(9)	4025.4(5)	14.3(3)
C2	1459(3)	5863.1(10)	3599.9(6)	14.5(3)
C3	1802(3)	4848(1)	3725.0(6)	13.8(3)
C4	-340(3)	4333.5(10)	3765.3(6)	12.8(3)
C5	-1718(3)	4828.5(11)	4189.4(7)	15.3(3)
C6	-1977(3)	5828.5(11)	4041.4(7)	16.0(3)
C7	-160(3)	7255.8(11)	3914.0(7)	16.4(3)
C8	1881(3)	7787.7(10)	3960.5(7)	15.4(3)
C9	2978(3)	8097.8(11)	3497.2(7)	19.8(3)
C10	4843(3)	8597.6(12)	3544.5(7)	21.7(3)
C11	5639(3)	8806.5(10)	4066.3(7)	17.7(3)
C12	4574(3)	8509.4(11)	4535.4(7)	16.5(3)
C13	2721(3)	7999.8(10)	4476.1(6)	15.2(3)
O14	7478(2)	9307.6(9)	4077.0(6)	26.6(3)
C15	8326(3)	9528.5(14)	4604.8(9)	31.0(4)
C16	3128(3)	4455.1(11)	3285.4(7)	16.9(3)
N17	4098(3)	4146.8(10)	2931.3(7)	24.8(3)
C18	-48(3)	3308.4(10)	3871.2(6)	12.9(3)
C19	699(3)	3095.3(11)	4462.0(6)	15.1(3)
C20	1311(3)	2110.6(11)	4515.1(6)	15.5(3)
O21	509(2)	1566.1(9)	4822.5(5)	24.8(3)
O22	2912(2)	1902.1(8)	4168.6(5)	20.4(3)
C23	3544(3)	961.9(12)	4143.5(7)	23.6(4)
C24	-2091(3)	2778.0(11)	3727.9(7)	16.9(3)
C25	-2258(3)	2554.3(12)	3110.6(7)	21.1(4)
C26	-737(3)	1811.4(12)	2941.8(7)	17.9(3)
C27	-1243(3)	906.5(13)	3052.4(7)	21.1(4)
C28	167(3)	208.4(12)	2929.6(8)	26.2(4)
C29	2117(3)	402.7(14)	2690.4(8)	27.7(4)
C30	2639(3)	1295.0(15)	2570.9(7)	27.5(4)
C31	1223(3)	1995.3(13)	2696.8(7)	23.1(4)

Table 3 Anisotropic Displacement Parameters ($Å^2 \times 10^3$) for bcorr_a. The Anisotropic displacement factor exponent takes the form: $-2\pi^2[h^2a^{*2}U_{11}+2hka^*b^*U_{12}+\ldots]$.

Atom	U_{11}	U_{22}	U_{33}	U_{23}	U_{13}	U_{12}
N1	15.8(6)	10.9(6)	16.2(6)	-2.7(5)	0.6(5)	1.1(5)
C2	17.4(8)	11.6(7)	14.5(7)	-0.5(6)	1.5(6)	0.1(6)
C3	13.3(7)	12.9(7)	15.3(7)	-0.7(6)	1.7(6)	1.1(6)
C4	13.5(7)	13.3(7)	11.7(7)	-0.9(5)	-0.6(6)	0.5(6)
C5	15.1(7)	15.4(7)	15.5(7)	-1.2(6)	2.0(6)	0.1(6)
C6	14.5(7)	15.1(7)	18.3(7)	-4.3(6)	-0.3(6)	2.5(6)
C7	18.1(8)	12.1(7)	18.9(7)	-1.8(6)	-3.1(6)	3.9(6)
C8	18.6(8)	10.9(7)	16.6(7)	-0.5(6)	-1.2(6)	3.0(6)
C9	27.4(8)	16.7(8)	15.4(7)	1.3(6)	-0.9(7)	4.4(7)
C10	28.0(9)	18.1(8)	19.0(8)	5.6(6)	6.8(7)	2.9(7)
C11	16.8(8)	10.9(7)	25.5(8)	1.4(6)	2.7(7)	-0.2(6)
C12	19.4(8)	12.7(7)	17.3(7)	-0.7(6)	-0.6(6)	3.0(6)
C13	19.3(7)	12.1(7)	14.4(7)	1.0(6)	2.5(6)	1.4(6)
O14	22.6(6)	20.4(6)	36.9(7)	2.9(5)	6.1(6)	-5.2(5)
C15	21.1(9)	25.7(10)	46.1(12)	-7.9(8)	-1.0(8)	-5.2(7)
C16	16.9(7)	12.3(7)	21.5(8)	2.6(6)	2.8(7)	0.5(6)
N17	24.5(8)	18.7(7)	31.3(8)	1.2(6)	13.0(7)	2.0(6)
C18	14.6(7)	11.5(7)	12.6(7)	-0.8(5)	0.5(6)	0.1(6)
C19	18.4(7)	14.1(7)	12.8(7)	-0.4(6)	0.8(6)	0.5(6)
C20	17.5(7)	17.0(8)	12.0(7)	-0.2(6)	-1.5(6)	0.8(6)
O21	29.1(7)	19.1(6)	26.1(6)	4.9(5)	8.4(5)	0.9(5)
O22	23.3(6)	17.1(6)	20.7(6)	2.7(4)	6.3(5)	4.6(5)
C23	30.3(10)	19.7(8)	21.0(8)	0.9(7)	3.4(7)	10.8(7)
C24	14.1(7)	16.8(7)	19.8(8)	-3.5(6)	-0.1(6)	-0.9(6)
C25	22.0(8)	18.3(8)	23.0(8)	-6.5(6)	-9.3(7)	4.1(7)
C26	20.5(8)	19.5(8)	13.7(7)	-5.6(6)	-4.9(6)	1.8(7)
C27	21.3(8)	21.9(9)	20.1(8)	-3.3(7)	1.4(7)	1.0(7)
C28	36.3(10)	21.0(8)	21.3(8)	-3.0(7)	-0.3(8)	7.9(8)
C29	28.1(9)	35.8(10)	19.3(8)	-10.1(7)	-5.3(7)	13.0(8)
C30	18.5(8)	48.3(11)	15.7(8)	-10.9(8)	-0.5(6)	-1.0(8)
C31	27.3(9)	26.9(9)	15.0(7)	-6.2(7)	-3.0(7)	-6.8(7)

Table 4 Bond Lengths for bcorr_a.

Atom	Atom	Length/Å	Atom	Atom	Length/Å
N1	C2	1.464(2)	O14	C15	1.425(3)
N1	C6	1.471(2)	C16	N17	1.147(2)
N1	C7	1.4775(19)	C18	C19	1.541(2)
C2	C3	1.540(2)	C18	C24	1.540(2)
C3	C4	1.546(2)	C19	C20	1.505(2)
C3	C16	1.472(2)	C20	O21	1.205(2)
C4	C5	1.529(2)	C20	O22	1.345(2)
C4	C18	1.541(2)	O22	C23	1.441(2)
C5	C6	1.524(2)	C24	C25	1.538(2)
C7	C8	1.505(2)	C25	C26	1.508(2)
C8	C9	1.395(2)	C26	C27	1.395(3)
C8	C13	1.394(2)	C26	C31	1.392(3)
C9	C10	1.387(3)	C27	C28	1.388(3)
C10	C11	1.396(3)	C28	C29	1.384(3)
C11	C12	1.391(2)	C29	C30	1.384(3)
C11	O14	1.369(2)	C30	C31	1.395(3)
C12	C13	1.391(2)			

Table 5 Bond Angles for bcorr_a.

Atom	Atom	Atom	Angle/°	Atom	Atom	Atom	Angle/°
C2	N1	C6	110.21(12)	C12	C13	C8	121.98(15)
C2	N1	C7	110.13(13)	C11	O14	C15	117.03(14)
C6	N1	C7	109.63(13)	N17	C16	C3	177.57(19)
N1	C2	C3	110.12(13)	C19	C18	C4	112.99(12)
C2	C3	C4	111.48(13)	C24	C18	C4	111.08(13)
C16	C3	C2	108.50(13)	C24	C18	C19	111.09(13)
C16	C3	C4	110.16(13)	C20	C19	C18	110.68(13)
C5	C4	C3	107.48(12)	O21	C20	C19	125.94(15)
C5	C4	C18	114.91(13)	O21	C20	O22	123.17(15)
C18	C4	C3	112.76(13)	O22	C20	C19	110.89(13)
C6	C5	C4	111.21(13)	C20	O22	C23	116.80(13)
N1	C6	C5	110.10(13)	C25	C24	C18	112.67(14)
N1	C7	C8	113.15(13)	C26	C25	C24	112.14(14)
C9	C8	C7	121.95(15)	C27	C26	C25	119.71(16)

C13	C8	C7	120.36(15)	C31	C26	C25	122.27(17)
C13	C8	C9	117.68(15)	C31	C26	C27	117.97(16)
C10	C9	C8	121.52(16)	C28	C27	C26	121.33(18)
C9	C10	C11	119.58(15)	C29	C28	C27	120.02(18)
C12	C11	C10	120.15(15)	C28	C29	C30	119.54(17)
O14	C11	C10	115.91(16)	C29	C30	C31	120.31(18)
O14	C11	C12	123.94(16)	C26	C31	C30	120.82(18)
C13	C12	C11	119.08(15)				

Table 6 Hydrogen Atom Coordinates (Å×10^4) and Isotropic Displacement Parameters (Å^2×10^3) for bcorr_a.

Atom	***x***	***y***	***z***	**U(eq)**
H2A	2853.28	6177.35	3586.59	17
H2B	765.53	5931.28	3235.89	17
H3	2574.74	4789.21	4083.55	17
H4	-1066.41	4397.43	3400.7	15
H5A	-3139.3	4537.51	4207.03	18
H5B	-1049.18	4776.88	4557.38	18
H6A	-2676.27	5883.14	3677.39	19
H6B	-2894.38	6130.8	4317.98	19
H7A	-1212.7	7506.56	4177.13	20
H7B	-745.44	7332.95	3538.2	20
H9	2434.1	7963.51	3141.25	24
H10	5574.35	8796.57	3223.86	26
H12	5105.5	8652.52	4891.38	20
H13	2005.72	7789.92	4796.73	18
H15A	7284.82	9890.72	4810.51	46
H15B	9643.65	9878.76	4559.29	46
H15C	8634.51	8968	4807.61	46
H18	1094.73	3091.49	3615.82	15
H19A	1938.99	3482.11	4555	18
H19B	-461.77	3236.03	4724.84	18
H23A	3641.51	715.67	4517.63	35
H23B	4935.95	913.9	3962.51	35
H23C	2484.05	616.76	3933.33	35
H24A	-2115.35	2204.92	3941.27	20
H24B	-3347.29	3141.71	3838.83	20

H25A	-3735.01	2362.61	3025.43	25
H25B	-1948.66	3108.38	2893.79	25
H27	-2580.6	765.33	3215.07	25
H28	-207.15	-402.92	3009.68	31
H29	3090.74	-73.01	2608.75	33
H30	3968.13	1431.03	2402.39	33
H31	1599.86	2605.42	2614.37	28

Experimental

Single crystals of $C_{26}H_{32}N_2O_3$ [bcorr_a] were []. A suitable crystal was selected and [] on a SuperNova, Dual, Cu at zero, EosS2 diffractometer. The crystal was kept at 100.01(10) K during data collection. Using Olex2 [1], the structure was solved with the ShelXT [2] structure solution program using Intrinsic Phasing and refined with the ShelXL [3] refinement package using Least Squares minimisation.

1. Dolomanov, O.V., Bourhis, L.J., Gildea, R.J, Howard, J.A.K. & Puschmann, H. (2009), J. Appl. Cryst. 42, 339-341.
2. Sheldrick, G.M. (2015). Acta Cryst. A71, 3-8.
3. Sheldrick, G.M. (2015). Acta Cryst. C71, 3-8.

Crystal structure determination of [bcorr_a]

Crystal Data for $C_{26}H_{32}N_2O_3$ (M =420.53 g/mol): orthorhombic, space group $P2_12_12_1$ (no. 19), a = 6.27180(10) Å, b = 14.71860(10) Å, c = 24.2813(2) Å, V = 2241.46(4) Å^3, Z = 4, T = 100.01(10) K, μ(CuKα) = 0.645 mm^{-1}, *Dcalc* = 1.246 g/cm^3, 43306 reflections measured ($7.022° \leq 2\Theta \leq 145.98°$), 4462 unique ($R_{int}$ = 0.0424, R_{sigma} = 0.0200) which were used in all calculations. The final R_1 was 0.0288 ($I > 2\sigma(I)$) and wR_2 was 0.0743 (all data).

Refinement model description

Number of restraints - 0, number of constraints - unknown.

Details:

1. Fixed Uiso
 At 1.2 times of:
 All C(H) groups, All C(H,H) groups
 At 1.5 times of:
 All C(H,H,H) groups
2.a Ternary CH refined with riding coordinates:
 C3(H3), C4(H4), C18(H18)
2.b Secondary CH2 refined with riding coordinates:
 C2(H2A,H2B), C5(H5A,H5B), C6(H6A,H6B), C7(H7A,H7B), C19(H19A,H19B), C24(H24A,

H24B), C25(H25A,H25B)
2.c Aromatic/amide H refined with riding coordinates:
C9(H9), C10(H10), C12(H12), C13(H13), C27(H27), C28(H28), C29(H29), C30(H30), C31(H31)
2.d Idealised Me refined as rotating group:
C15(H15A,H15B,H15C), C23(H23A,H23B,H23C)

Appendix II. Supplementary Information for Chapter 3.

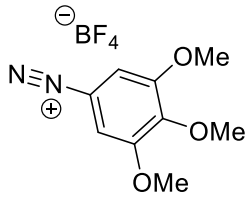

3,4,5-trimethoxybenzenediazonium tetrafluoroborate: A 250 mL RB flask containing 3,4,5-trimethoxyaniline (9.09 g, 49.6 mmol) dissolved in 150 mL THF (0.3 M) was cooled to −10 ℃ and HBF_4 48 wt.% in water (17.7 mL, 135 mmol, 2.7 equiv) was added dropwise over 15-20 minutes. *t*-butyl nitrite (7.5 mL, 63.1 mmol, 1.3 equiv) was then added drop-wise over 25 minutes, and the mixture was stirred for 15 minutes. After this time, the precipitate was collected by vacuum filtration, rinsed generously with Et_2O, and dried in vacuo to give 13.03 g (93%) of a tan/pale yellow precipitate used without further purification. Spectral data matches those previously reported.[1] **^{1}H NMR** (300 MHz; DMSO-d_6): δ 8.15 (s, 2H), 4.00 (s, 3H), 3.87 (s, 6H).

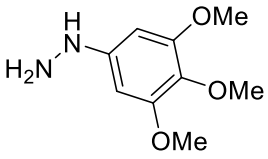

(3,4,5-trimethoxyphenyl)hydrazine: To a solution of tin(II)chloride dihydrate (3.0 g, 13.3 mmol, 2.5 equiv) in 6 M HCl (20 mL) at −10 ℃ (ice/brine) was added 3,4,5-trimethoxybenzenediazonium tetrafluoroborate (1.5 g, 5.3 mmol, 1 equiv) portion-wise over 20 min. After stirring for 2 hours at the same temperature, 25 mL DCM was added along with 12 M KOH (20 mL), keeping the temperature below 0 ℃. At this point, the foamy off-white solution became clear and the layers were separated. The aqueous mixture was then extracted again with DCM (1 x 25 mL). The combined organic extract was then dried (Na_2SO_4) and concentrated in vacuo to 1/3 the volume (~15 mL). The dry DCM/hydrazine solution was then used immediately in the next step without further purification.

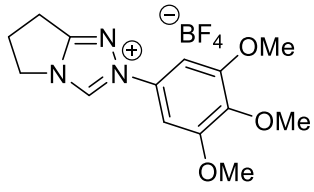

2-(3,4,5-trimethoxyphenyl)-6,7-dihydro-5H-pyrrolo[2,1-c][1,2,4]triazol-2-ium tetrafluoroborate: Prepared according to a literature procedure[2], with minor modifications. To a flame-dried flask under Ar was added 0.38 mL 2-pyrolidinone along with 10 mL anhydrous DCM. Trimethyloxonium tetrafluoroborate (743 mg, 5.0 mmol, 1 equiv) was then added quickly, in one portion, and the mixture was stirred until homogenous (~3 hr). After this time, the dried crude solution of (3,4,5-trimethoxyphenyl)hydrazine (5.3 mmol in ~15 mL DCM) was added and the mixture stirred for an additional 8 hr. The resultant deep red solution was concentrated in vacuo until most of the DCM was removed (~2 mL total volume) and diluted with EtOAc (25 mL) causing a precipitate to form. The pink/orange precipitate was then collected by vacuum filtration and dried in vacuo (30 min) to give 505 mg (1.43 mmol, 29%) of the corresponding hydrazinium.[3] The crude powder was then diluted with 10 mL MeCN and 1 mL trimethylorthoformate (9.1 mmol, 6.5 equiv), and the mixture was heated to reflux for

12 hr. After this time, the reaction was allowed to cool to rt and concentrated in vacuo. The crude residue was dissolved in a minimum amount of DCM (~20 mL) and the title compound precipitated upon addition of 5 mL EtOAc. The precipitate was then collected by vacuum filtration, and rinsed with Et_2O to give 434 mg (1.2 mmol, 24% overall yield) of pure azolium as a colorless powder. **^{1}H-NMR** (400 MHz; acetone-d_6): δ 10.25 (s, 1H), 7.24 (s, 2H), 4.63 (t, J = 7.6 Hz, 2H), 3.93 (s, 6H), 3.81 (s, 3H), 3.56 (t, J = 7.6 Hz, 2H), 2.93 – 3.00 (m, 2H). **^{13}C-NMR** (101 MHz; acetone-d_6): δ 163.4, 154.3, 139.7, 137.8, 98.9, 59.9, 56.0, 47.5, 26.7, 21.5. **^{19}F-NMR** (101 MHz; acetone-d_6): δ -151.58 **IR** (ATR, neat) 3144, 2946, 1609, 1588, 1473, 1236, 1128 cm-1.
HRMS (ESI + APCI): m/z [M+H] calcd 276.14, found 276.14.

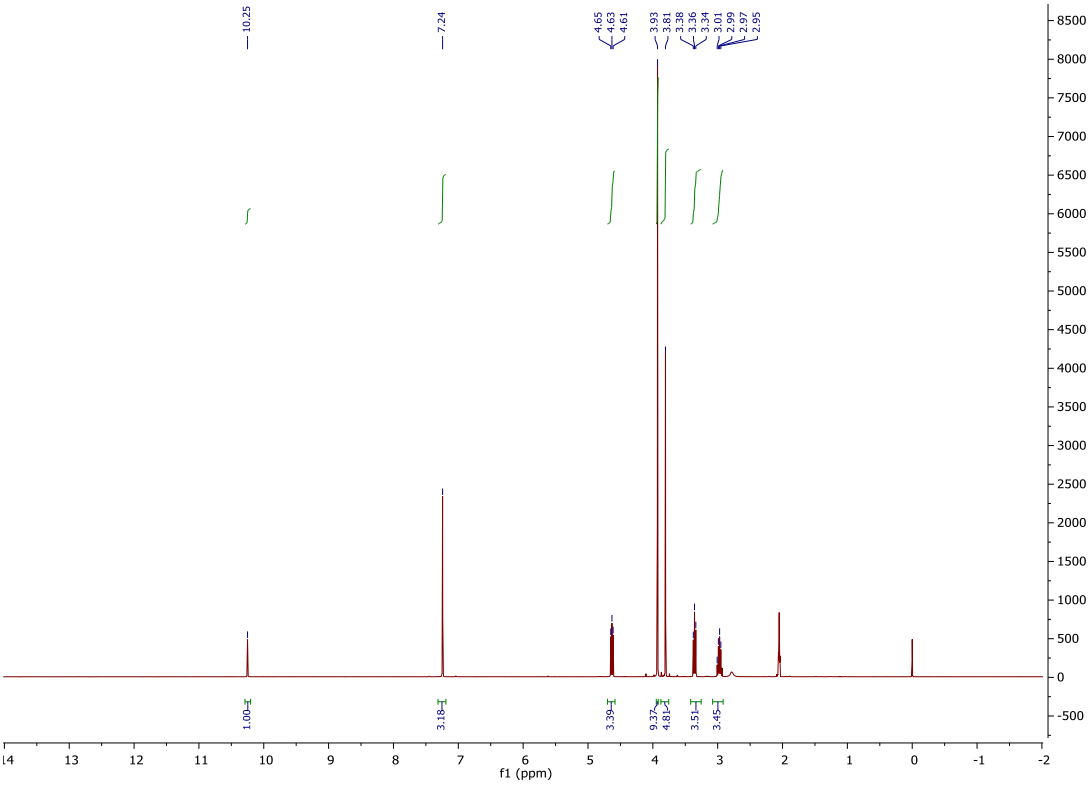

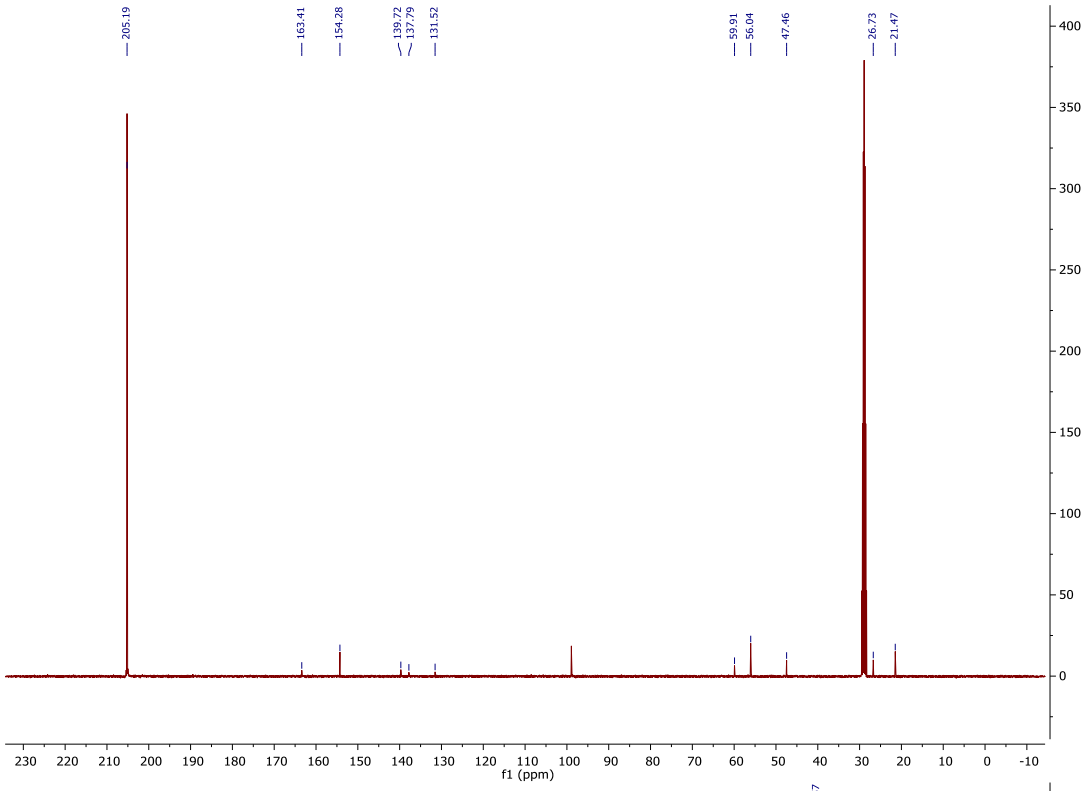
205.19
163.41
154.28
139.72
137.79
131.52
59.91
56.04
47.46
26.73
21.47
f1 (ppm)

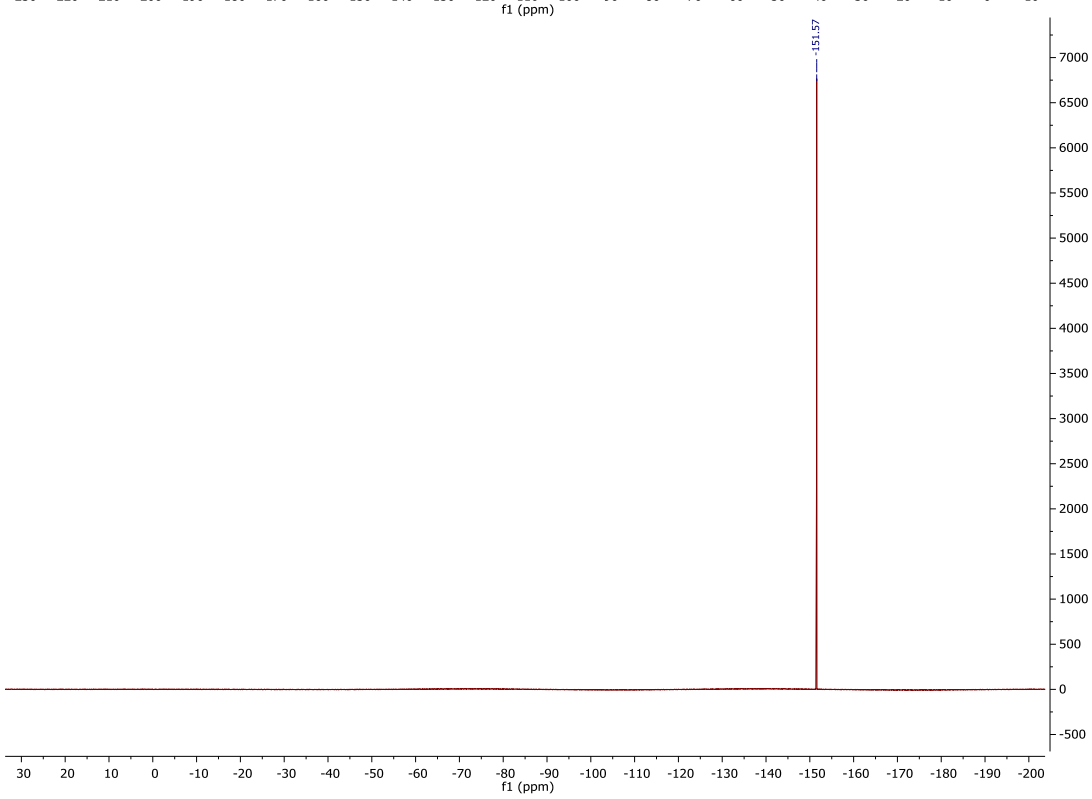
151.57
f1 (ppm)

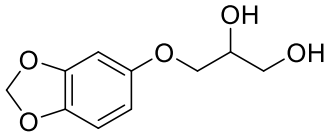

3-(benzo[d][1,3]dioxol-5-yloxy)propane-1,2-diol: Prepared according to a literature procedure. A 100 mL round bottom flask was charged with sesamol (6.906 g, 50.0 mmol) and dissolved in 30 mL EtOH. To this solution was added a solution of NaOH (2.50 g, 62.5 mmol, 1.2 eq.) in 10 mL H_2O and the mixture was heated to reflux for 10 min. After this time, a solution of 3-chloro-1,2-propane diol (5.0 mL, 6.61 g, 60.0 mmol, 1.25 eq.) in 5 mL EtOH was added and the resulting mixture was allowed to reflux overnight (~8 hr) until TLC indicated complete reaction. After this time, solution was cooled to rt and volatiles were removed *in vacuo*. The resulting residue was diluted with EtOAc (50 mL) and H_2O (50 mL), and the layers separated. The aqueous layer was extracted with EtOAc (6 x25 mL) and the combined organic extracts were dried with $MgSO_4$, filtered, and concentrated *in vacuo* to give a pale orange off-white solid (10.9 g) which was used in the next step without further purification. Rf= 0.12 in (3:2 Hexanes:EtOAc); quant., **1H-NMR** (400 MHz; $(CD_3)_2CO$): δ 6.71 (d, *J* = 8.4 Hz, 1H), 6.53 (d, *J* = 2.8 Hz, 1H), 6.37 (dd, *J* = 8.4, 2.8 Hz, 1H), 5.91 (s, 2H), 4.11 – 3.87 (m, 4H), 3.72 – 3.59 (m, 3H) **13C NMR** (101 MHz; $(CD_3)_2CO$): δ 154.7, 148.3, 141.6, 107.7, 105.7, 101.1, 97.8, 70.5, 70.4, 63.2. **IR** (neat) 3320, 2933, 2894, 1487, 1194, 1038, 928 cm-1; **LRMS** (ESI) *m/z* calcd 212.1, found 212.0

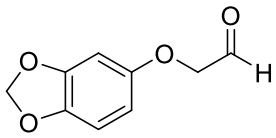

2-(benzo[d][1,3]dioxol-5-yloxy)acetaldehyde: Prepared according to a literature procedure.**Error! Bookmark not defined.** To a vigorously stirred solution of silica gel (50 g) in 350 mL CH_2Cl_2 was added a solution of 6.952 g $NaIO_4$ (32.5 mmol) in 50 mL H_2O, followed by a solution of 5.305 g 3-(benzo[d][1,3]dioxol-5-yloxy)propane-1,2-diol (25.0 mmol) in 50 mL CH_2Cl_2. The resulting mixture was allowed to stir at rt open to the air for 2 hr until TLC completed complete reaction. After this time, the reaction mixture was filtered over a bed of silica gel and the silica gel was rinsed with ~1 L of CH_2Cl_2. The Solvent was then removed *in vacuo* to give 3.63 g (20.5 mmol) 2-(benzo[d][1,3]dioxol-5-yloxy)acetaldehyde as an analytically pure white solid. Rf= 0.42 in (3:2 Hexanes:EtOAc); 82 % yield, **1H-NMR** (400 MHz; $(CD_3)_2CO$): δ 9.75 (s, 1H), 6.73 (d, *J* = 8.8 Hz, 1H), 6.57 (d, *J* = 2.4 Hz, 1H), 6.38 (dd, *J* = 8.4, 2.8 Hz, 1H), 5.94 (s, 2H), 4.67 (s, 2H) **13C NMR** (101 MHz; $(CD_3)_2CO$): δ 198.4, 153.6, 148.5, 142.3, 107.8, 105.9, 101.3, 97.9, 73.5. **IR** (neat) 2900, 2832, 1738, 1503, 1488, 1187, 1037 cm-1; **LRMS** (ESI) *m/z* calcd 180.0, found 180.0

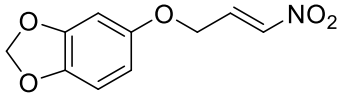

(E)-5-((3-nitroallyl)oxy)benzo[d][1,3]dioxole: To an oven-dried round bottom flask was added 3.42 g 2-(benzo[d][1,3]dioxol-5-yloxy)acetaldehyde (19.0 mmol), 1.5 mL nitromethane (28.0 mmol), and 1:1 THF/*t*-BuOH (25 mL). This solution was then cooled to 0 °C and 426 mg potassium tert-butoxide (3.8 mmol) was added in one portion. The reaction was allowed to stir at 0 °C for 15 min then warmed to room temperature and stirred for another 2 h until TLC indicated complete reaction. After completion, saturated aqueous NH_4Cl solution (50 mL) was added to quench the reaction and then the aqueous layer was extracted with CH_2Cl_2

(4 x 50 mL). The combined organic extracts were then dried (Na_2SO_4) and concentrated *in vacuo*. After drying the crude residue under vacuum (4 mm) for 0.5 h, CH_2Cl_2 (50 mL) was added and the solution was cooled to 0 °C. Trifluoroacetic anhydride (3.0 mL, 10.9 mmol) was then added followed by the slow dropwise addition of 5.6 mL Et_3N (40 mmol). After stirring for ~15 min at 0 °C the reaction was diluted with H_2O (30 mL) and CH_2Cl_2 (50 mL) and the layers separated. The organic layer was then washed with sat. aq. NH_4Cl (2 x 30 mL), dried (Na_2SO_4) and concentrated *in vacuo* to give brown-yellow solid, which was then purified by column chromatography (3:1 hexanes:ethyl acetate) to give 2.893 g (13.0 mmol) of (E)-5-((3-nitroallyl)oxy)benzo[d][1,3]dioxole as a bright yellow solid. Rf= 0.4 in (3:1 Hexanes:EtOAc); 68 % yield, **1H-NMR** (400 MHz; $(CD_3)_2CO$): δ 7.47 (dt, *J* = 13.6, 3.6 Hz, 1H), 7.39 (dt, *J* = 13.6, 2.0 Hz, 1H), 6.76 (d, *J* = 8.4 Hz, 1H), 6.65 (d, *J* = 2.4 Hz, 1H), 6.47 (dd, *J* = 8.4, 2.4 Hz, 1H), 5.95 (s, 2H), 4.11 (dd, *J* = 3.6, 2.0 Hz, 2H), **13C NMR** (101 MHz; $(CD_3)_2CO$): δ 153.3, 148.5, 142.4, 139.7, 137.9, 107.8, 106.0, 101.4, 101.4, 98.0, 64.6 **IR** (neat) 3439, 3124, 1635, 1435, 933,
733 cm-1; **LRMS** (ESI) *m/z* calcd 223.1, found 223.0

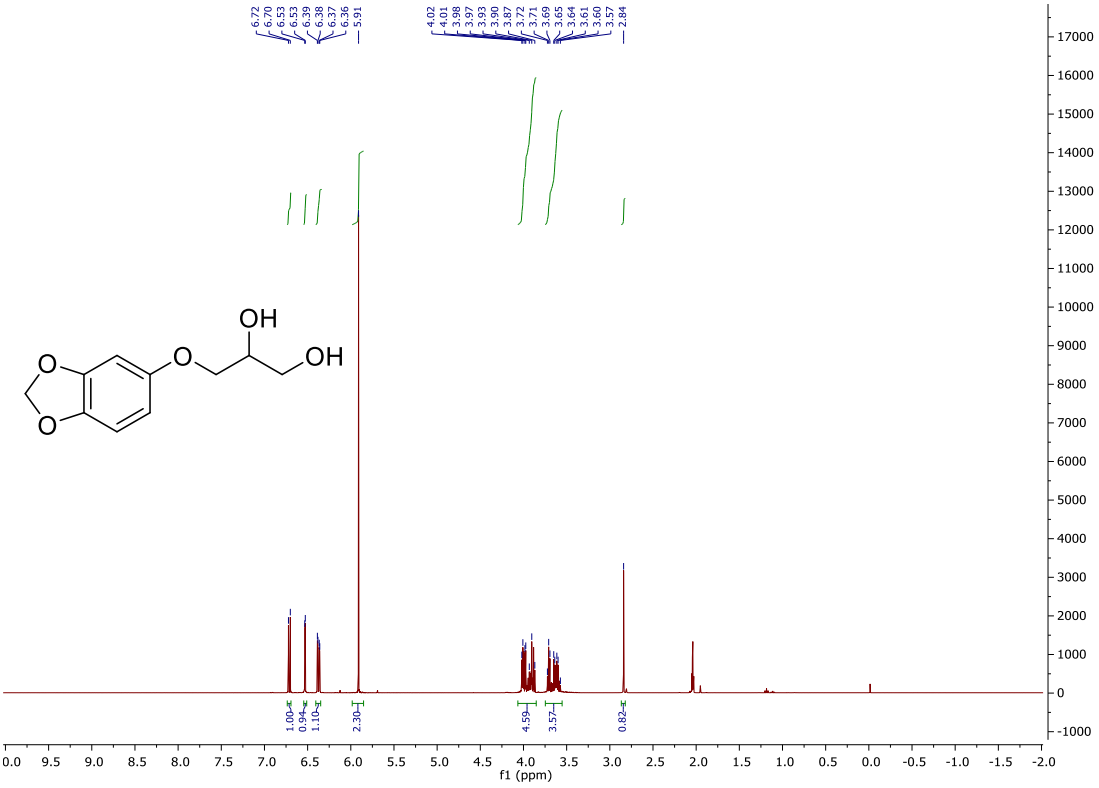

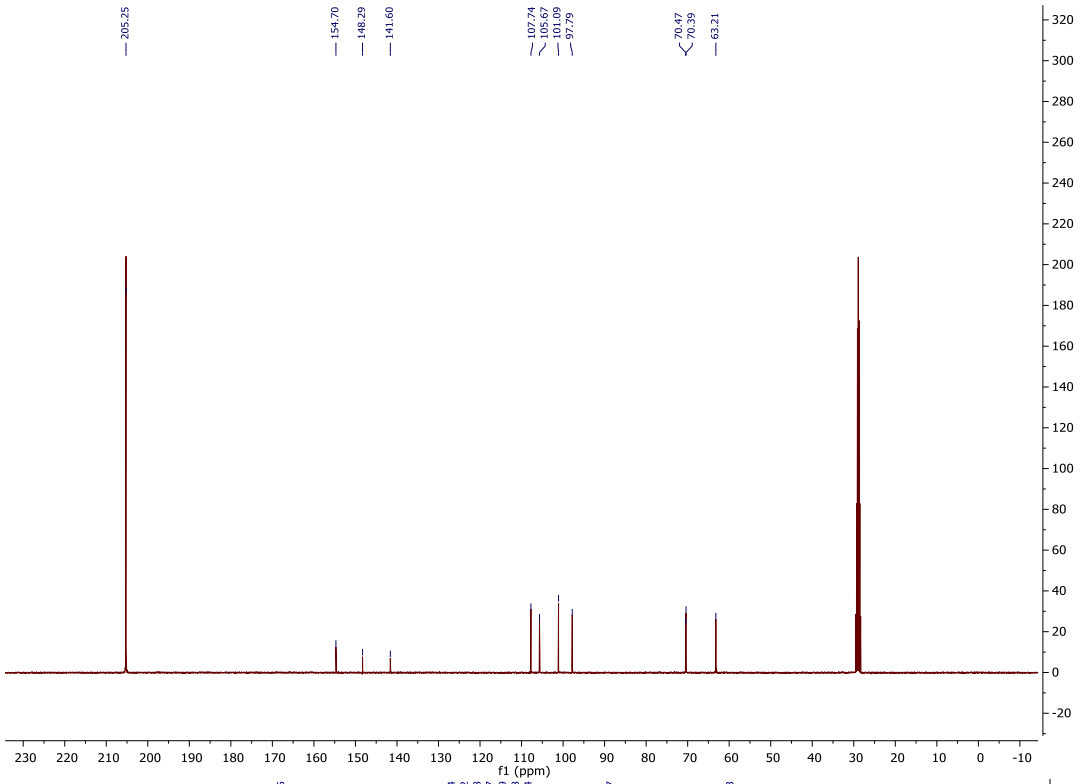
205.25
154.70
148.29
141.60
107.74
105.67
101.09
97.79
70.47
70.39
63.21
f1 (ppm)

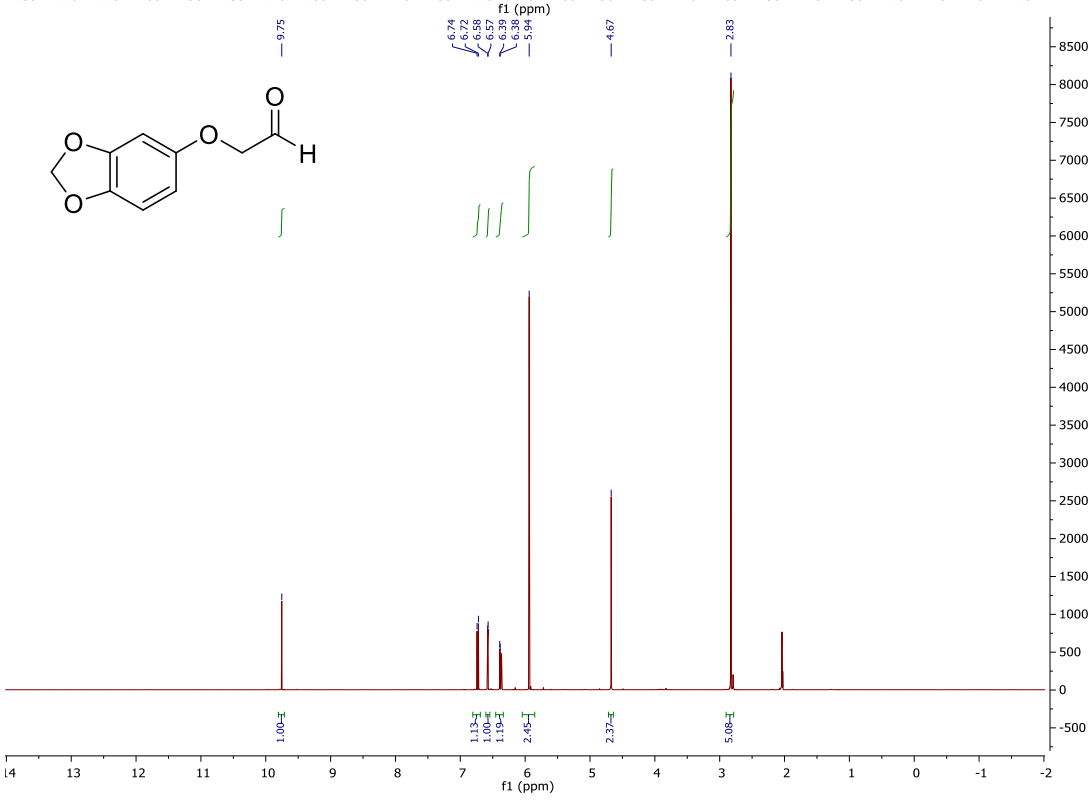
9.75
6.74
6.72
6.58
6.57
6.39
6.38
5.94
4.67
2.83
O
O
O
H
1.00
1.13
1.00
1.19
2.45
2.37
5.08
f1 (ppm)

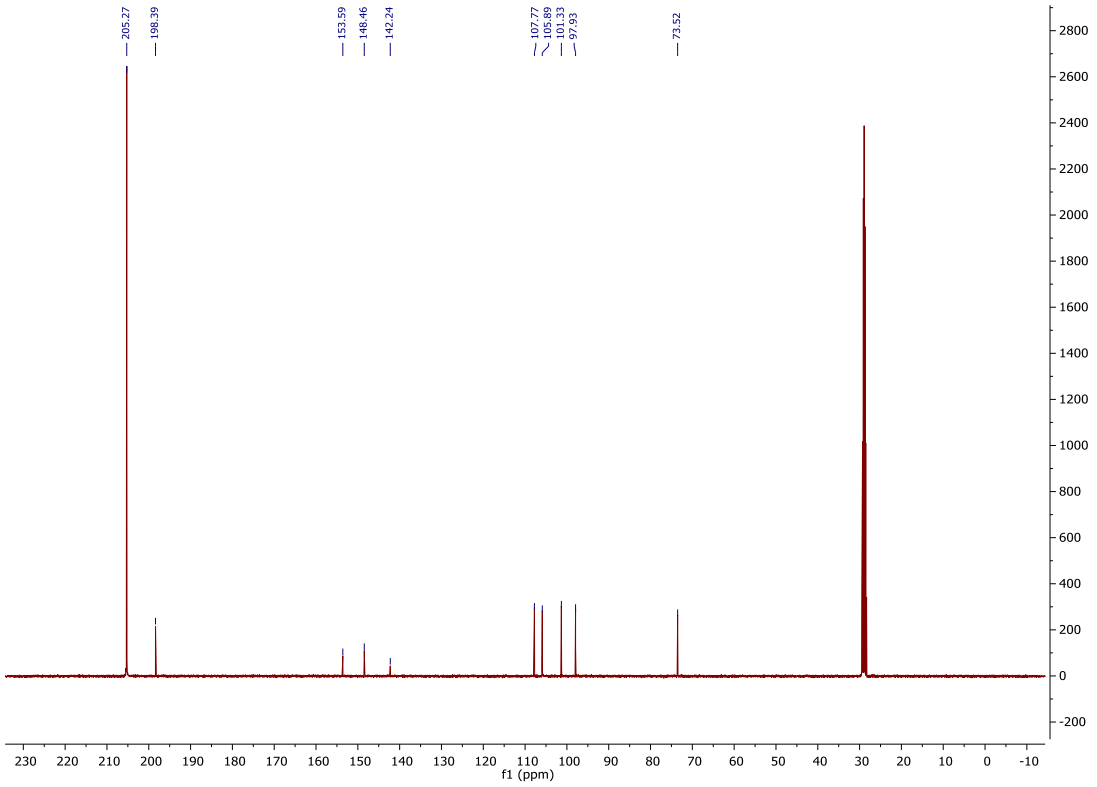
205.27
198.39
153.59
148.46
142.24
107.77
105.89
101.33
97.93
73.52
f1 (ppm)

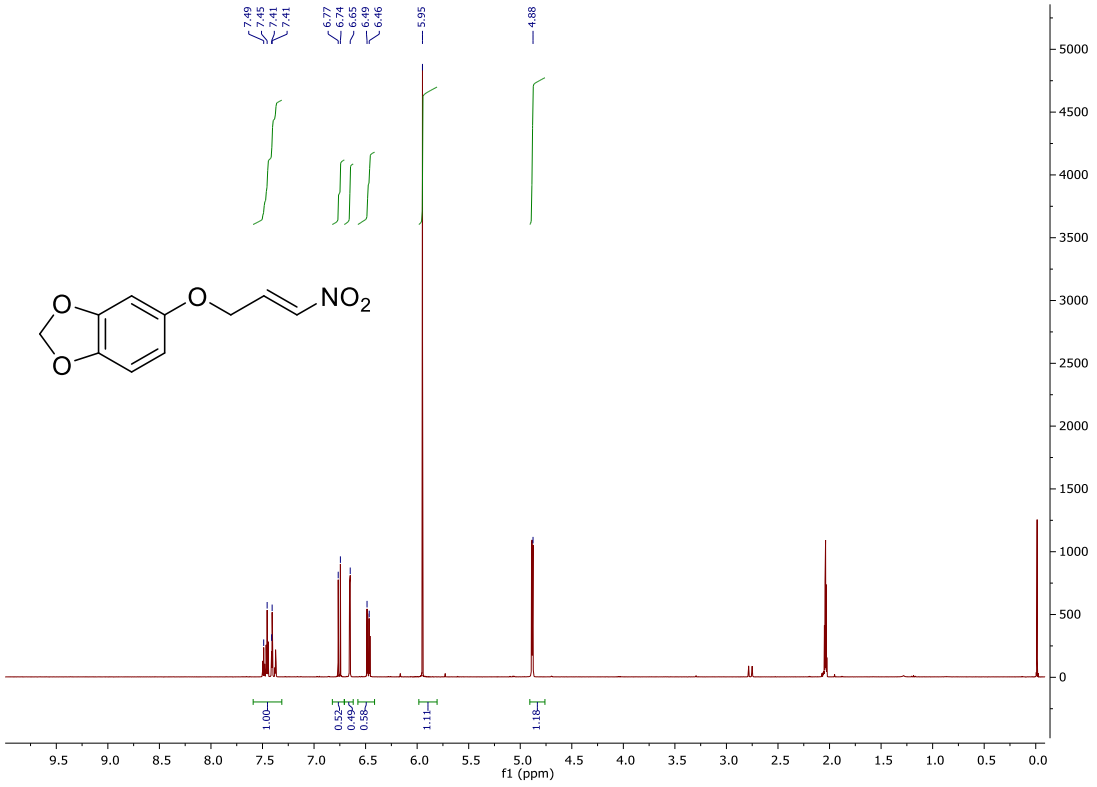
7.49
7.45
7.41
7.41
6.77
6.74
6.65
6.49
6.46
5.95
4.88
O
O
O
NO2
1.00
0.52
0.49
0.58
1.11
1.18
f1 (ppm)

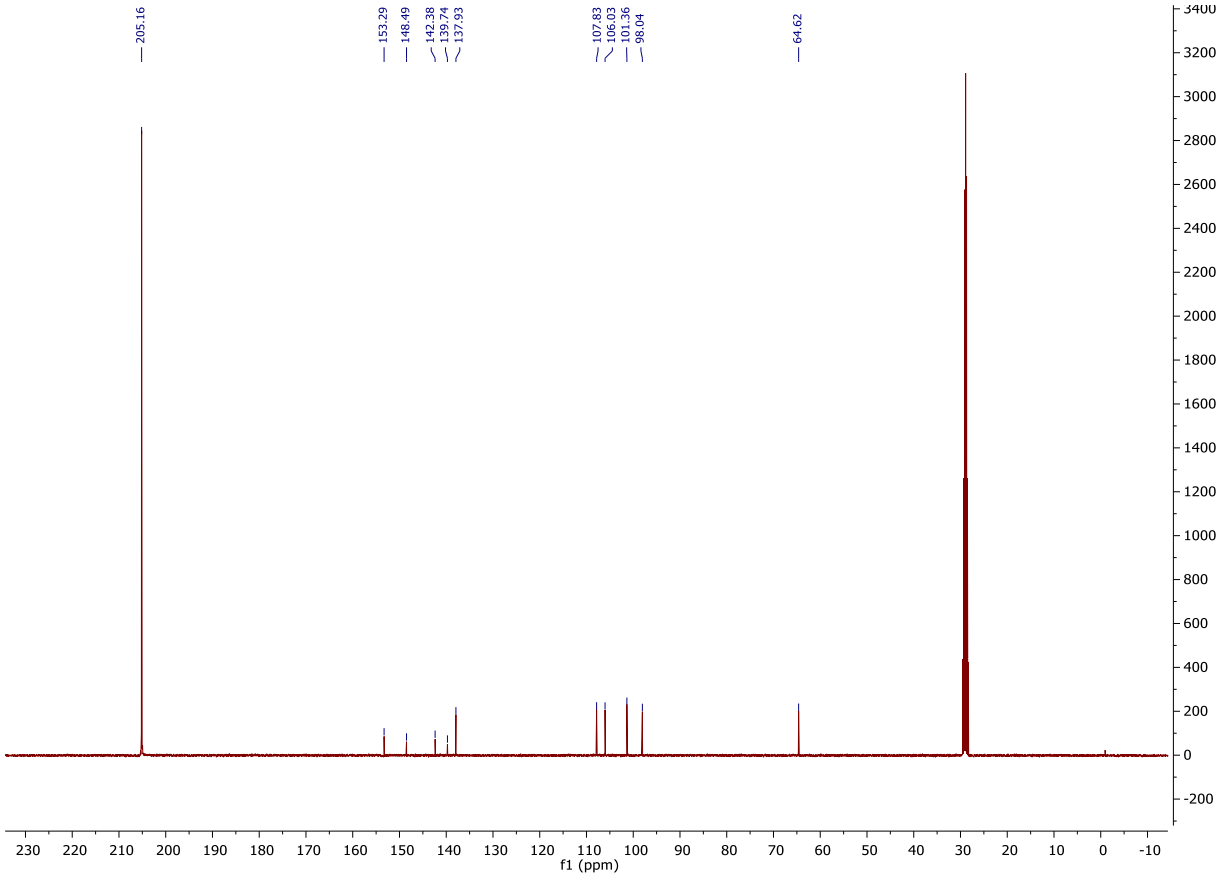

[1] N. H. Nguyen, C. Cougnon, F. Gohier, *J. Org. Chem.* **2009**, *74*, 3955.
[2] N. A. White, T. Rovis, *J. Am. Chem. Soc.* **2014**, *136*, 14674.
[3] (Z)-2-(pyrrolidin-2-ylidene)-1-(3,4,5-trimethoxyphenyl)hydrazin-1-ium tetrafluoroborate